

# OPTICAL MULTI-COLOR PHOTOMETRY OF SPECTROPHOTOMETRIC STANDARD STARS

Arlo U. Landolt<sup>1,2</sup>

*Department of Physics & Astronomy, Louisiana State University, Baton Rouge, LA  
70803-4001*

landolt@phys.lsu.edu

and

Alan K. Uomoto<sup>1</sup>

*Carnegie Observatories, 813 Santa Barbara St., Pasadena, CA 91101-1292*

au@ociw.edu

## ABSTRACT

Photoelectric data on the Johnson-Kron-Cousins *UBVRI* broadband photometric system are provided for a set of stars which have been used as spectrophotometric standard stars at the Hubble Space Telescope.

*Subject headings:* stars: standard — photometry: broad-band — photometry: standardization

---

<sup>1</sup>Visiting Astronomer, Kitt Peak National Observatory.

<sup>2</sup>Visiting Astronomer, Cerro Tololo Inter-American Observatory, National Optical Astronomical Observatories, which are operated by the Association of Universities for Research in Astronomy, under contract with the National Science Foundation.

## 1. Introduction

A document originally prepared by Bohlin et al. (1990) and published as Turnshek et al. (1990), provided two lists of stars to be used as spectrophotometric standard stars by the Hubble Space Telescope (HST) instruments. One table listed some stars which either had known ultraviolet fluxes or which could have their ultraviolet fluxes measured with the International Ultraviolet Explorer (IUE) satellite. A second table identified stars which might prove useful standard stars but which were too faint to be observed with the IUE. These stars could be used to intercompare calibrations for the different HST instruments.

The papers by Bohlin et al. (1990) and Turnshek et al. (1990) discussed the considerations that led to selecting these spectrophotometric standard star candidates. Their goal was to construct a list of stars lengthy enough to encompass all HST instrument calibration requirements but short enough to minimize data collection efforts. An effort also was made to identify objects accessible to both HST and ground-based instrumentation. They chose at least two stars for each calibration requirement to avoid possible variability in any individual star. They avoided strong-lined stars because objects with such spectra complicate absolute calibration effects. Finally, stars covering a large magnitude range were included to allow instrumentation linearity checks.

All of the stars in this program were observed at the behest of HST staff, with the majority of the stars being taken from lists in Bohlin et al. (1990) and Turnshek et al. (1990). It may be noted that an early version of the photometry presented in this paper is the basis for the photometry of stars in common with those in the HST Calspec database.

## 2. Observations

The Kitt Peak National Observatory (KPNO) 1.3-m telescope was scheduled for this program for 101 nights in the interval 1985 September to 1991 June. Of those scheduled nights, 49, or 48.5 percent, provided usable photometric data.

The broad-band *UBVRI* photometric observations all were obtained with the same RCA 31034A-02 (KPNO serial no. H 18862) type photomultiplier used in a pulse counting mode. The photomultiplier always was kept in cold box no. 51 and was operated at -1600 volts. The 1.3-m telescope was operated in its chopping mode; ten seconds were spent on a star, and then ten seconds on the sky, over a twenty second interval of time. The data were recorded on magnetic tape, and were reduced on the IBM 3090 computer at the Louisiana State University System Network Computer Center.

The KPNO “J” *UBVRI* filter set was used throughout the data acquisition process at KPNO, with one exception. The 1985 September and December observing runs made use of an ultraviolet *U* filter combination of Corning 9863, plus a solid  $\text{CuSO}_4$  crystal. The same *BVRI* filters were used throughout the program. Their specifications, plus the specification for the *U* filter used for all except the late 1985 September and December runs, as laid down by Bessell (1979), are given in Table 1.

On average, 23 *UBVRI* standard stars, as defined by Landolt (1983), were observed each night together with the program stars. Standard stars were observed in groups of four or five periodically throughout the night. Each such group, physically close together on the sky, contained stars in as wide a color range as possible. An attempt was made to ensure that the standard star observations encompassed as wide a range in air mass as did the program stars. Almost all program star measures were taken at less than 1.5 air masses. The exception was the star AGK+81°266 whose northern declination meant that data for it were obtained between 1.56 and 1.75 air masses.

A complete data set for a star consisted of a series of measures *IRVBUUBVRI*. Throughout the process, the sky was sampled once per second via the telescope’s chopping mode. A 17.7 second of arc diaphragm was used (because that was the most reasonable size diaphragm available given the instrument setup). Counting intervals, i.e., the time spent on a star, ranged from no less than ten seconds for the brightest stars to sixty seconds for the faintest stars. The longest integrations were constrained by the lack of an automatic guiding mode; one had to depend upon the telescope drive to keep the star centered for the duration of the observation. Fortunately, the KPNO 1.3-m was a very stable telescope! Data reduction procedures followed the precepts outlined by Schulte & Crawford (1961).

Extinction coefficients were extracted from three or four standard stars possessing a range in color index which were followed over to an air mass of 2.1, or so. Each night’s data were reduced using the primary extinction coefficients derived from that night, whenever possible. Average secondary extinction coefficients, for a given run, were used. The average extinction coefficient values found over the seventy month observational interval of this project are given in Table 2. It is interesting to compare these *UBV* extinction coefficient values with those from earlier years’ data obtained at KPNO (Landolt 1967, 1973), and this is done in Table 3. One notes that, within the errors of the data, extinction coefficients essentially have remained unchanged, although, of course, there exist on occasion wide variations from night to night, and even during a night (Landolt 2007). Therefore, mean extinction coefficients only should be used with great caution.

A more detailed description of extinction coefficient behavior and the data reduction procedures employed by the author may be found in Landolt (2007).

The final computer printout for each night’s reductions contained the magnitude and color indices for each of the standard stars. Since the time of observation was recorded for each measurement, it was possible to plot the residuals in the  $V$  magnitude and in the different color indices for each standard star against Universal Time for a given night. These plots permitted small corrections to be made to all program star measures. The corrections usually were less than a few hundredths of a magnitude. Such corrections took into account small changes in both atmospheric and instrumental conditions which occurred during the course of a night’s observations.

A problem was discovered near the end of the observing session in 1986 November in the sense that frost had formed on the coldbox’s Fabry lens at some point during the course of the run. The subsequent data analysis showed no discernible effect on the derived values of the program stars’ color indices. However, small trends did appear in the  $V$  magnitudes. To be on the safe side, all of the data from that observing run were discarded.

### 3. Discussion

A total of 32 stars, distributed over the sky, made up this observational program. The data were reduced night by night with the results having been tied into the  $UBVRI$  photometric system defined by Landolt (1983) standard stars. A thorough check was made to ensure that the  $U$  data obtained during the 1985 September and December observing sessions were on the same  $U$  filter system with which the remaining and majority of the data were acquired.

A check on the accuracy of the magnitude and color index transformations was made via a comparison of the magnitudes and color indices of the stars from Landolt (1983) which were used as standards herein, with the magnitudes and color indices of these same standard stars obtained during this project. The comparisons, the delta quantities, were in the sense data from this program *minus* corresponding magnitudes and color indices from Landolt (1992), since this latter paper was a successor to Landolt (1983).

Figures 1-6 illustrate the plots of the delta quantities on the ordinates versus the color indices on the abscissas. Nonlinearities are apparent in the figures. Inspection of each figure allowed the nonlinear “breakpoints” to be chosen. They are indicated below in association with the appropriate nonlinear transformation relation, which relations were derived by least squares from the data appearing in Figures 1-6.

The nonlinear transformation relations, then, had the form, where  $c =$  catalogue and  $obs =$  observed:

$$(B - V)_c = +0.00268 + 1.02847(B - V)_{obs} \quad (B - V) < +0.1, \\ \pm 0.00322 \pm 0.01879$$

$$(B - V)_c = +0.00709 + 0.98474(B - V)_{obs} \quad + 0.1 < (B - V) < +1.0, \\ \pm 0.00163 \pm 0.00314$$

$$(B - V)_c = -0.00835 + 1.00688(B - V)_{obs} \quad (B - V) > +1.0, \\ \pm 0.00679 \pm 0.00518$$

$$V_c = -0.00036 - 0.01444(B - V)_c + V_{obs} \quad (B - V) < +0.1, \\ \pm 0.00379 \pm 0.02213$$

$$V_c = -0.00112 - 0.00271(B - V)_c + V_{obs} \quad + 0.1 < (B - V) < +1.0, \\ \pm 0.00163 \pm 0.00312$$

$$V_c = -0.00692 + 0.00713(B - V)_c + V_{obs} \quad (B - V) > +1.0, \\ \pm 0.00558 \pm 0.00426$$

$$(U - B)_c = -0.01701 + 0.96496(U - B)_{obs} \quad (U - B) < -0.2, \\ \pm 0.00643 \pm 0.00746$$

$$(U - B)_c = -0.00565 + 0.99602(U - B)_{obs} \quad - 0.2 < (U - B) < +0.5, \\ \pm 0.00567 \pm 0.02805$$

$$(U - B)_c = -0.02240 + 1.01788(U - B)_{obs} \quad (U - B) > +0.5, \\ \pm 0.00771 \pm 0.00565$$

$$(V - R)_c = +0.00133 + 0.96767(V - R)_{obs} \quad (V - R) < +0.1, \\ \pm 0.00073 \pm 0.00818$$

$$(V - R)_c = -0.00267 + 0.99641(V - R)_{obs} \quad + 0.1 < (V - R) < +0.5,$$

$$\pm 0.00268 \pm 0.00451$$

$$(V - R)_c = -0.00129 + 1.00502(V - R)_{obs} \quad (V - R) > +0.5, \\ \pm 0.00307 \pm 0.00432$$

$$(R - I)_c = -0.00155 + 0.99765(R - I)_{obs} \quad (R - I) < +0.1, \\ \pm 0.00125 \pm 0.01193$$

$$(R - I)_c = -0.00258 + 1.00789(R - I)_{obs} \quad + 0.1 < (R - I) < +0.5, \\ \pm 0.00155 \pm 0.00506$$

$$(R - I)_c = +0.00753 + 0.98853(R - I)_{obs} \quad (R - I) > +0.5, \\ \pm 0.00228 \pm 0.00347$$

$$(V - I)_c = -0.00116 + 0.98201(V - I)_{obs} \quad (V - I) < +0.1, \\ \pm 0.00350 \pm 0.01750$$

$$(V - I)_c = -0.00228 + 0.99807(V - I)_{obs} \quad + 0.1 < (V - I) < +1.0, \\ \pm 0.00166 \pm 0.00288$$

$$(V - I)_c = +0.00683 + 0.99628(V - I)_{obs} \quad (V - I) > +1.0. \\ \pm 0.00397 \pm 0.00291$$

Once these relations were applied to the recovered magnitudes and color indices of the standard stars used in this project, the data were on the broadband *UBVRI* photometric system defined by the standard stars in Landolt (1992). Next the now corrected for nonlinear transformation standard star magnitudes and color indices once again were compared to the published values in the sense corrected values *minus* published magnitudes and color indices. The fact that the nonlinear effects have been corrected successfully is illustrated in Figures 7-12. Hence, the data in this paper have been transformed to the photometric system defined in Landolt (1992).

Two of the stars herein (BPM 16274 and HD 49798) are too far south to be observed from

KPNO. Hence these stars were observed at the Cerro Tololo Inter-American Observatory (CTIO) as part of a standard star observational program there (Landolt 1992). The CTIO *UBVRI* data were tied into the same standard stars (Landolt 1983) as were the northern data. The data reductions were handled in the same fashion as were the KPNO reductions. Several stars on the KPNO program could be observed from both hemispheres, and this was done to further check that data from the two observatories were tied together as best as one could do.

The final magnitude and color indices for the stars in this program are tabulated in Table 4. Each star was observed an average of 35 times on 17 nights. Most of the stars' identifications were provided by the Space Telescope Science Institute (STScI) staff; a few were taken from the literature. Finding charts are provided herein via Figures 13-43.

The coordinates for the stars in Table 4 were computed by STScI staff for the equinox J2000. Proper motion terms were included where necessary.

Columns 4 - 9 in Table 4 give the final magnitude and color indices on the *UBVRI* photometric system as defined by Landolt (1992). Column 10 indicates the number of times,  $n$ , that each star was observed. Column 11 gives the number of nights,  $m$ , that each star was observed. The numbers in columns 4 - 9 are mean magnitudes and color indices. Hence, the errors tabulated in columns 12 - 17 are mean errors of the mean magnitude and color indices (see Landolt 1983, p. 450).

#### 4. Comments on Individual Stars

G 24-9: One of the program stars, G24-9, was found to be variable in light. It was reported to be quite faint (Landolt 1985), at  $V = 18.3$ , on 1985 October 7.11 UT. This observation has not been included in the averaged magnitude and color indices in Table 4. Such a large drop in brightness of some 2.6 magnitudes would point toward the occurrence of an eclipse. The observation led to G24-9's designation as V1412 Aql (Kholopov et al. 1989). Confirmation appeared in the literature (Carilli et al. 1988; Zuckerman & Becklin 1988). In addition, on other occasions, the  $V$  magnitude of G24-9 seems to show more scatter than was evidenced for other stars of similar brightness in this program. The approximate 0.25 magnitude variation otherwise observed may indicate that one component is variable in light. On the other hand, there is a faint nearby star, not visible on the acquisition monitor, and several arc seconds distant, whose relative location slowly is changing due to G24-9's large proper motion. The relatively small variations may be due to that faint star's sometime presence within the photometer's diaphragm, and at other times its exclusion.

Filippenko & Greenstein (1984) classified G24-9 as a DQ7 white dwarf. G24-9’s nearness to its optical companion means that under any circumstances it is not a good standard star anyway, especially since it has not been possible to properly calibrate G24-9.

BD+75°325: The star BD+75°325 was considered by Bartolini et al. (1982) to be a possible variable star of small amplitude, perhaps 0.03 magnitude. It has been assigned the suspected variable star name NSV 17739 (Kazarovets et al. 1998). Data taken on one night indicated the presence of a period of 0.0465116 days. However small variations on other nights did not fit that period. The data in this paper were taken on 16 nights over a period of 63 months between 1985 December 14 and 1991 March 25. No more than two or three data points were taken on any one night. The mean error of a single observation is about 0.04 magnitude, much too large for a star so bright. So, the current data agree with the short term amplitude found by Bartolini et al. (1982). What is more interesting, though, is that Bartolini et al. quote a  $V$  magnitude of 8.9 (their Table 1), whereas the current data indicate  $V = 9.548$ , in agreement with the Hipparcos value of  $V = 9.55$  (HIP 40047). On the other hand, if one reads off an average  $\Delta m$  of  $-0.06$  from their Figure 4, and applies that quantity to a  $V$  of 9.60, taken from SIMBAD, for their primary comparison star, BD+74°356, one finds  $V = 9.54$ , on average, for their measurements of BD+75°325. Therefore, overall, the star has had no long term light variation of note. The fact that both the Bartolini et al. (1982) data and the current results show a variation of three or four percent is a firm indication that the star is variable in light. And, the quoted  $V = 8.9$  either is not a  $V$  magnitude, or is a typo.

Feige 34: Feige 34 is listed by Thejll et al. (1995) as a binary based on a measured infrared flux excess.

HZ 44: The star HZ 44 has been assigned the suspected variable star designation NSV 19768 (Kazarovets et al. 1998) apparently on the basis on one discrepant measurement (Kilkenny 1977). The data herein in Table 4 indicate that HZ 44 is constant in light at the level of the accuracy quoted. Ulla & Thejll (1998) list HZ 44 as a suspected binary based on a measured infrared flux excess, but note the possibility of a filter wheel problem.

BD+17°4708: This star long has been used as a primary spectrophotometric standard star (Oke & Gunn 1983). Lu et al. (1987) showed, via speckle observations, that BD+17°4708 = G 126-62 is an astrometric binary with a period of 29.6 years.

BD+33°2642: A long used spectrophotometric standard star surrounded by a faint planetary nebula (Napiwotzki 1993). The star also exhibits radial velocity variations (Napiwotzki et al. 2001; De Marco et al. 2004).

BD+26°2606: This star long has been used as a primary spectrophotometric standard



star (Oke & Gunn 1983). Carney & Latham (1987) showed that BD+26°2606 = G 166-45 was a double lined spectroscopic binary. It also is a high proper motion star (Perryman et al. 1997, and see Volume 8 of the Hipparcos Catalogue). The Hipparcos Catalogue shows a range in brightness of 0.1 magnitude. The present data indicate that the error of a single observation is  $0.0045 \times 6 = 0.027$  magnitude, a bit larger than one might expect for so bright a star.

BD+28°4211: Massey & Gronwall (1990) reported that this star, long used as a spectrophotometric standard, had a companion at position angle  $240^\circ$  and with a separation of  $2.8''$ . Ulla & Thejll (1998) list BD+28°4211 as a suspected binary based on a measured infrared flux excess.

Feige 110: The star Feige 110 has been assigned the suspected variable star number NSV 14503 (Kazarovets et al. 1998) apparently on the basis of the  $V$  magnitude discrepancy found by Graham (1969) between his and those belonging to Eggen & Greenstein (1965) (11.81 versus 11.50, respectively). The  $V$  magnitude of 11.832 reported herein in Table 4 agrees with Graham (1969). Furthermore, the small error indicated in Table 4 emphasizes that Feige 110 is constant in light. Ulla & Thejll (1998) list this star as a suspected binary based on a measured infrared flux excess, but note the possibility of a filter wheel problem.

HD 49798: Finally, a few comments on the star HD 49798 = UCAC2 12836082 [ $\alpha = 06^h48^m04.7^s$ ;  $\delta = -44^\circ18'58.4''$ ; 2000.0;  $\mu_\alpha = -4.9$  mas/yr,  $\mu_\delta = +7.6$  mas/yr, all from UCAC2]. It had been included in the list of spectrophotometric standard stars for which  $UBVRI$  photometry was desirable for HST needs, but was too bright to be included in the main observational program. Hence HD 49798 was observed on several nights at a CTIO 0.4-m telescope, and at the 0.61-m Lowell telescope located at CTIO. A total of six measures were made on five different nights, resulting in  $V = 8.287 \pm 0.0024$ ,  $(B - V) = -0.270 \pm 0.0024$ ,  $(U - B) = -1.259 \pm 0.0029$ ,  $(V - R) = -0.104 \pm 0.0012$ ,  $(R - I) = -0.149 \pm 0.0020$ , and  $(V - I) = -0.256 \pm 0.0012$ . The errors again are mean errors of the mean.

It is a pleasure to thank the staffs of KPNO and CTIO for their hospitality and assistance. Helpful comments on drafts of this paper were made by Drs. John A. Graham and Philip Massey. AUL is most indebted to Dr. David A. Turnshek and his then colleagues at STScI, and to Dr. Ralph C. Bohlin of the STScI for the finding charts and for their support and consultation throughout the project. Thanks go to Dr. T. Kinman who verified certain instrumental characteristics during the late stages of the preparation of this paper. B. Skiff updated AUL with techniques to ensure that the coordinates and proper motions are modern and accurate. Drs. Howard Bond and Jay Holberg provided suggestions regarding spectral types. The appearance of this paper's Figures and Tables is due to the skills of James

L. Clem and Karen Richard, to whom AUL is very grateful. This observational program has been supported by grants to AUL from the Air Force Office of Scientific Research (AFOSR) grant no. 82-0192, by STScI grant no. CW-0004-85, and by NSF grants AST 9114457 and 0503871.

### A. Appendix I

Knowledge of the sensitivity of a photomultiplier (any detector, for that matter) as a function of wavelength, as well as the transmission characteristics of the filters used in a photometric program is needed for the theoretical modeling of a photometric system. Unfortunately, such information never was available or obtainable for the RCA 31034A-02 (KPNO no. H 18862) used to obtain the data described in this paper. Such information for that brand photomultiplier may be found in Landolt (1992) [ Please consult Table 11 and Figures 51 - 54, therein.].

On the other hand, the transmission characteristics of the KPNO “J” *UBVRI* filter set were measured at KPNO by Mr. Ed Carder, using a Lambda 9 Spectrophotometer. He used a slit that gave a resolution of 10 Angstroms. Tables 5-9 provide the measured transmission characteristics of the *UBVRI* filters in the KPNO “J” filter set. Figures 44-48 illustrate the transmission characteristics for the KPNO “J” filter set.

### B. Appendix II

Observational programs sometimes demand the best available coordinate and motion information for standard stars. Table 10 provides the most recent coordinates and proper motions for the program stars in Table 4. All coordinates are for the epoch J2000. The 2MASS-PSC positions come from The Two Micron All Sky Survey (2MASS) (Skrutskie et al. 2006). The UCAC2 positions came from The Second US Naval Observatory CCD Astrograph Catalogue (UCAC2) (Zacharias et al. 2004). Representative spectral types are listed in Table 10. The literature sources for these spectral types appear in the last column.

## REFERENCES

Bartolini, C., Bonifazi, A., Pecci, F. F., Oculi, L., Piccioni, A., Serra, R., & Dantona, F. 1982, *Ap&SS*, 83, 287

- Bessell, M. S. 1979, *PASP*, 91, 589
- Bohlin, R. C., Harris, A. W., Holm, A. V., & Gry, C. 1990, *ApJS*, 73, 413
- Carney, B. W., & Latham, D. W. 1987, *AJ*, 93, 116
- Carilli, C., Conner, S., & Green, D. W. E. 1988, *IAU Circ.*, 4648, 2
- De Marco, O., Bond, H. E., Harmer, D., & Fleming, A. J. 2004, *ApJ*, 602, L93
- Eggen, O. J., & Greenstein, J. L. 1965, *ApJ*, 141, 83
- Filippenko, A., & Greenstein, J. L. 1984, *PASP*, 96, 530
- Graham, J. A. 1969, in *Low-Luminosity Stars*, S. S. Kumar, Editor, (Gordon & Breach: New York), 139
- Hanson, R. B., Klemola, A. R., Jones, B. F., & Monet, D. G. 2004, *AJ*, 128, 1430
- Kazarovets, E. V., Samus, N. N., & Durlevich, O. V. 1998, *Informational Bulletin on Variable Stars*, 4655, 1
- Kholopov, P. N., Samus, N. N., Kazarovets, B. V., Frolov, M. S., & Kireeva, N. N. 1989, *Informational Bulletin on Variable Stars*, 3323, 1
- Kilkenny, D. 1977, *MNRAS*, 181, 611
- Klemola, A. R., Jones, B. F., & Hanson, R. B. 1987, *AJ*, 94, 501
- Landolt, A. U. 1967, *AJ*, 72, 1012
- Landolt, A. U. 1973, *AJ*, 78, 959
- Landolt, A. U. 1983, *AJ*, 88, 439
- Landolt, A. U. 1985, *IAU Circ.*, 4125, 2
- Landolt, A. U. 1992, *AJ*, 104, 340
- Landolt, A. U. 2007, *The Future of Photometric, Spectrophotometric, and Polarimetric Standardization*, C. Sterken, Editor, *ASP Conference Series*, in press
- Lu, P. K., Demarque, P., van Alena, W., McAlister, H., & Hartkopf, W. 1987, *AJ*, 94, 1318
- Massey, P., & Gronwall, C. 1990, *ApJ*, 358, 344

- McCook, G. P., & Sion, E. M. 2006, <http://www.astronomy.villanova.edu/WDCatalog/index.html>
- Monet, D. G., et al. 2003, *AJ*, 125, 984
- Napiwotzki, R. 1993, *Acta Astronomica*, 43, 415
- Napiwotzki, R., Herrmann, M., Heber, U., & Altmann, M. 2001, *Post-AGB Objects as a Phase of Stellar Evolution*, ed. R. Szczerba & S. K. Gorny (Dordrecht: Kluwer), 277
- Oke, J. B. 1990, *AJ*, 99, 1621
- Oke, J. B., & Gunn, J. E. 1983, *ApJ*, 266, 713
- Perryman, M. A. C., et al. 1997, *A&A*, 323, L49
- Roman, N. G. 1955, *ApJS*, 2, 195
- Schulte, D., & Crawford, D. L., 1961, *Kitt Peak National Observatory Contribution No. 10*
- Skrutskie, M. F., et al. 2006, *AJ*, 131, 1163
- Thejll, P., Ulla, A., & MacDonald, J. 1995, *A&A*, 303, 773
- Turnshek, D. A., Bohlin, R. C., Williamson, R. L., II, Lupie, O. L., Koornneef, J., & Morgan, D. H. 1990, *AJ*, 99, 1243
- Ulla, A., & Thejll, P. 1998, *A&AS*, 132, 1
- Urban, S. E., Zacharias, N., & Wycoff, G. L. 2004, *VizieR Online Data Catalog*, 1294, 0
- Zacharias, N., Urban, S. E., Zacharias, M. I., Wycoff, G. L., Hall, D. M., Monet, D. G., & Rafferty, T. J. 2004, *AJ*, 127, 3043
- Zuckerman, B., & Becklin, E. 1988, *IAU Circ.*, 4652, 3

Table 1. KPNO *UBVRI* Filter Set J

<i>V</i>	2mm GG 495 + 1mm BG 18
<i>B</i>	1mm BG 12 + 2mm GG 385 + 1mm BG 18
<i>U</i>	1mm UG 2 + CuSO <sub>4</sub>
<i>R</i>	2mm OG 570 + 2mm KG 3
<i>I</i>	3mm RGN 9

Table 2. Extinction at Kitt Peak

Magnitude or Color Index	Coefficient Symbol	Average Coefficient Value	Range in Values
<i>V</i>	$Q_y$	+0.162	+0.081 to +0.256
<i>B</i> – <i>V</i>	$k_1$	+0.119	+0.046 to +0.223
	$k_2$	–0.020	–0.042 to +0.000
<i>U</i> – <i>B</i>	$k_3$	+0.341	+0.267 to +0.463
	$k_4$	–0.013	–0.042 to +0.018
<i>V</i> – <i>R</i>	$k_5$	+0.043	+0.021 to +0.082
	$k_6$	–0.003	–0.038 to +0.017
<i>R</i> – <i>I</i>	$k_7$	+0.044	–0.003 to +0.074
	$k_8$	+0.004	–0.010 to +0.017
<i>V</i> – <i>I</i>	$k_9$	+0.087	+0.047 to +0.127
	$k_{10}$	+0.001	–0.028 to +0.014

Table 3. Extinction at Kitt Peak at Three Epochs

Magnitude or Color Index	Coefficient Symbol	1967	1969-1972	1985-1991
$V$	$Q_y$	$+0.171 \pm 0.016$	$+0.150$	$+0.162 \pm 0.040$
$B - V$	$k_1$	$+0.085 \pm 0.008$	$+0.080$	$+0.119 \pm 0.028$
	$k_2$	$-0.029 \pm 0.002$	$-0.030$	$-0.020 \pm 0.009$
$U - B$	$k_3$	$+0.326 \pm 0.025$	$+0.340$	$+0.341 \pm 0.037$
	$k_4$	$-0.020 \pm 0.005$	$-0.020$	$-0.013 \pm 0.014$

Table 4. *UBVRI* Photometry of Spectrophotometric Standard Stars

Star	$\alpha$ (2000)		$\delta$	<i>V</i>	<i>B</i> - <i>V</i>	<i>U</i> - <i>B</i>	<i>V</i> - <i>R</i>	<i>R</i> - <i>I</i>	<i>V</i> - <i>I</i>	<i>n</i>	<i>m</i>	<i>V</i>	Mean Error of the Mean					
	h	m											s	°	'	"	<i>B</i> - <i>V</i>	<i>U</i> - <i>B</i>
G158 100	00	33	54	-12	07	57	14.891	+0.681	-0.061	+0.424	+0.418	+0.840	0.0021	0.0047	0.0059	0.0030	0.0063	0.0068
BPM 16274	00	50	03	-52	08	17	14.206	-0.049	-0.803	-0.104	-0.119	-0.222	0.0016	0.0025	0.0043	0.0028	0.0074	0.0081
HZ 4	03	55	22	+09	47	19	14.506	+0.086	-0.675	-0.074	-0.060	-0.136	0.0028	0.0015	0.0028	0.0020	0.0042	0.0046
LB 227	04	09	29	+17	07	54	15.323	+0.055	-0.718	-0.085	-0.108	-0.192	0.0035	0.0032	0.0034	0.0042	0.0131	0.0143
HZ 2	04	12	44	+11	51	50	13.877	-0.090	-0.884	-0.107	-0.111	-0.217	0.0014	0.0015	0.0029	0.0017	0.0024	0.0024
G191 B2B	05	05	31	+52	49	54	11.781	-0.326	-1.205	-0.149	-0.181	-0.327	0.0023	0.0014	0.0026	0.0016	0.0017	0.0025
G193 74	07	53	27	+52	29	36	15.674	+0.256	-0.563	+0.163	+0.161	+0.324	0.0055	0.0037	0.0039	0.0055	0.0064	0.0094
BD+75°325	08	10	49	+74	57	58	9.548	-0.334	-1.212	-0.150	-0.187	-0.336	0.0018	0.0010	0.0020	0.0008	0.0018	0.0018
LDS 235B	08	47	32	-18	59	36	15.682	-0.118	-0.957	-0.100	-0.120	-0.219	0.0064	0.0057	0.0068	0.0091	0.0304	0.0335
AGK+81°266	09	21	19	+81	43	29	11.936	-0.340	-1.204	-0.154	-0.191	-0.345	0.0024	0.0013	0.0030	0.0013	0.0021	0.0019
F 34	10	39	37	+43	06	10	11.181	-0.343	-1.225	-0.138	-0.144	-0.283	0.0025	0.0011	0.0041	0.0013	0.0018	0.0018
GD 140	11	37	06	+29	47	59	12.492	-0.086	-0.936	-0.106	-0.114	-0.222	0.0024	0.0013	0.0038	0.0013	0.0025	0.0028
HZ 21	12	13	56	+32	56	31	14.688	-0.327	-1.236	-0.149	-0.201	-0.350	0.0022	0.0016	0.0033	0.0022	0.0043	0.0049
F 66	12	37	24	+25	04	00	10.509	-0.289	-1.103	-0.133	-0.166	-0.300	0.0025	0.0012	0.0036	0.0008	0.0013	0.0015
F 67	12	41	52	+17	31	20	11.822	-0.343	-1.218	-0.147	-0.190	-0.337	0.0025	0.0012	0.0043	0.0010	0.0017	0.0018
G60 54	13	00	10	+03	28	56	15.808	+0.644	-0.096	+0.379	+0.385	+0.764	0.0027	0.0040	0.0063	0.0027	0.0067	0.0060
HZ 44	13	23	35	+36	08	00	11.673	-0.291	-1.196	-0.141	-0.181	-0.322	0.0016	0.0011	0.0027	0.0009	0.0011	0.0014
GRW+70°5824	13	38	52	+70	17	08	12.773	-0.091	-0.875	-0.100	-0.104	-0.206	0.0027	0.0017	0.0022	0.0013	0.0017	0.0020
BD+26°2606	14	49	02	+25	42	26	9.714	+0.438	-0.242	+0.296	+0.308	+0.605	0.0025	0.0022	0.0030	0.0008	0.0037	0.0035
GD 190	15	44	19	+18	06	49	14.677	-0.121	-1.019	-0.090	-0.079	-0.172	0.0045	0.0022	0.0052	0.0022	0.0040	0.0040
BD+33°2642	15	52	00	+32	56	55	10.828	-0.166	-0.856	-0.056	-0.076	-0.133	0.0020	0.0020	0.0043	0.0009	0.0009	0.0011
G138 31	16	27	54	+09	12	24	16.117	+0.358	-0.467	+0.218	+0.216	+0.434	0.0061	0.0069	0.0057	0.0071	0.0098	0.0128
G24 9	20	13	56	+06	42	55	15.751	+0.425	-0.443	+0.275	+0.223	+0.503	0.0129	0.0122	0.0067	0.0089	0.0134	0.0163
LDS 749B	21	32	16	+00	15	14	14.674	-0.040	-0.917	-0.001	+0.001	-0.002	0.0020	0.0018	0.0036	0.0027	0.0041	0.0053
L930 80	21	47	36	-07	44	07	14.804	-0.084	-0.968	-0.036	-0.045	-0.085	0.0027	0.0027	0.0023	0.0020	0.0064	0.0070
BD+28°4211	21	51	11	+28	51	52	10.509	-0.341	-1.246	-0.147	-0.176	-0.322	0.0027	0.0018	0.0039	0.0011	0.0012	0.0018
BD+17°4708	22	11	31	+18	05	32	9.464	+0.443	-0.183	+0.298	+0.320	+0.618	0.0026	0.0015	0.0021	0.0011	0.0009	0.0013
NGC 7293	22	29	38	-20	50	13	13.524	-0.366	-1.264	-0.165	-0.210	-0.374	0.0021	0.0021	0.0033	0.0021	0.0040	0.0046
F 110	23	19	58	-05	09	56	11.832	-0.305	-1.167	-0.138	-0.180	-0.313	0.0018	0.0010	0.0033	0.0012	0.0022	0.0020
LTT 9491	23	19	35	-17	05	30	14.111	+0.021	-0.853	+0.041	+0.020	+0.062	0.0028	0.0028	0.0030	0.0036	0.0070	0.0104
GD 248	23	26	07	+16	00	21	15.112	+0.094	-0.775	+0.078	+0.055	+0.135	0.0028	0.0026	0.0050	0.0030	0.0061	0.0059

Table 5. Transmission characteristics of the  $U$  filter in KPNO's  $UBVRI$  filter set J

$\lambda$	% T	$\lambda$	% T	$\lambda$	% T	$\lambda$	% T	$\lambda$	% T
3000	10.495	3260	58.085	3520	77.045	3780	69.440	4040	4.785
3010	12.090	3270	59.380	3530	77.320	3790	67.845	4050	3.785
3020	13.805	3280	60.665	3540	77.640	3800	66.085	4060	2.980
3030	15.530	3290	61.890	3550	77.805	3810	64.185	4070	2.315
3040	17.360	3300	63.010	3560	78.005	3820	62.125	4080	1.790
3050	19.300	3310	64.110	3570	78.185	3830	59.920	4090	1.365
3060	21.225	3320	65.060	3580	78.305	3840	57.460	4100	1.030
3070	23.250	3330	66.060	3590	78.435	3850	54.860	4110	0.770
3080	25.270	3340	67.025	3600	78.500	3860	52.220	4120	0.575
3090	27.315	3350	67.915	3610	78.490	3870	49.295	4130	0.430
3100	29.405	3360	68.710	3620	78.485	3880	46.240	4140	0.320
3110	31.490	3370	69.445	3630	78.400	3890	43.075	4150	0.235
3120	33.545	3380	70.175	3640	78.370	3900	39.745	4160	0.170
3130	35.595	3390	70.880	3650	78.255	3910	36.420	4170	0.125
3140	37.660	3400	71.465	3660	78.015	3920	33.115	4180	0.090
3150	39.615	3410	72.125	3670	77.860	3930	29.835	4190	0.065
3160	41.540	3420	72.770	3680	77.490	3940	26.605	4200	0.045
3170	43.425	3430	73.290	3690	77.060	3950	23.480	4210	0.035
3180	45.260	3440	73.860	3700	76.635	3960	20.575	4220	0.025
3190	47.085	3450	74.370	3710	76.175	3970	17.820	4230	0.015
3200	48.885	3460	74.805	3720	75.570	3980	15.260	4240	0.015
3210	50.630	3470	75.210	3730	74.790	3990	12.935	4250	0.010
3220	52.190	3480	75.610	3740	73.865	4000	10.805		
3230	53.770	3490	76.015	3750	72.980	4010	8.950		
3240	55.265	3500	76.395	3760	71.880	4020	7.345		
3250	56.675	3510	76.720	3770	70.800	4030	5.960		



Table 6. Transmission characteristics of the  $B$  filter in KPNO's  $UBVRI$  filter set J

$\lambda$	% T	$\lambda$	% T	$\lambda$	% T	$\lambda$	% T	$\lambda$	% T
3520	0.000	4100	51.560	4680	49.205	5260	1.830	5840	0.100
3530	0.010	4110	52.030	4690	48.175	5270	1.655	5850	0.085
3540	0.030	4120	52.505	4700	47.140	5280	1.495	5860	0.070
3550	0.065	4130	52.930	4710	46.030	5290	1.360	5870	0.055
3560	0.125	4140	53.380	4720	44.925	5300	1.245	5880	0.050
3570	0.220	4150	53.760	4730	43.765	5310	1.140	5890	0.040
3580	0.360	4160	54.150	4740	42.575	5320	1.055	5900	0.035
3590	0.565	4170	54.580	4750	41.390	5330	0.980	5910	0.030
3600	0.850	4180	54.965	4760	40.185	5340	0.925	5920	0.035
3610	1.230	4190	55.315	4770	38.965	5350	0.875	5930	0.030
3620	1.700	4200	55.665	4780	37.780	5360	0.830	5940	0.030
3630	2.270	4210	55.965	4790	36.520	5370	0.805	5950	0.025
3640	2.950	4220	56.330	4800	35.235	5380	0.775	5960	0.025
3650	3.745	4230	56.525	4810	33.935	5390	0.760	5970	0.030
3660	4.650	4240	56.810	4820	32.620	5400	0.745	5980	0.030
3670	5.645	4250	56.985	4830	31.300	5410	0.740	5990	0.030
3680	6.720	4260	57.200	4840	30.015	5420	0.740	6000	0.030
3690	7.900	4270	57.370	4850	28.710	5430	0.745	6010	0.030
3700	9.165	4280	57.595	4860	27.490	5440	0.760	6020	0.030
3710	10.475	4290	57.730	4870	26.305	5450	0.775	6030	0.030
3720	11.820	4300	57.885	4880	25.110	5460	0.810	6040	0.030
3730	13.255	4310	58.005	4890	23.995	5470	0.845	6050	0.030
3740	14.635	4320	58.175	4900	22.875	5480	0.890	6060	0.030
3750	16.120	4330	58.255	4910	21.845	5490	0.940	6070	0.030
3760	17.535	4340	58.335	4920	20.835	5500	1.000	6080	0.030
3770	18.990	4350	58.435	4930	19.890	5510	1.065	6090	0.030
3780	20.410	4360	58.470	4940	19.020	5520	1.140	6100	0.030
3790	21.905	4370	58.530	4950	18.195	5530	1.220	6110	0.025
3800	23.375	4380	58.610	4960	17.440	5540	1.290	6120	0.025
3810	24.805	4390	58.630	4970	16.735	5550	1.360	6130	0.025
3820	26.170	4400	58.655	4980	16.040	5560	1.420	6140	0.025
3830	27.520	4410	58.700	4990	15.370	5570	1.475	6150	0.025
3840	28.865	4420	58.700	5000	14.680	5580	1.515	6160	0.020
3850	30.180	4430	58.655	5010	13.970	5590	1.540	6170	0.020
3860	31.440	4440	58.655	5020	13.230	5600	1.550	6180	0.020
3870	32.690	4450	58.545	5030	12.460	5610	1.540	6190	0.020
3880	33.885	4460	58.390	5040	11.670	5620	1.520	6200	0.015

Table 6—Continued

$\lambda$	% T	$\lambda$	% T	$\lambda$	% T	$\lambda$	% T	$\lambda$	% T
3890	35.025	4470	58.295	5050	10.890	5630	1.490	6210	0.015
3900	36.180	4480	58.075	5060	10.130	5640	1.445	6220	0.015
3910	37.340	4490	57.875	5070	9.415	5650	1.390	6230	0.015
3920	38.325	4500	57.725	5080	8.745	5660	1.320	6240	0.015
3930	39.345	4510	57.495	5090	8.120	5670	1.245	6250	0.015
3940	40.320	4520	57.320	5100	7.560	5680	1.160	6260	0.015
3950	41.295	4530	57.120	5110	7.020	5690	1.070	6270	0.010
3960	42.180	4540	56.880	5120	6.535	5700	0.980	6280	0.010
3970	43.045	4550	56.650	5130	6.080	5710	0.885	6290	0.010
3980	43.880	4560	56.380	5140	5.645	5720	0.790	6300	0.005
3990	44.650	4570	56.040	5150	5.220	5730	0.705	6310	0.010
4000	45.420	4580	55.655	5160	4.810	5740	0.610	6320	0.005
4010	46.160	4590	55.275	5170	4.425	5750	0.530	6330	0.005
4020	46.805	4600	54.840	5180	4.050	5760	0.455	6340	0.005
4030	47.515	4610	54.350	5190	3.705	5770	0.385	6350	0.005
4040	48.140	4620	53.790	5200	3.365	5780	0.325	6360	0.005
4050	48.785	4630	53.220	5210	3.050	5790	0.275	6370	0.000
4060	49.375	4640	52.565	5220	2.760	5800	0.230	6380	0.000
4070	49.980	4650	51.830	5230	2.495	5810	0.185	6390	0.000
4080	50.505	4660	51.025	5240	2.245	5820	0.150	6400	0.000
4090	51.035	4670	50.135	5250	2.030	5830	0.125		

Table 7. Transmission characteristics of the  $V$  filter in KPNO's  $UBVRI$  filter set J

$\lambda$	% T	$\lambda$	% T	$\lambda$	% T	$\lambda$	% T	$\lambda$	% T
4500	0.025	5100	76.505	5700	66.865	6300	19.130	6900	1.310
4510	0.030	5110	77.025	5710	66.260	6310	18.525	6910	1.230
4520	0.035	5120	77.525	5720	65.565	6320	17.920	6920	1.165
4530	0.040	5130	77.950	5730	64.870	6330	17.320	6930	1.100
4540	0.045	5140	78.375	5740	64.170	6340	16.735	6940	1.045
4550	0.050	5150	78.755	5750	63.430	6350	16.145	6950	0.975
4560	0.060	5160	78.990	5760	62.750	6360	15.590	6960	0.930
4570	0.065	5170	79.315	5770	61.980	6370	15.045	6970	0.880
4580	0.070	5180	79.560	5780	61.280	6380	14.505	6980	0.835
4590	0.080	5190	79.790	5790	60.470	6390	13.985	6990	0.785
4600	0.090	5200	79.970	5800	59.725	6400	13.490	7000	0.740
4610	0.105	5210	80.115	5810	58.925	6410	13.000	7010	0.695
4620	0.115	5220	80.275	5820	58.185	6420	12.520	7020	0.650
4630	0.130	5230	80.395	5830	57.350	6430	12.045	7030	0.620
4640	0.150	5240	80.505	5840	56.505	6440	11.585	7040	0.585
4650	0.180	5250	80.555	5850	55.690	6450	11.150	7050	0.550
4660	0.215	5260	80.595	5860	54.835	6460	10.740	7060	0.520
4670	0.260	5270	80.625	5870	54.045	6470	10.315	7070	0.490
4680	0.330	5280	80.635	5880	53.225	6480	9.900	7080	0.455
4690	0.420	5290	80.625	5890	52.365	6490	9.510	7090	0.435
4700	0.540	5300	80.565	5900	51.460	6500	9.125	7100	0.410
4710	0.700	5310	80.525	5910	50.635	6510	8.760	7110	0.390
4720	0.930	5320	80.485	5920	49.760	6520	8.405	7120	0.360
4730	1.235	5330	80.395	5930	48.880	6530	8.045	7130	0.345
4740	1.645	5340	80.350	5940	47.990	6540	7.705	7140	0.325
4750	2.190	5350	80.200	5950	47.165	6550	7.390	7150	0.295
4760	2.900	5360	80.075	5960	46.260	6560	7.095	7160	0.280
4770	3.820	5370	79.980	5970	45.355	6570	6.770	7170	0.270
4780	4.975	5380	79.835	5980	44.495	6580	6.490	7180	0.250
4790	6.400	5390	79.670	5990	43.620	6590	6.210	7190	0.240
4800	8.120	5400	79.465	6000	42.725	6600	5.940	7200	0.220
4810	10.190	5410	79.270	6010	41.870	6610	5.660	7210	0.210
4820	12.595	5420	79.105	6020	40.985	6620	5.420	7220	0.195
4830	15.300	5430	78.850	6030	40.105	6630	5.165	7230	0.180
4840	18.310	5440	78.610	6040	39.205	6640	4.935	7240	0.175
4850	21.550	5450	78.335	6050	38.360	6650	4.720	7250	0.160
4860	25.000	5460	78.150	6060	37.485	6660	4.490	7260	0.155

Table 7—Continued

$\lambda$	% T	$\lambda$	% T	$\lambda$	% T	$\lambda$	% T	$\lambda$	% T
4870	28.500	5470	77.820	6070	36.645	6670	4.290	7270	0.145
4880	32.140	5480	77.495	6080	35.755	6680	4.095	7280	0.135
4890	35.775	5490	77.180	6090	34.945	6690	3.915	7290	0.125
4900	39.375	5500	76.905	6100	34.070	6700	3.705	7300	0.120
4910	42.895	5510	76.520	6110	33.220	6710	3.535	7310	0.115
4920	46.245	5520	76.180	6120	32.415	6720	3.365	7320	0.105
4930	49.445	5530	75.725	6130	31.555	6730	3.190	7330	0.100
4940	52.435	5540	75.330	6140	30.730	6740	3.050	7340	0.090
4950	55.215	5550	74.995	6150	29.930	6750	2.895	7350	0.085
4960	57.735	5560	74.535	6160	29.150	6760	2.750	7360	0.080
4970	60.060	5570	74.100	6170	28.370	6770	2.610	7370	0.080
4980	62.215	5580	73.605	6180	27.595	6780	2.480	7380	0.070
4990	64.160	5590	73.135	6190	26.845	6790	2.355	7390	0.070
5000	65.935	5600	72.620	6200	26.085	6800	2.245	7400	0.060
5010	67.565	5610	72.165	6210	25.315	6810	2.120	7410	0.055
5020	69.055	5620	71.620	6220	24.590	6820	2.010	7420	0.055
5030	70.320	5630	71.100	6230	23.850	6830	1.910	7430	0.050
5040	71.510	5640	70.530	6240	23.155	6840	1.805	7440	0.050
5050	72.590	5650	69.925	6250	22.440	6850	1.715	7450	0.045
5060	73.535	5660	69.430	6260	21.755	6860	1.625	7460	0.045
5070	74.415	5670	68.775	6270	21.095	6870	1.540	7470	0.040
5080	75.170	5680	68.180	6280	20.425	6880	1.460		
5090	75.840	5690	67.485	6290	19.775	6890	1.380		

Table 8. Transmission characteristics of the  $R$  filter in KPNO's  $UBVRI$  filter set J

$\lambda$	% T	$\lambda$	% T	$\lambda$	% T	$\lambda$	% T	$\lambda$	% T
5470	0.000	6440	71.125	7410	32.765	8380	5.770	9350	0.640
5480	0.005	6450	70.895	7420	32.310	8390	5.690	9360	0.610
5490	0.015	6460	70.550	7430	31.880	8400	5.525	9370	0.590
5500	0.030	6470	70.310	7440	31.500	8410	5.455	9380	0.580
5510	0.065	6480	69.935	7450	31.035	8420	5.300	9390	0.600
5520	0.130	6490	69.650	7460	30.690	8430	5.195	9400	0.545
5530	0.250	6500	69.465	7470	30.270	8440	5.085	9410	0.530
5540	0.450	6510	69.115	7480	29.920	8450	4.940	9420	0.545
5550	0.795	6520	68.790	7490	29.540	8460	4.815	9430	0.475
5560	1.340	6530	68.485	7500	29.095	8470	4.760	9440	0.495
5570	2.155	6540	68.145	7510	28.645	8480	4.675	9450	0.475
5580	3.335	6550	67.815	7520	28.295	8490	4.565	9460	0.460
5590	4.960	6560	67.555	7530	27.940	8500	4.455	9470	0.455
5600	7.100	6570	67.190	7540	27.510	8510	4.380	9480	0.500
5610	9.740	6580	66.880	7550	27.125	8520	4.300	9490	0.440
5620	12.870	6590	66.620	7560	26.750	8530	4.180	9500	0.405
5630	16.470	6600	66.230	7570	26.350	8540	4.050	9510	0.480
5640	20.380	6610	65.895	7580	25.995	8550	3.945	9520	0.415
5650	24.555	6620	65.595	7590	25.665	8560	3.920	9530	0.405
5660	28.910	6630	65.255	7600	25.250	8570	3.755	9540	0.405
5670	33.210	6640	64.905	7610	24.950	8580	3.725	9550	0.380
5680	37.530	6650	64.565	7620	24.500	8590	3.550	9560	0.375
5690	41.675	6660	64.220	7630	24.110	8600	3.560	9570	0.385
5700	45.520	6670	63.860	7640	23.735	8610	3.610	9580	0.370
5710	49.305	6680	63.565	7650	23.445	8620	3.515	9590	0.330
5720	52.730	6690	63.230	7660	23.005	8630	3.435	9600	0.335
5730	55.855	6700	62.880	7670	22.675	8640	3.420	9610	0.325
5740	58.705	6710	62.585	7680	22.360	8650	3.345	9620	0.380
5750	61.245	6720	62.120	7690	22.010	8660	3.215	9630	0.275
5760	63.540	6730	61.755	7700	21.620	8670	3.105	9640	0.350
5770	65.590	6740	61.445	7710	21.320	8680	3.080	9650	0.310
5780	67.455	6750	60.990	7720	21.000	8690	3.040	9660	0.290
5790	69.010	6760	60.650	7730	20.645	8700	2.940	9670	0.295
5800	70.365	6770	60.285	7740	20.250	8710	2.875	9680	0.305
5810	71.680	6780	59.860	7750	19.960	8720	2.750	9690	0.260
5820	72.800	6790	59.455	7760	19.610	8730	2.740	9700	0.300
5830	73.760	6800	59.090	7770	19.280	8740	2.675	9710	0.280

Table 8—Continued

$\lambda$	% T	$\lambda$	% T	$\lambda$	% T	$\lambda$	% T	$\lambda$	% T
5840	74.550	6810	58.645	7780	18.990	8750	2.575	9720	0.265
5850	75.365	6820	58.210	7790	18.645	8760	2.550	9730	0.225
5860	75.935	6830	57.810	7800	18.360	8770	2.485	9740	0.250
5870	76.505	6840	57.385	7810	18.080	8780	2.410	9750	0.270
5880	77.005	6850	57.015	7820	17.720	8790	2.375	9760	0.210
5890	77.380	6860	56.550	7830	17.440	8800	2.320	9770	0.230
5900	77.750	6870	56.100	7840	17.140	8810	2.240	9780	0.200
5910	78.050	6880	55.755	7850	16.840	8820	2.200	9790	0.240
5920	78.290	6890	55.285	7860	16.505	8830	2.135	9800	0.240
5930	78.465	6900	54.880	7870	16.250	8840	2.100	9810	0.165
5940	78.665	6910	54.420	7880	15.995	8850	2.030	9820	0.190
5950	78.815	6920	54.015	7890	15.630	8860	2.010	9830	0.245
5960	78.990	6930	53.525	7900	15.330	8870	1.975	9840	0.220
5970	78.995	6940	53.125	7910	15.095	8880	1.910	9850	0.175
5980	79.070	6950	52.640	7920	14.855	8890	1.870	9860	0.190
5990	79.120	6960	52.200	7930	14.565	8900	1.830	9870	0.170
6000	79.110	6970	51.765	7940	14.270	8910	1.795	9880	0.190
6010	79.110	6980	51.295	7950	14.035	8920	1.755	9890	0.170
6020	79.175	6990	50.940	7960	13.840	8930	1.725	9900	0.150
6030	79.105	7000	50.470	7970	13.605	8940	1.645	9910	0.205
6040	79.045	7010	50.055	7980	13.250	8950	1.635	9920	0.185
6050	79.000	7020	49.560	7990	13.020	8960	1.590	9930	0.150
6060	78.910	7030	49.210	8000	12.780	8970	1.535	9940	0.130
6070	78.875	7040	48.700	8010	12.535	8980	1.520	9950	0.185
6080	78.700	7050	48.225	8020	12.345	8990	1.500	9960	0.135
6090	78.720	7060	47.795	8030	12.060	9000	1.450	9970	0.210
6100	78.540	7070	47.345	8040	11.815	9010	1.410	9980	0.165
6110	78.420	7080	46.870	8050	11.545	9020	1.335	9990	0.160
6120	78.365	7090	46.445	8060	11.355	9030	1.335	10000	0.145
6130	78.140	7100	46.030	8070	11.170	9040	1.305	10010	0.130
6140	77.995	7110	45.605	8080	10.970	9050	1.325	10020	0.115
6150	77.810	7120	45.165	8090	10.720	9060	1.270	10030	0.150
6160	77.670	7130	44.730	8100	10.515	9070	1.165	10040	0.100
6170	77.485	7140	44.280	8110	10.245	9080	1.190	10050	0.125
6180	77.310	7150	43.865	8120	10.085	9090	1.145	10060	0.085
6190	77.155	7160	43.400	8130	9.890	9100	1.115	10070	0.115
6200	76.995	7170	42.975	8140	9.690	9110	1.120	10080	0.120

Table 8—Continued

$\lambda$	% T	$\lambda$	% T	$\lambda$	% T	$\lambda$	% T	$\lambda$	% T
6210	76.835	7180	42.520	8150	9.485	9120	1.100	10090	0.090
6220	76.560	7190	42.100	8160	9.305	9130	1.070	10100	0.090
6230	76.325	7200	41.675	8170	9.115	9140	1.000	10110	0.145
6240	76.160	7210	41.230	8180	8.925	9150	1.020	10120	0.025
6250	75.925	7220	40.855	8190	8.690	9160	0.955	10130	0.065
6260	75.695	7230	40.295	8200	8.595	9170	0.950	10140	0.090
6270	75.460	7240	39.890	8210	8.390	9180	0.920	10150	0.165
6280	75.275	7250	39.490	8220	8.190	9190	0.895	10160	0.120
6290	74.990	7260	39.095	8230	8.040	9200	0.890	10170	0.065
6300	74.770	7270	38.600	8240	7.865	9210	0.890	10180	0.110
6310	74.540	7280	38.150	8250	7.755	9220	0.865	10190	0.100
6320	74.340	7290	37.810	8260	7.515	9230	0.805	10200	0.100
6330	74.090	7300	37.330	8270	7.345	9240	0.770	10210	0.090
6340	73.845	7310	36.920	8280	7.185	9250	0.815	10220	0.085
6350	73.545	7320	36.500	8290	7.100	9260	0.775	10230	0.120
6360	73.310	7330	36.070	8300	6.935	9270	0.705	10240	0.110
6370	73.090	7340	35.640	8310	6.755	9280	0.695	10250	0.085
6380	72.805	7350	35.205	8320	6.655	9290	0.730	10260	0.055
6390	72.510	7360	34.770	8330	6.455	9300	0.695	10270	0.095
6400	72.330	7370	34.425	8340	6.330	9310	0.710	10280	0.070
6410	71.970	7380	34.010	8350	6.195	9320	0.695	10290	0.105
6420	71.660	7390	33.565	8360	6.090	9330	0.665	10300	0.090
6430	71.480	7400	33.170	8370	5.950	9340	0.640	10310	0.105

Table 9. Transmission characteristics of the *I* filter in KPNO’s *UBVRI* filter set J

$\lambda$	% T	$\lambda$	% T	$\lambda$	% T	$\lambda$	% T	$\lambda$	% T
6860	0.000	7890	89.435	8920	86.015	9950	71.760	10980	31.660
6870	0.000	7900	89.440	8930	85.950	9960	71.535	10990	31.250
6880	0.010	7910	89.335	8940	85.910	9970	71.315	11000	30.810
6890	0.020	7920	89.545	8950	85.885	9980	71.005	11010	30.370
6900	0.035	7930	89.695	8960	85.780	9990	70.755	11020	29.885
6910	0.060	7940	89.655	8970	85.710	10000	70.460	11030	29.525
6920	0.105	7950	89.215	8980	85.610	10010	70.210	11040	29.030
6930	0.165	7960	89.625	8990	85.535	10020	69.940	11050	28.610
6940	0.255	7970	89.630	9000	85.415	10030	69.735	11060	28.185
6950	0.385	7980	89.480	9010	85.335	10040	69.405	11070	27.760
6960	0.565	7990	89.275	9020	85.255	10050	69.155	11080	27.285
6970	0.810	8000	89.360	9030	85.090	10060	68.855	11090	26.855
6980	1.130	8010	89.595	9040	85.060	10070	68.630	11100	26.480
6990	1.535	8020	89.585	9050	84.940	10080	68.280	11110	26.060
7000	2.065	8030	89.370	9060	84.930	10090	68.015	11120	25.620
7010	2.705	8040	89.580	9070	84.835	10100	67.770	11130	25.180
7020	3.495	8050	89.115	9080	84.735	10110	67.465	11140	24.735
7030	4.435	8060	89.195	9090	84.610	10120	67.110	11150	24.330
7040	5.530	8070	89.535	9100	84.525	10130	66.835	11160	23.985
7050	6.810	8080	89.465	9110	84.435	10140	66.505	11170	23.600
7060	8.220	8090	89.235	9120	84.375	10150	66.235	11180	23.165
7070	9.820	8100	89.235	9130	84.330	10160	65.895	11190	22.795
7080	11.540	8110	89.190	9140	84.250	10170	65.640	11200	22.420
7090	13.390	8120	89.010	9150	84.165	10180	65.270	11210	21.990
7100	15.455	8130	89.275	9160	84.090	10190	64.920	11220	21.595
7110	17.620	8140	88.995	9170	83.960	10200	64.595	11230	21.240
7120	19.895	8150	89.235	9180	83.860	10210	64.290	11240	20.940
7130	22.255	8160	89.150	9190	83.770	10220	63.985	11250	20.510
7140	24.755	8170	89.170	9200	83.675	10230	63.660	11260	20.170
7150	27.250	8180	89.105	9210	83.600	10240	63.295	11270	19.740
7160	29.750	8190	88.870	9220	83.425	10250	62.920	11280	19.435
7170	32.365	8200	88.795	9230	83.380	10260	62.555	11290	19.065
7180	34.980	8210	88.730	9240	83.240	10270	62.295	11300	18.780
7190	37.525	8220	88.830	9250	83.105	10280	61.880	11310	18.435
7200	40.205	8230	88.895	9260	83.060	10290	61.525	11320	18.030
7210	42.695	8240	88.975	9270	82.965	10300	61.160	11330	17.590
7220	45.210	8250	89.270	9280	82.885	10310	60.800	11340	17.210



Table 9—Continued

$\lambda$	% T	$\lambda$	% T	$\lambda$	% T	$\lambda$	% T	$\lambda$	% T
7230	47.695	8260	88.800	9290	82.755	10320	60.470	11350	16.885
7240	50.065	8270	88.685	9300	82.605	10330	60.115	11360	16.615
7250	52.390	8280	88.380	9310	82.535	10340	59.740	11370	16.325
7260	54.730	8290	88.740	9320	82.435	10350	59.305	11380	16.025
7270	56.890	8300	88.500	9330	82.315	10360	58.935	11390	15.595
7280	58.930	8310	88.495	9340	82.240	10370	58.530	11400	15.330
7290	60.965	8320	88.425	9350	82.095	10380	58.160	11410	15.060
7300	62.780	8330	88.475	9360	82.000	10390	57.755	11420	14.740
7310	64.635	8340	88.465	9370	82.025	10400	57.375	11430	14.480
7320	66.460	8350	88.395	9380	81.775	10410	56.950	11440	14.150
7330	67.985	8360	88.395	9390	81.650	10420	56.530	11450	13.840
7340	69.620	8370	88.565	9400	81.610	10430	56.105	11460	13.575
7350	71.020	8380	88.115	9410	81.345	10440	55.750	11470	13.275
7360	72.420	8390	88.310	9420	81.250	10450	55.385	11480	13.070
7370	73.815	8400	88.045	9430	81.090	10460	54.980	11490	12.770
7380	74.970	8410	88.190	9440	80.985	10470	54.580	11500	12.465
7390	76.090	8420	88.265	9450	80.905	10480	54.175	11510	12.170
7400	77.185	8430	87.930	9460	80.700	10490	53.785	11520	11.945
7410	78.055	8440	88.340	9470	80.585	10500	53.320	11530	11.630
7420	79.090	8450	87.870	9480	80.435	10510	52.895	11540	11.405
7430	80.045	8460	88.040	9490	80.260	10520	52.565	11550	11.155
7440	80.640	8470	87.630	9500	80.170	10530	52.115	11560	10.860
7450	81.455	8480	88.020	9510	80.045	10540	51.640	11570	10.565
7460	82.200	8490	88.190	9520	79.965	10550	51.205	11580	10.300
7470	82.900	8500	87.965	9530	79.765	10560	50.820	11590	10.105
7480	83.380	8510	88.105	9540	79.610	10570	50.300	11600	9.880
7490	83.765	8520	88.215	9550	79.475	10580	49.905	11610	9.700
7500	84.400	8530	87.805	9560	79.380	10590	49.465	11620	9.450
7510	84.765	8540	87.605	9570	79.160	10600	49.020	11630	9.245
7520	85.375	8550	87.620	9580	79.005	10610	48.590	11640	9.045
7530	85.795	8560	87.815	9590	78.845	10620	48.150	11650	8.825
7540	86.060	8570	87.435	9600	78.735	10630	47.655	11660	8.660
7550	86.405	8580	87.920	9610	78.590	10640	47.205	11670	8.375
7560	86.655	8590	87.280	9620	78.390	10650	46.800	11680	8.240
7570	86.895	8600	88.265	9630	78.240	10660	46.360	11690	8.045
7580	86.900	8610	87.810	9640	78.045	10670	45.930	11700	7.875
7590	87.545	8620	87.735	9650	77.925	10680	45.450	11710	7.700

Table 9—Continued

$\lambda$	% T	$\lambda$	% T	$\lambda$	% T	$\lambda$	% T	$\lambda$	% T
7600	87.545	8630	87.710	9660	77.770	10690	45.010	11720	7.520
7610	87.845	8640	87.625	9670	77.555	10700	44.530	11730	7.305
7620	87.955	8650	87.600	9680	77.415	10710	44.090	11740	7.085
7630	88.390	8660	87.550	9690	77.165	10720	43.620	11750	6.945
7640	88.225	8670	87.475	9700	77.000	10730	43.155	11760	6.875
7650	88.305	8680	87.430	9710	76.895	10740	42.710	11770	6.660
7660	88.450	8690	87.385	9720	76.650	10750	42.250	11780	6.500
7670	88.580	8700	87.370	9730	76.470	10760	41.820	11790	6.360
7680	88.760	8710	87.205	9740	76.310	10770	41.385	11800	6.205
7690	88.825	8720	87.300	9750	76.130	10780	40.935	11810	6.030
7700	88.970	8730	87.220	9760	75.925	10790	40.435	11820	5.920
7710	89.100	8740	87.190	9770	75.765	10800	39.920	11830	5.710
7720	89.120	8750	87.175	9780	75.560	10810	39.450	11840	5.595
7730	89.330	8760	87.170	9790	75.370	10820	38.970	11850	5.415
7740	89.370	8770	87.050	9800	75.145	10830	38.450	11860	5.265
7750	89.295	8780	86.965	9810	74.900	10840	38.095	11870	5.100
7760	89.165	8790	86.915	9820	74.750	10850	37.615	11880	4.935
7770	89.235	8800	86.770	9830	74.520	10860	37.120	11890	4.700
7780	89.425	8810	86.710	9840	74.360	10870	36.640	11900	4.585
7790	89.405	8820	86.660	9850	74.090	10880	36.290	11910	4.660
7800	89.495	8830	86.550	9860	73.890	10890	35.855	11920	4.520
7810	89.600	8840	86.515	9870	73.640	10900	35.380	11930	4.475
7820	89.370	8850	86.460	9880	73.435	10910	34.865	11940	4.305
7830	89.425	8860	86.340	9890	73.200	10920	34.480	11950	4.230
7840	89.630	8870	86.275	9900	72.920	10930	33.985	11960	4.120
7850	89.515	8880	86.315	9910	72.690	10940	33.520	11970	4.055
7860	89.625	8890	86.220	9920	72.465	10950	33.065	11980	3.915
7870	89.630	8900	86.130	9930	72.240	10960	32.625	11990	3.805
7880	89.560	8910	86.065	9940	72.000	10970	32.155	12000	3.830

Table 10. Accurate Coordinates and Proper Motions for Stars in Table 4.

Star Name	2MASS-PSC UCAC2	$\alpha$ (2000) h m s	$\delta$ ° ' "	$\mu_\alpha$ (mas/yr)	$\mu_\delta$ (mas/yr)	$\mu$ Ref.	Sp. Type	Sp. Type Ref.
G158 100	00335445-1207588	00 33 54.46	-12 07 58.8	155.6	-192.9	1	sdG	8
BPM 16274	00500367-5208155	00 50 03.68	-52 08 15.6	132	44	2	DA2	6
HZ 4	03552198+0947180	03 55 21.99	+09 47 18.0	168	4	2	DA4	6
LB 227	04092888+1707542	04 09 28.89	+17 07 54.3	104	-24	2	DA3	6
HZ 2	04124355+1151487	04 12 43.55	+11 51 48.8	48.3	-84.9	3	DA3	6
G191 B2B	05053063+5250032	05 05 30.63	+52 50 03.2	24	-128	2	DA1	6
G193 74	07532726+5229315	07 53 27.26	+52 29 31.5	-92.4	-252.0	1	DC7	6
BD +75° 325	08104947+7457579	08 10 49.48	+74 57 57.9	154	-192	2	O5p	7
LDS 235B	08472944-1859498	08 10 49.490	+74 57 57.93	28.34	9.55	4	DB4	6
AGK+81° 266	09211915+8143274	09 21 19.16	+81 43 27.5	-188	34	2	sdO	7
F 34	10393674+4306092	10 39 36.74	+43 06 09.2	-70.52	-50.14	4	DA	6
GD 140	11370512+2947581	11 37 05.12	+29 47 58.1	9.9	-26.2	5	DA3	6
HZ 21	12135625+3256314	12 13 56.25	+32 56 31.4	-148.3	-11.6	5	DO2	6
F 66	12372352+2503598	12 37 23.52	+25 03 59.8	-102	36	2	sdO	8
F 67	12415179+1731197	12 41 51.79	+17 31 19.8	2.2	-26.7	5	sdO	8
G60 54	13000906+0328409	13 00 09.06	+03 28 41.0	-6.8	-38.1	5	DC9	6
HZ 44	13233526+3607595	13 23 35.27	+36 07 59.6	-430.74	-876.3	1	sdO	7
GRW+70° 5824	13385054+7017077	13 38 50.54	+70 17 07.7	-432	-864	2	DA2	6
BD+26° 2606	14490235+2542092	14 49 02.35	+25 42 09.2	-1197.03	-26.17	5	sdF4	9
GD 190	15441945+1806442	15 44 19.46	+18 06 44.3	-8.9	-347.3	5	DB2	6
BD+33° 2642	15515988+3256543	15 51 59.88	+32 56 54.4	0.8	-129.2	1	B2IV	7
G138 31	16275347+0912159	16 27 53.48	+09 12 15.9	6	-118	2	DC8	6
G24 9	20135551+0642481	20 13 55.51	+06 42 48.2	-14.6	1.5	5	DQ7	6
LDS 749B	21321623+0015144	21 32 16.24	+00 15 14.4	-109.2	-466.5	1	DB4	6
L930 80	21473725-0744121	21 47 37.25	-07 44 12.2	-76	-462	2	DB4	6
BD+28° 4211	21511102+2851504	21 51 11.02	+28 51 50.4	253.5	-129.6	5	DA	6
BD+17° 4708	22113136+1805341	22 11 31.37	+18 05 34.1	-35.8	-58.0	5	sdF6	9
NGC 7293	22293854-2050136	22 29 38.54	-20 50 13.6	509.0	58.4	5	DA0	6
F 110	23195840-0509561	23 19 58.41	-05 09 56.2	37.3	-3.9	5	DOp	7
LTT 9491	23193537-1705284	23 19 35.38	-17 05 28.5	-9.8	-4.2	5	DB3	6
GD 248	23260659+1600195	23 26 06.59	+16 00 19.6	240.5	25.2	1	DC5	6
				238	14	2		
				-42	-108	2		

1. (Klemola et al. 1987) [Lick NPM1 Catalogue]
2. (Monet et al. 2003) [USNO-B1.0]
3. (Hanson et al. 2004) [Lick NPM2 Catalogue]

4. (Urban et al. 2004) [UCAC2-BSS]
5. (Zacharias et al. 2004) [UCAC2]
6. (McCook & Sion 2006)
7. (Bohlin et al. 1990)
8. (Oke 1990)
9. (Roman 1955)

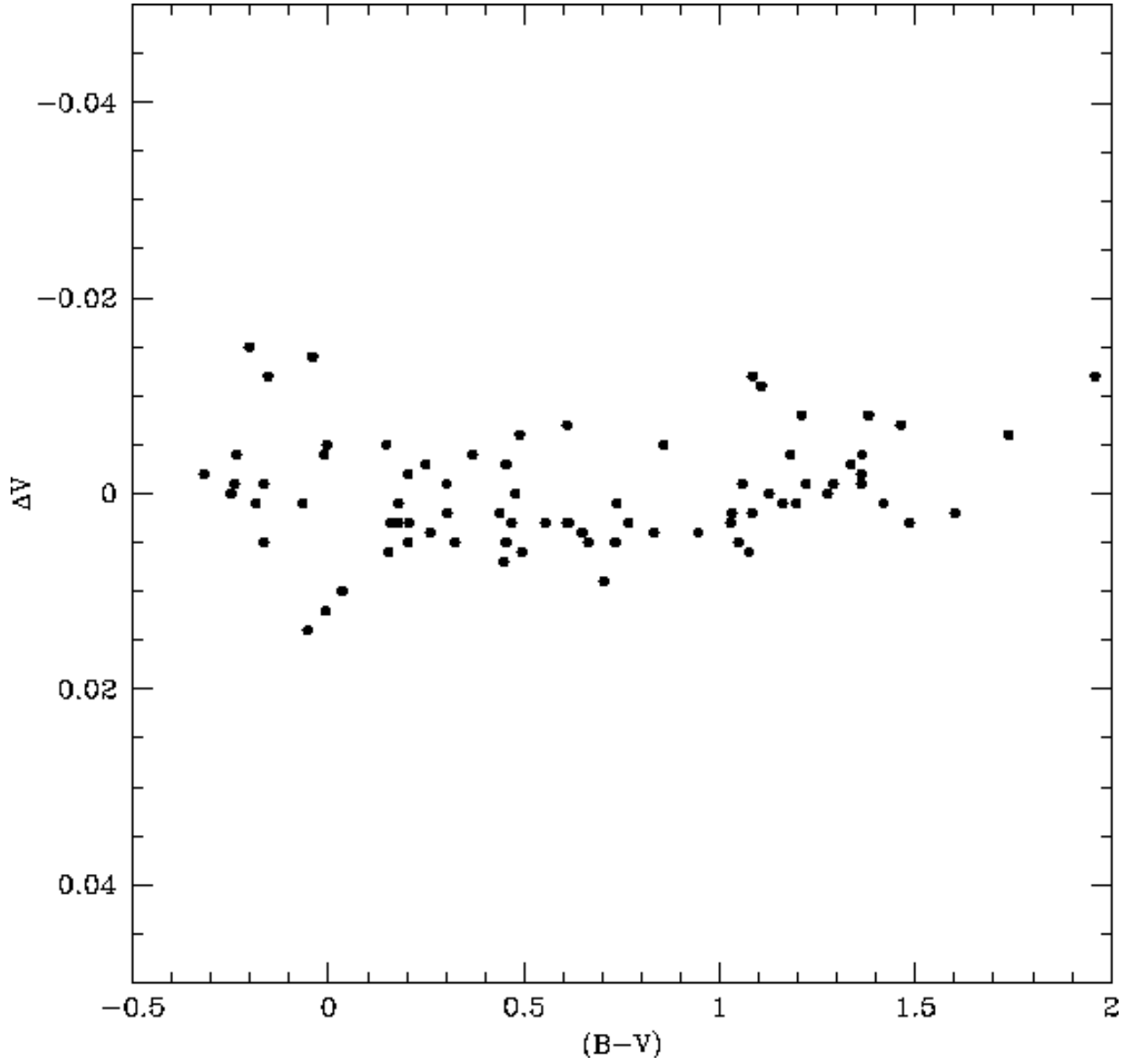


Fig. 1.— A comparison of the  $V$  magnitudes tied into Landolt (1983) standard stars as a function of the Landolt (1992) equatorial standard's  $(B - V)$  color indices.

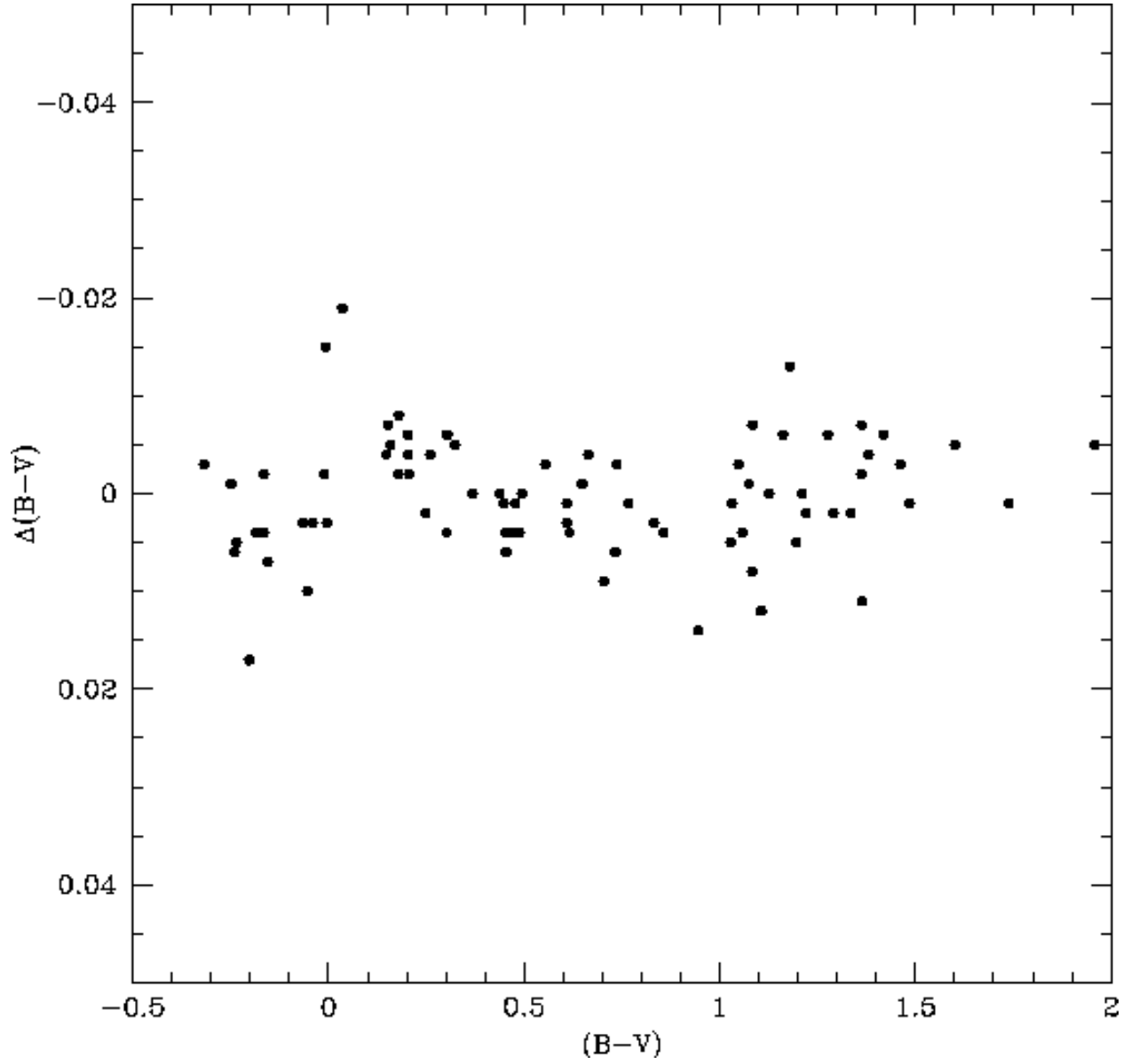


Fig. 2.— A comparison of the  $(B - V)$  color indices tied into Landolt (1983) standard stars as a function of the Landolt (1992) equatorial standard's  $(B - V)$  color indices.

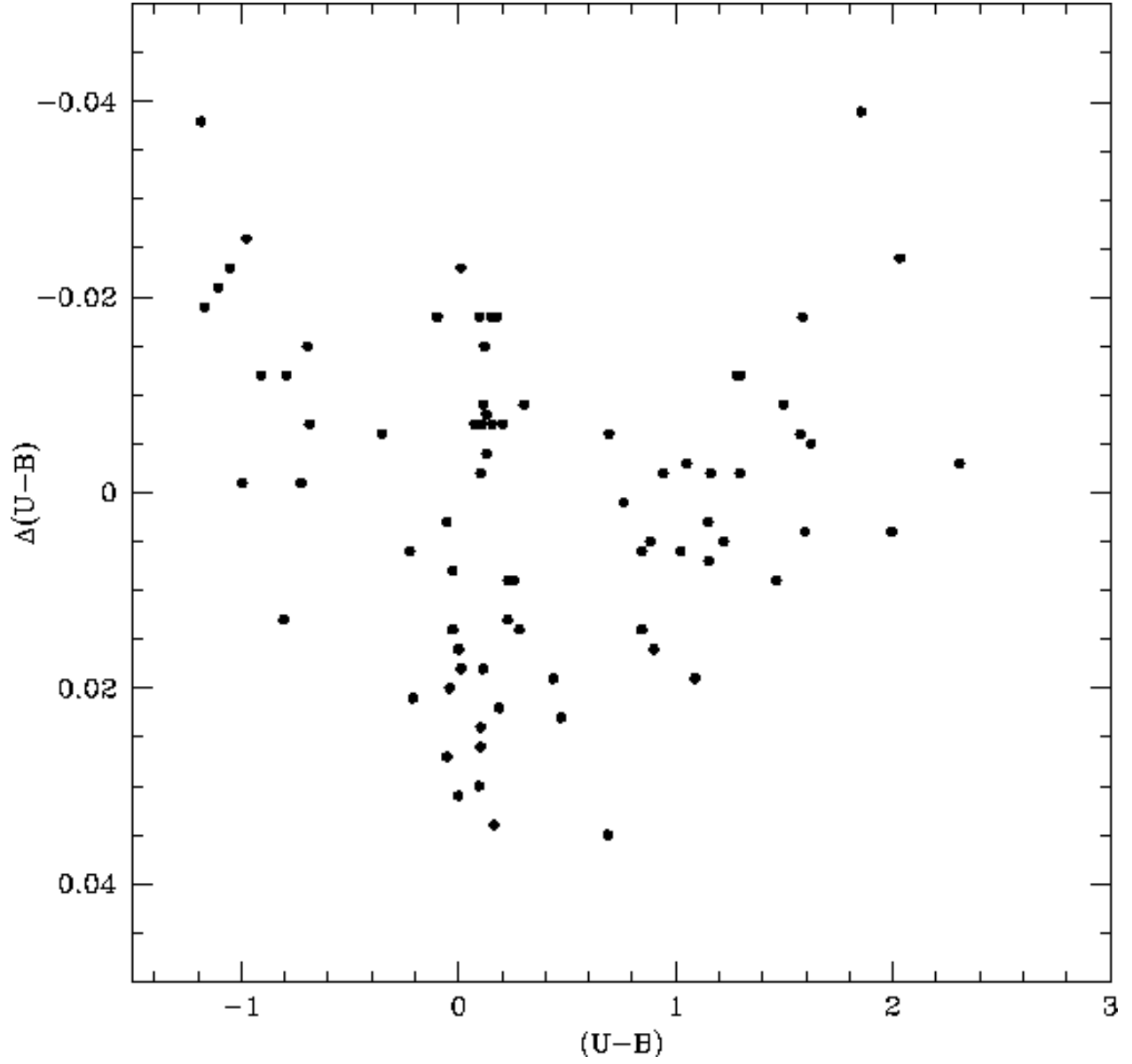


Fig. 3.— A comparison of the  $(U - B)$  color indices tied into Landolt (1983) standard stars as a function of the Landolt (1992) equatorial standard's  $(U - B)$  color indices.

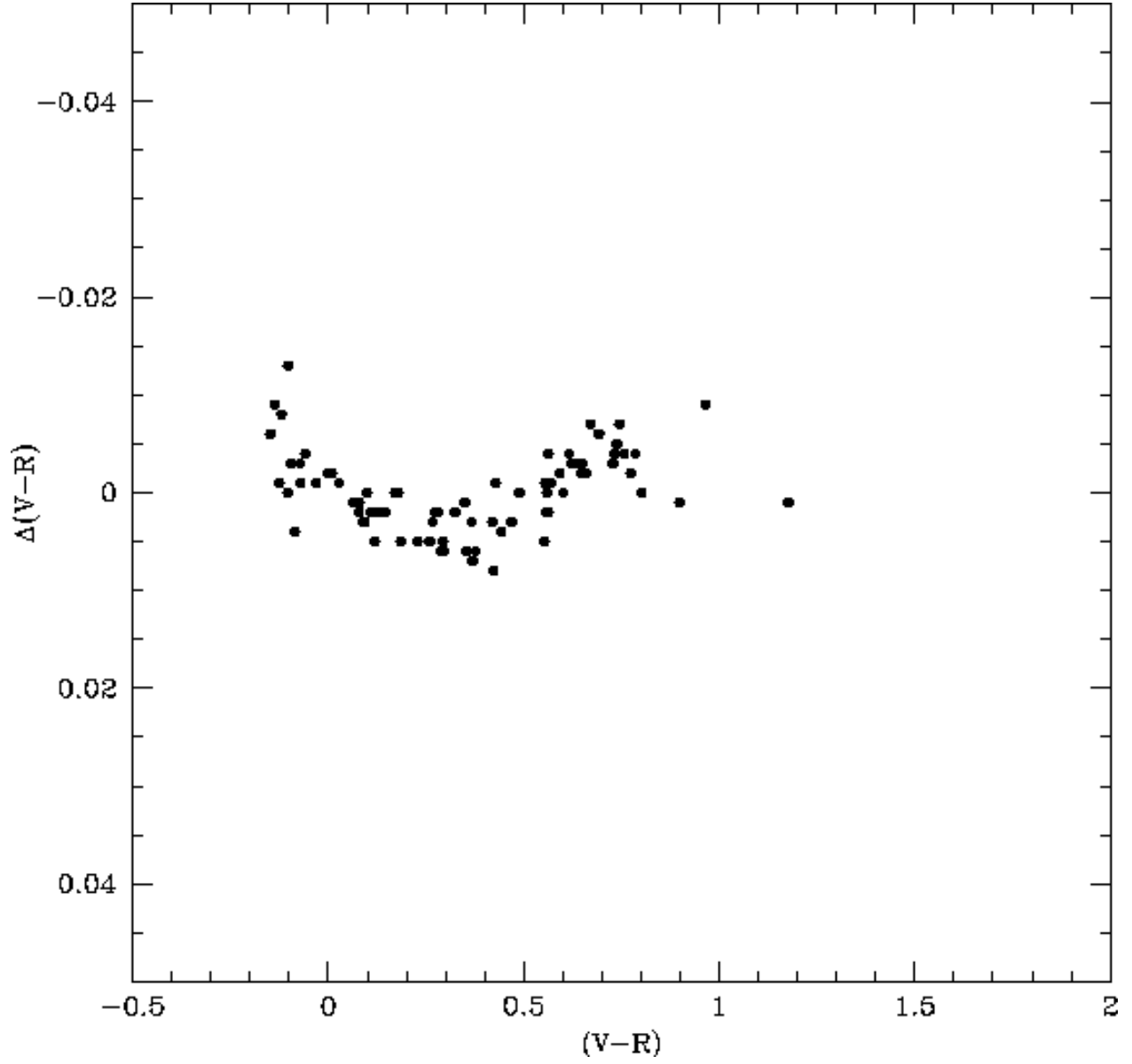


Fig. 4.— A comparison of the  $(V - R)$  color indices tied into Landolt (1983) standard stars as a function of the Landolt (1992) equatorial standard's  $(V - R)$  color indices.



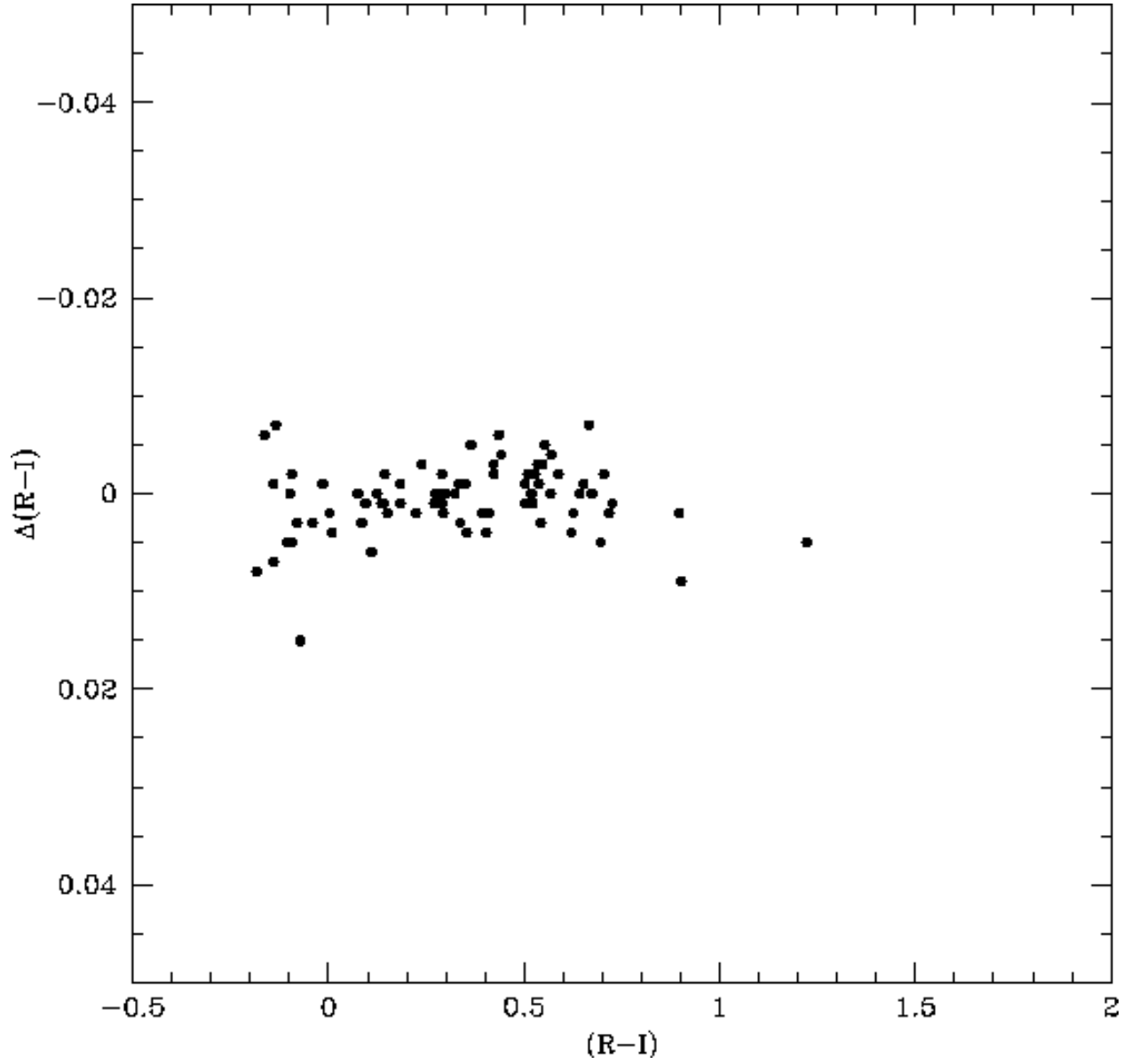


Fig. 5.— A comparison of the  $(R - I)$  color indices tied into Landolt (1983) standard stars as a function of the Landolt (1992) equatorial standard's  $(R - I)$  color indices.

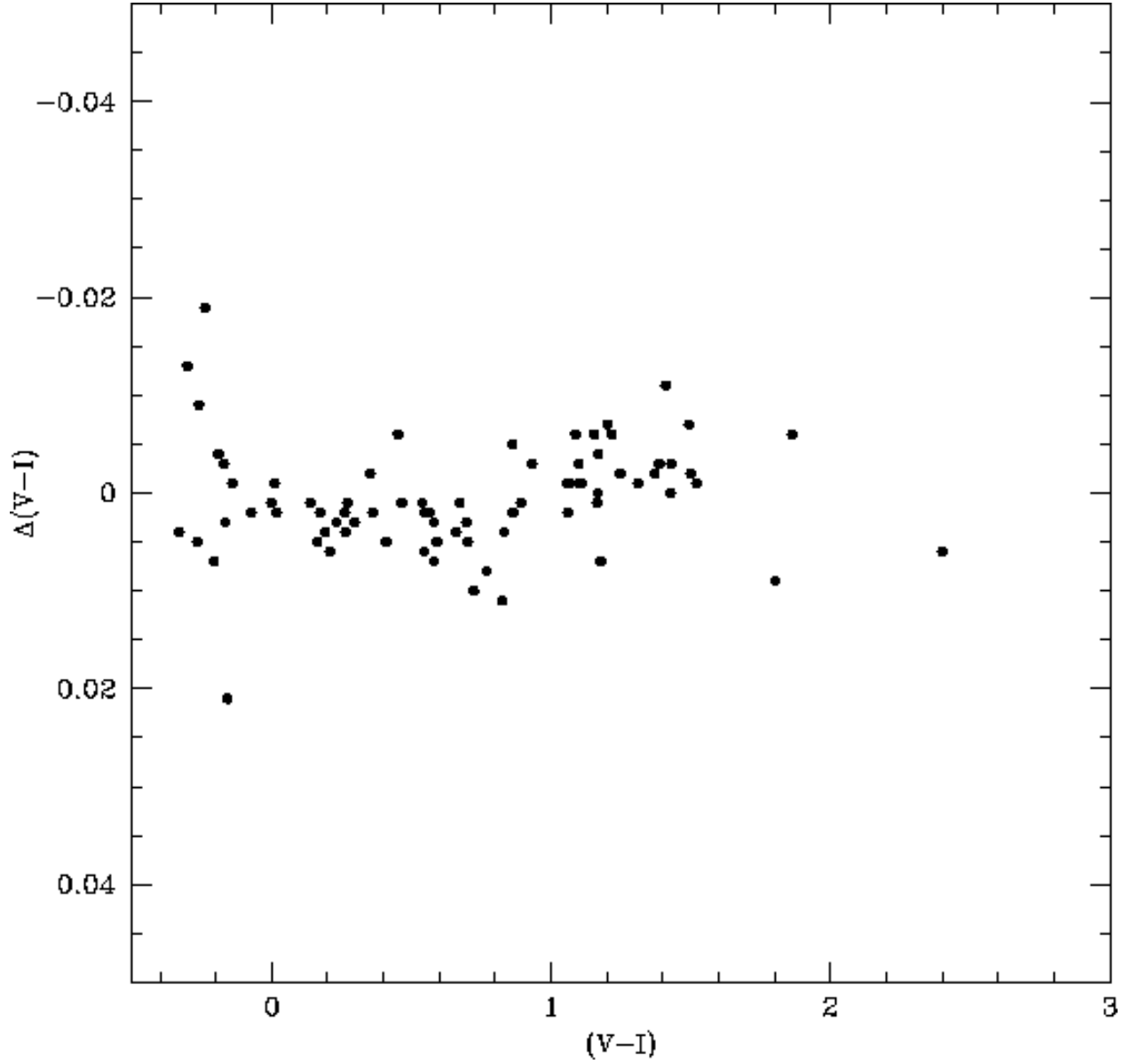


Fig. 6.— A comparison of the  $(V - I)$  color indices tied into Landolt (1983) standard stars as a function of the Landolt (1992) equatorial standard's  $(V - I)$  color indices.

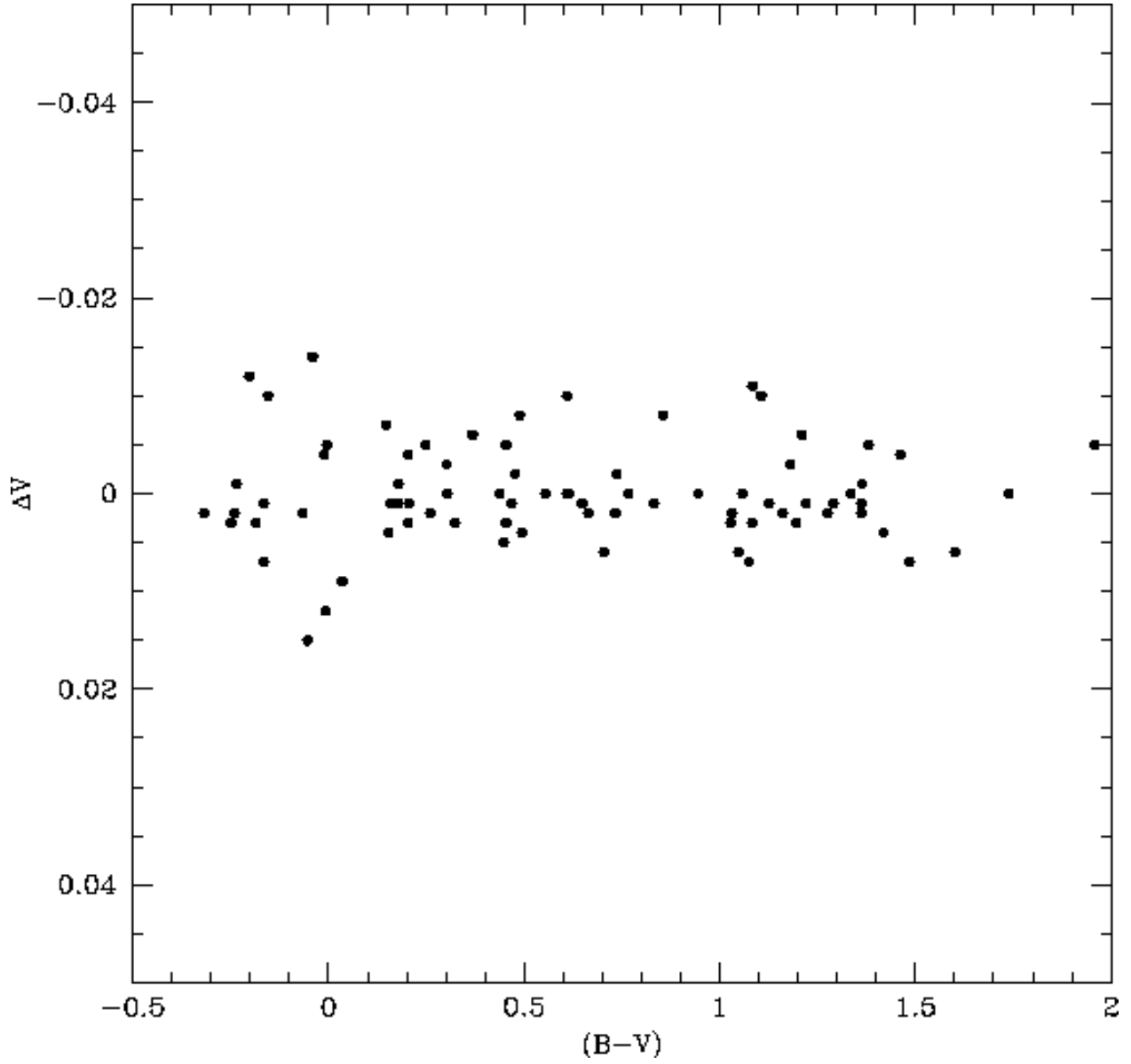


Fig. 7.— A comparison of the  $V$  magnitudes tied into Landolt (1992) standard stars as a function of the Landolt (1992) equatorial standard's  $(B - V)$  color indices.

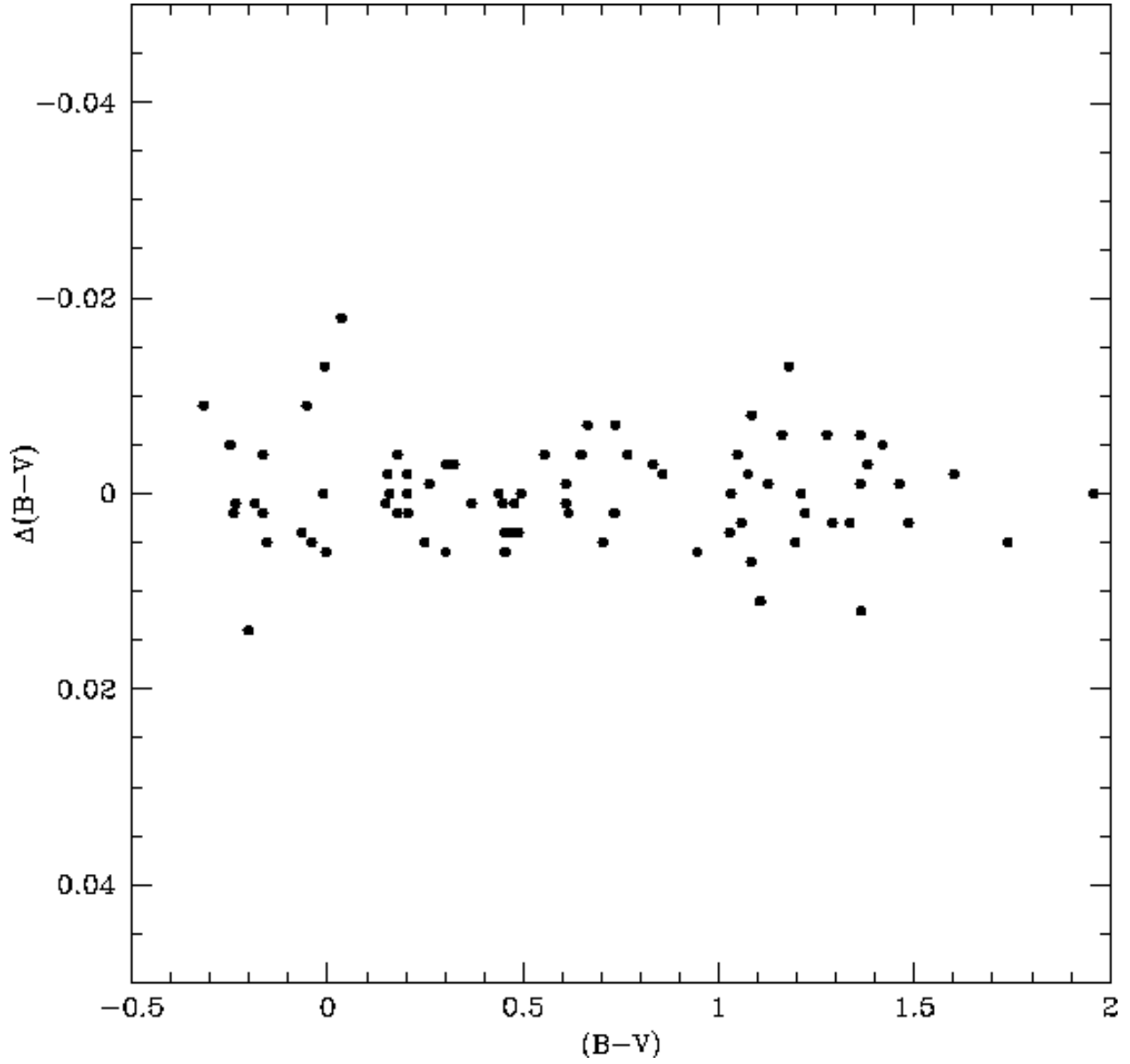


Fig. 8.— A comparison of the  $(B - V)$  color indices tied into Landolt (1992) standard stars as a function of the Landolt (1992) equatorial standard's  $(B - V)$  color indices.

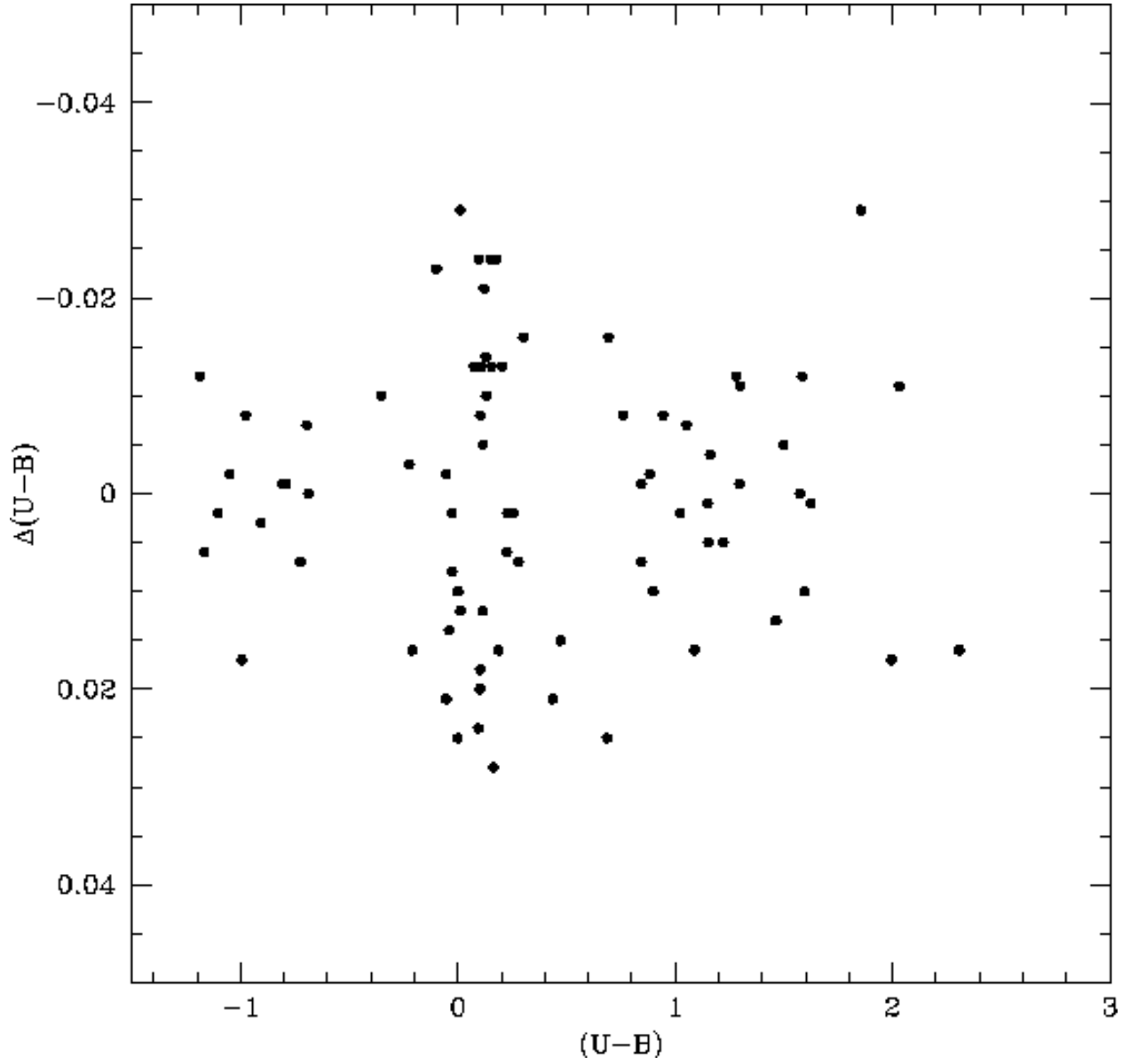


Fig. 9.— A comparison of the  $(U - B)$  color indices tied into Landolt (1992) standard stars as a function of the Landolt (1992) equatorial standard's  $(U - B)$  color indices.

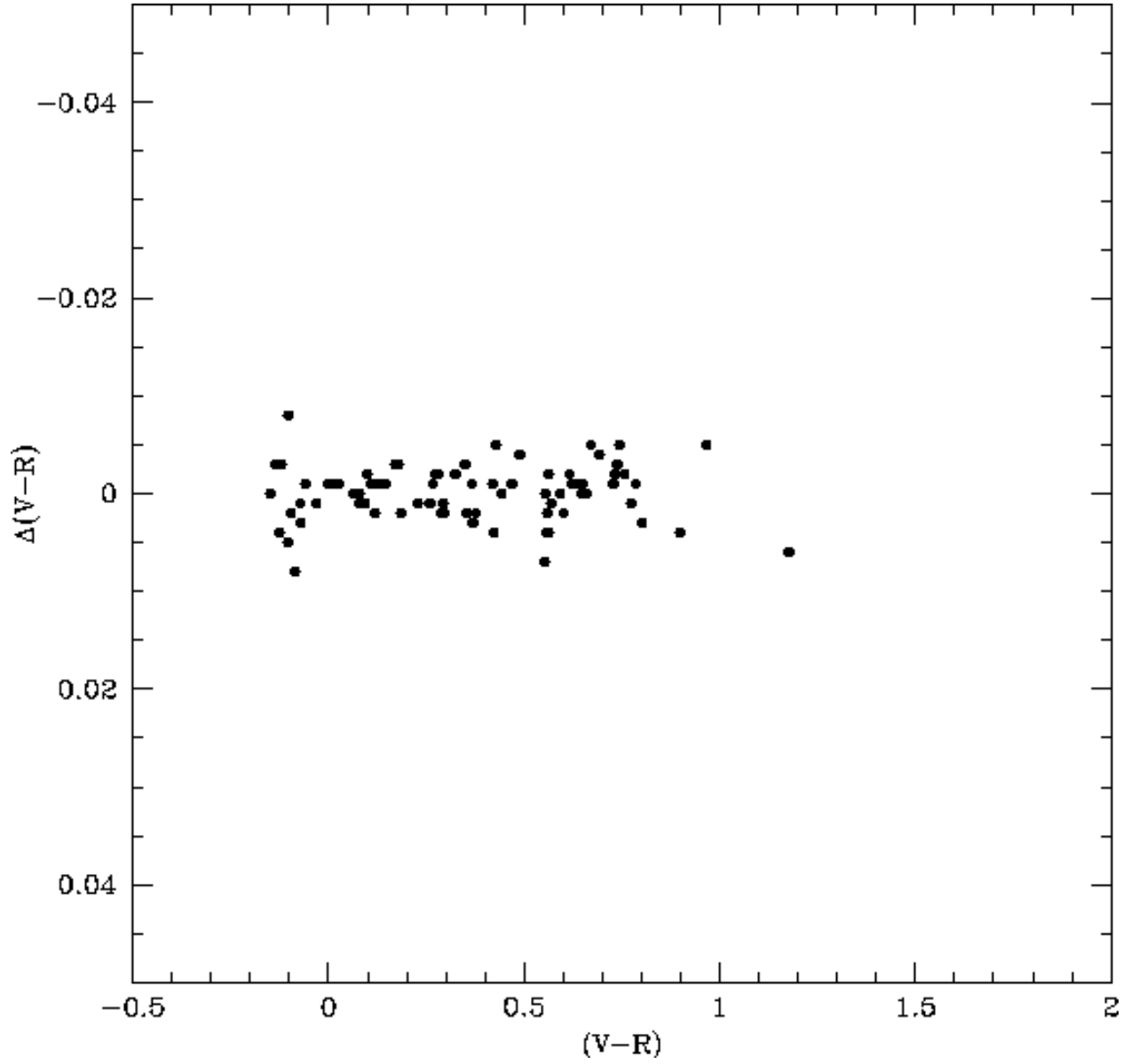


Fig. 10.— A comparison of the  $(V - R)$  color indices tied into Landolt (1992) standard stars as a function of the Landolt (1992) equatorial standard's  $(V - R)$  color indices.

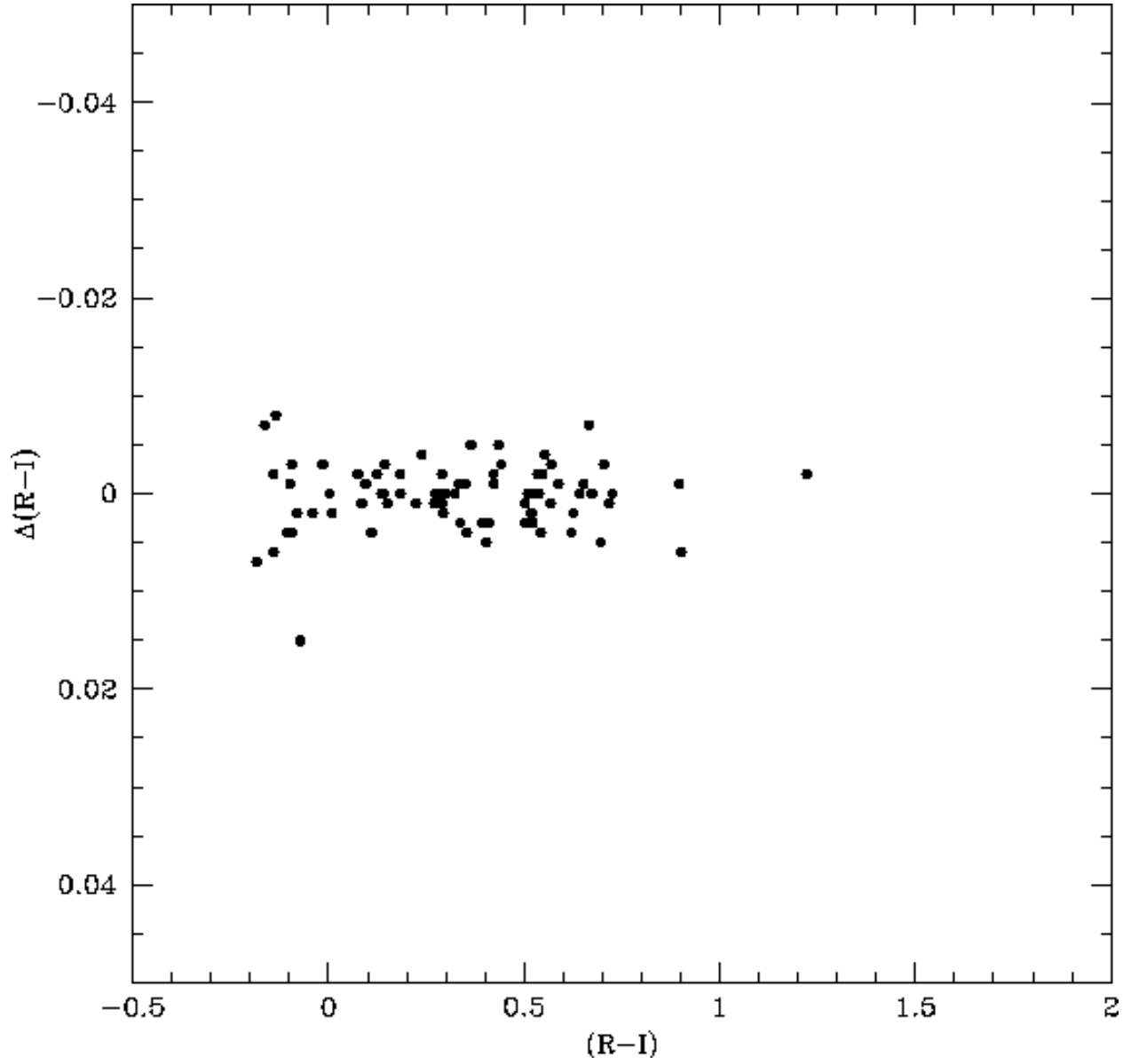


Fig. 11.— A comparison of the  $(R - I)$  color indices tied into Landolt (1992) standard stars as a function of the Landolt (1992) equatorial standard's  $(R - I)$  color indices.

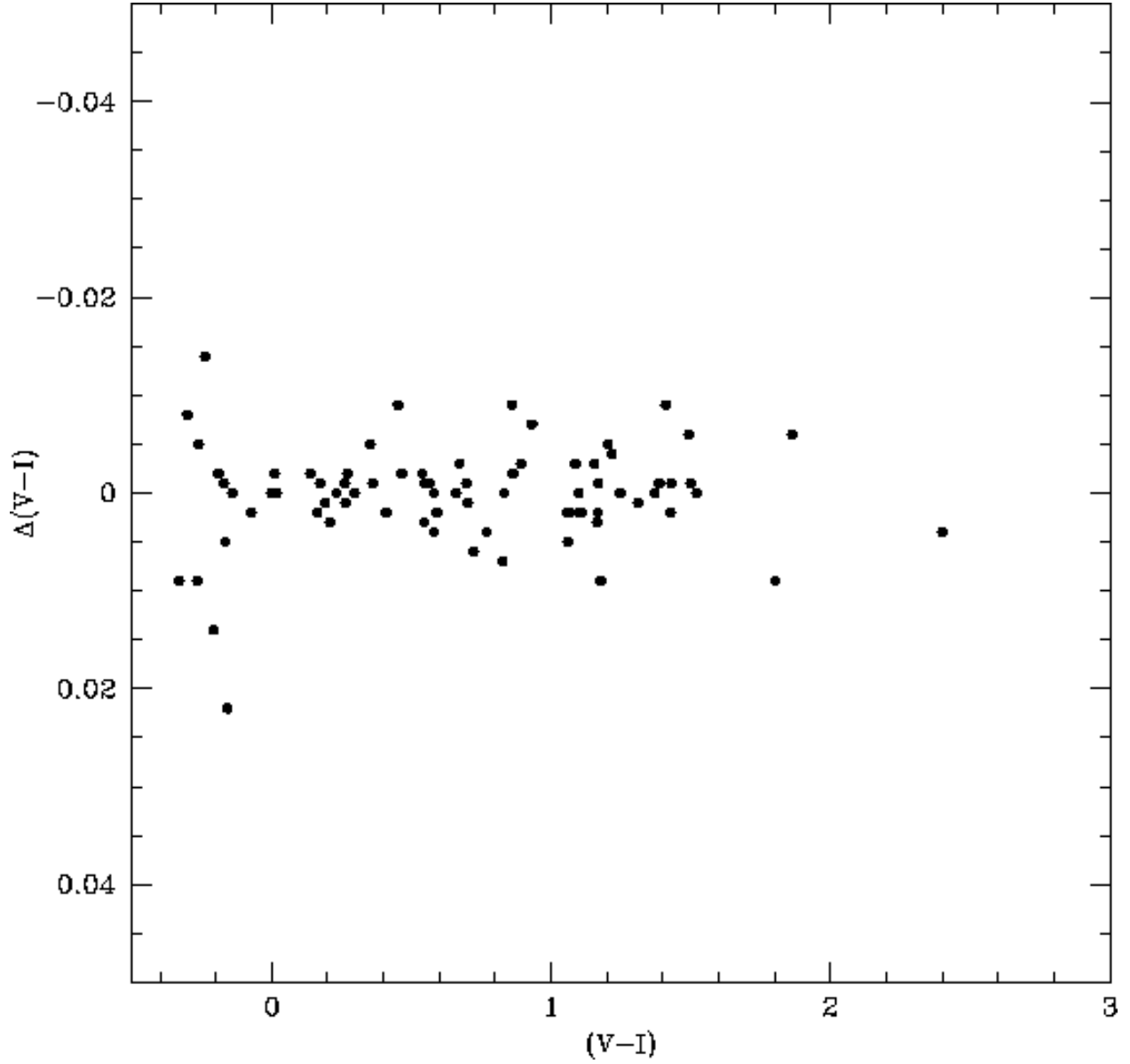


Fig. 12.— A comparison of the  $(V - I)$  color indices tied into Landolt (1992) standard stars as a function of the Landolt (1992) equatorial standard's  $(V - I)$  color indices.



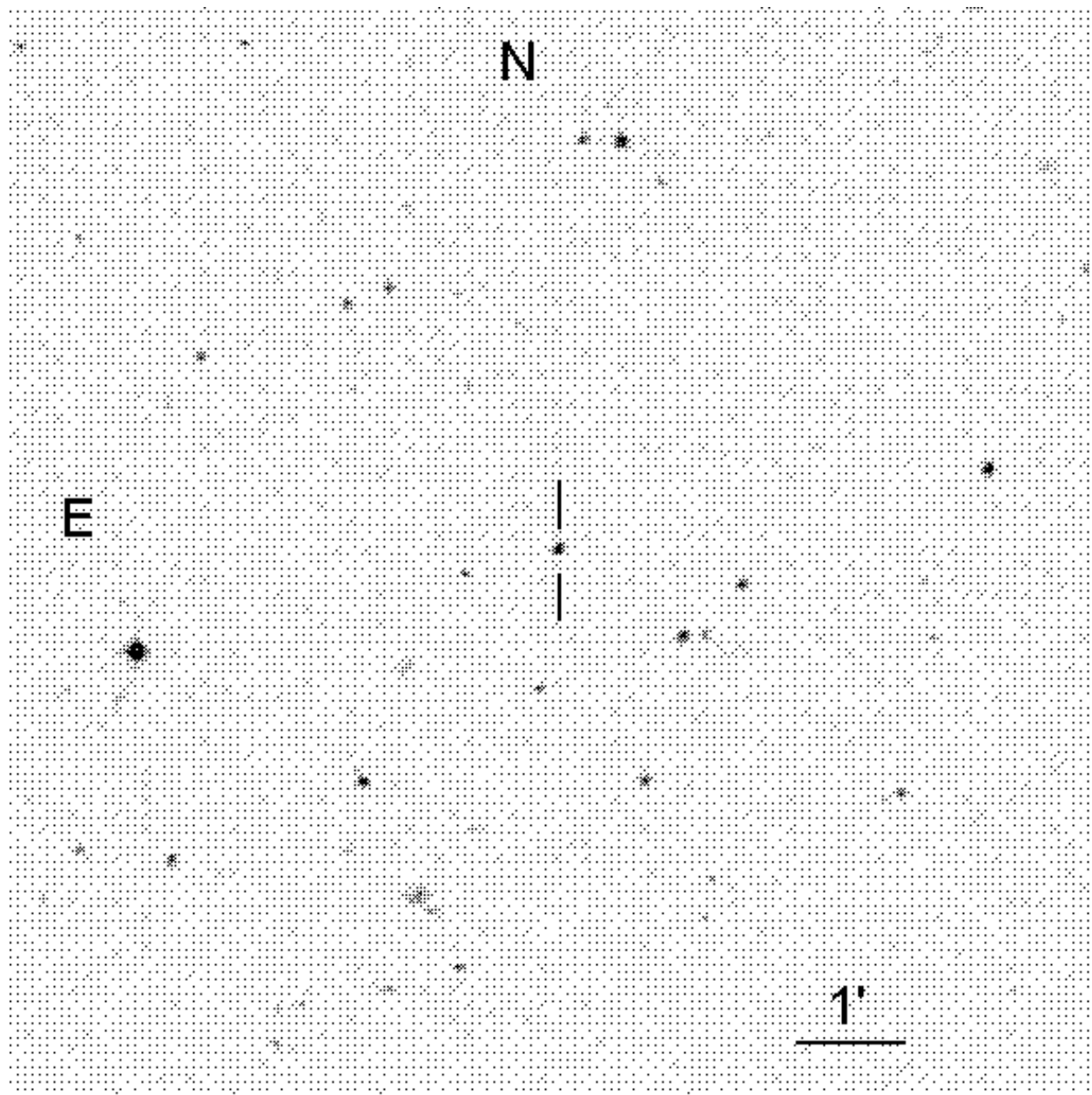


Fig. 13.— The field, 10 arc minutes on a side, of the star G 158-100.

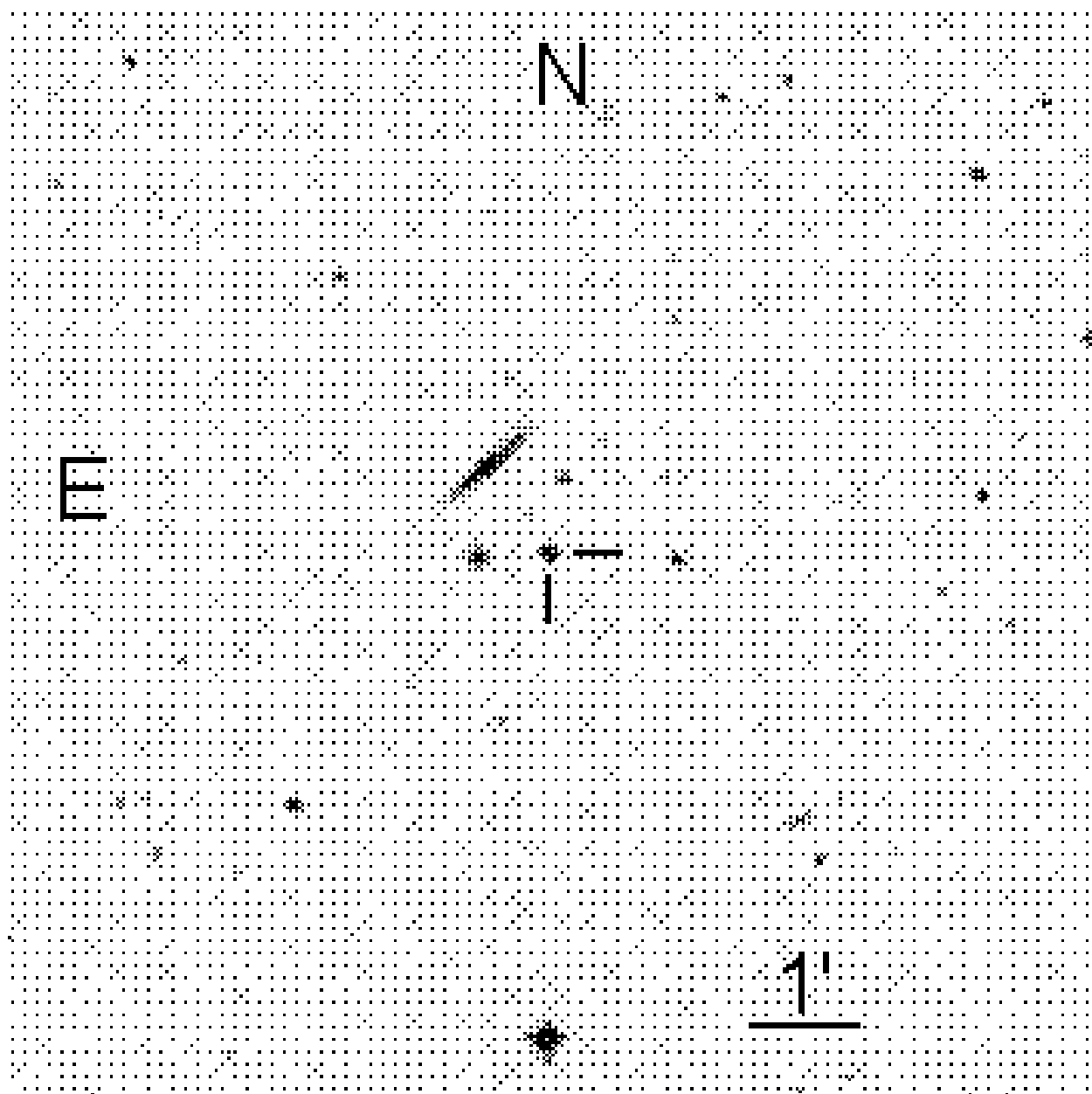


Fig. 14.— The field, 10 arc minutes on a side, of the star BPM 16274.

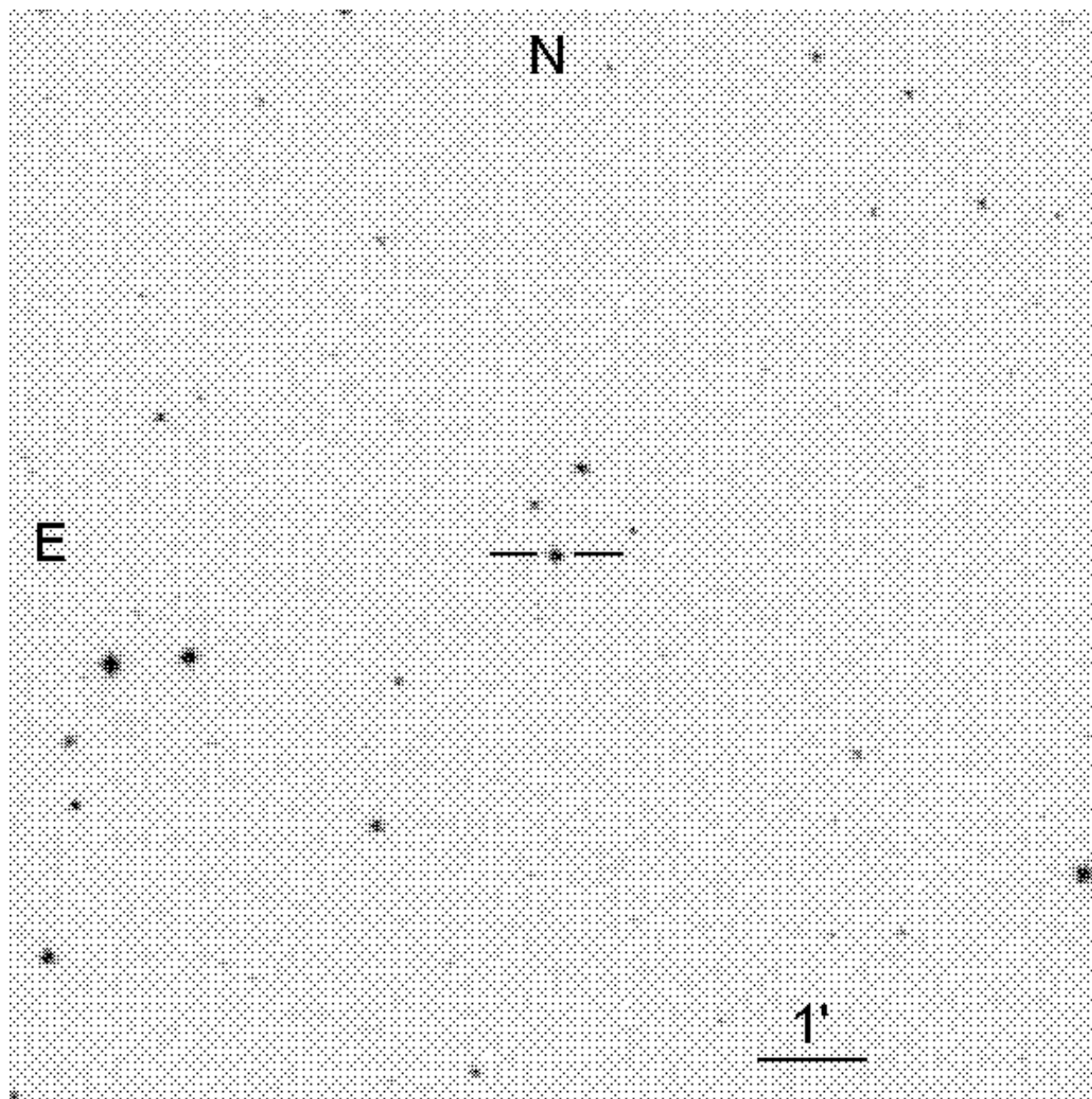


Fig. 15.— The field, 10 arc minutes on a side, of the star HZ 4.

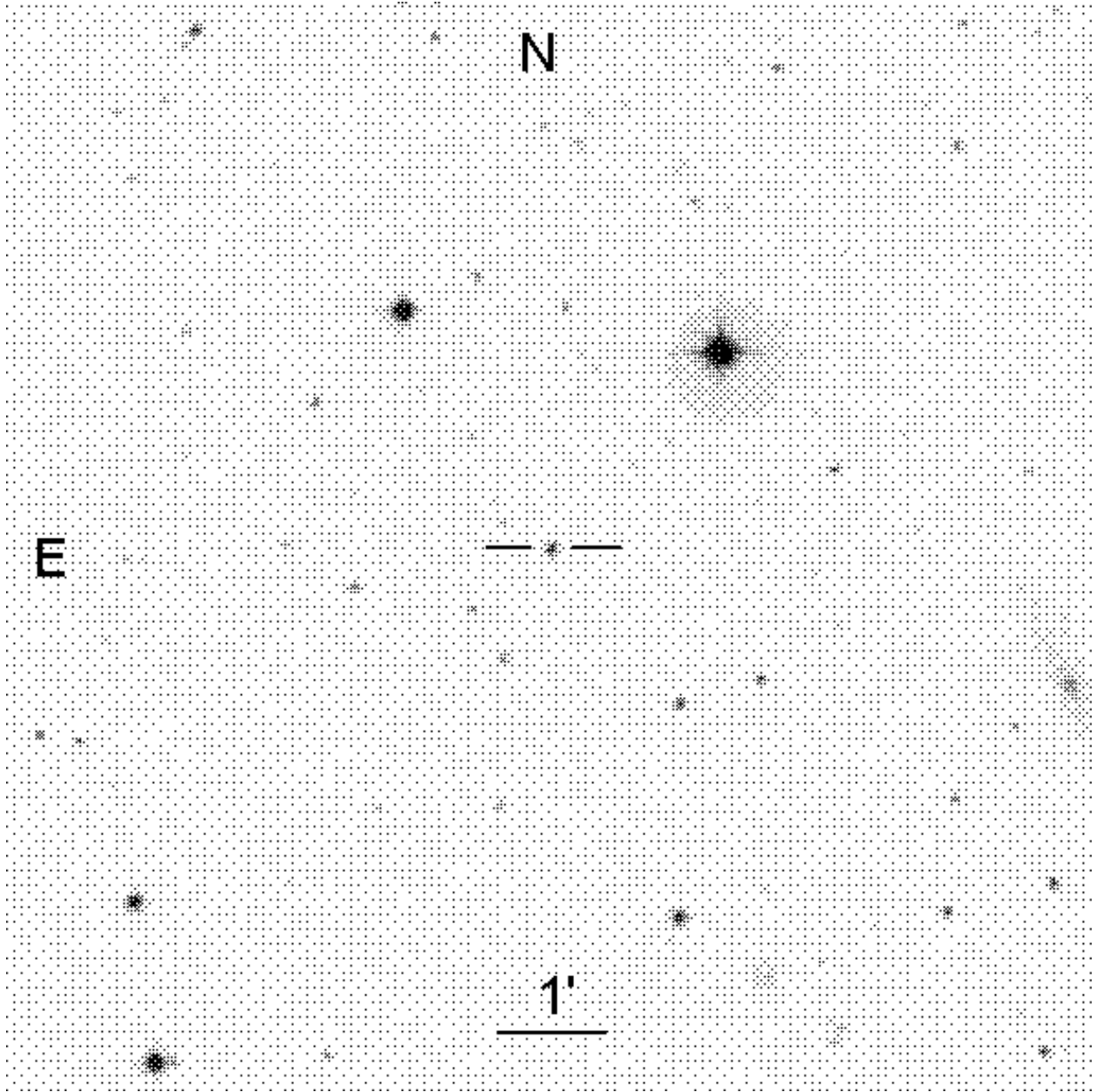


Fig. 16.— The field, 10 arc minutes on a side, of the star LB 227.

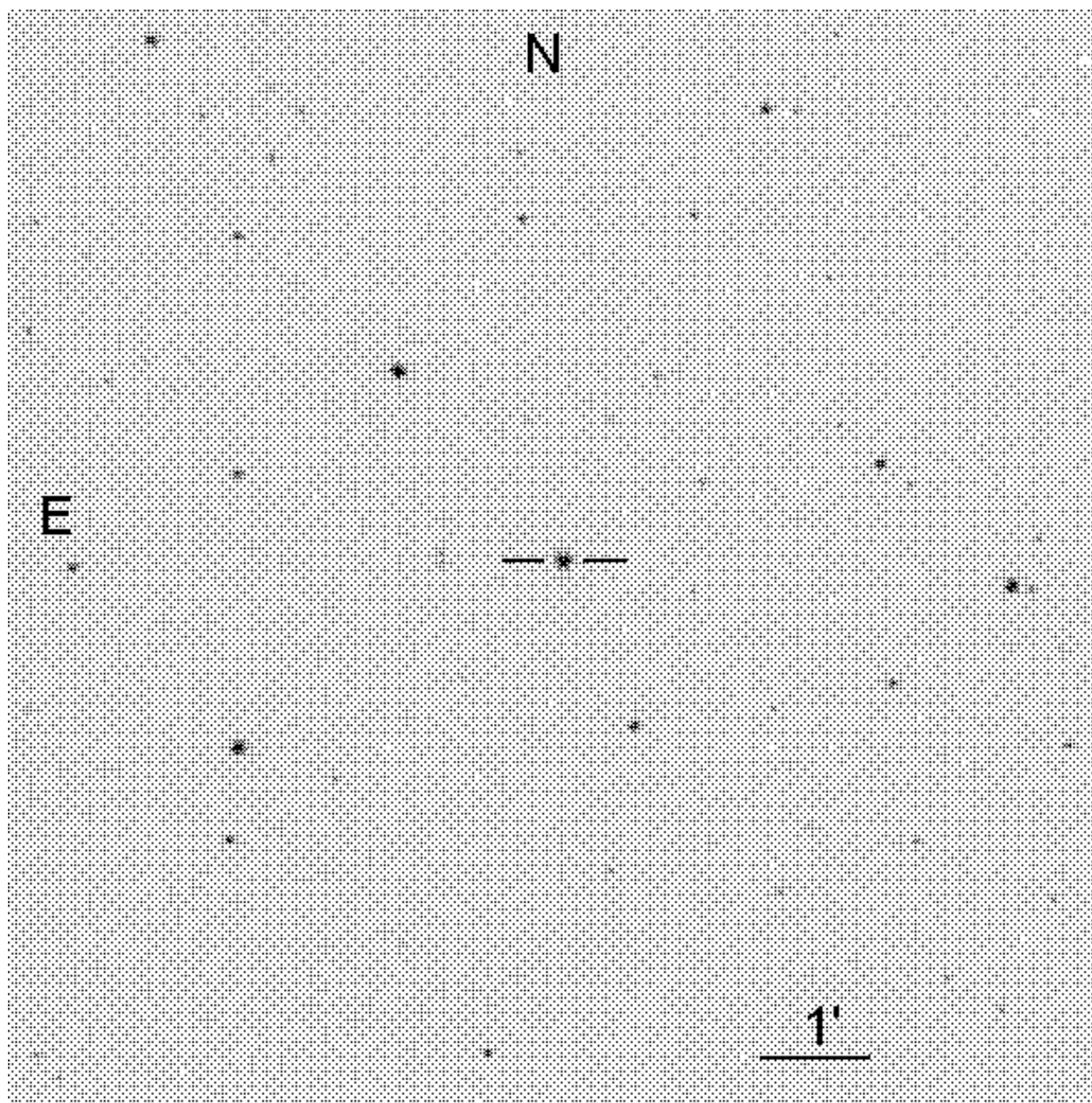


Fig. 17.— The field, 10 arc minutes on a side, of the star HZ 2.

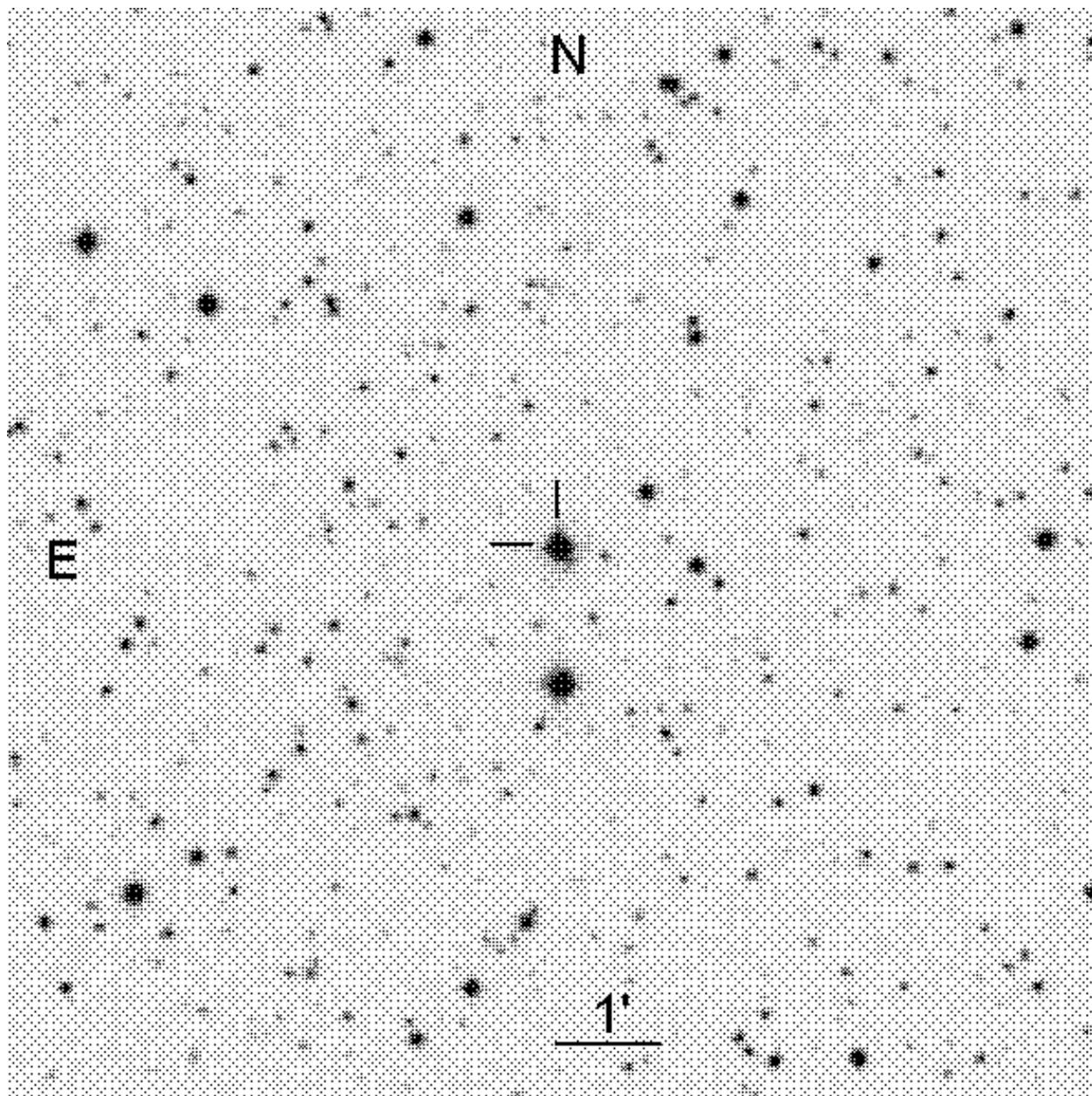


Fig. 18.— The field, 10 arc minutes on a side, of the star G 191-B2B.

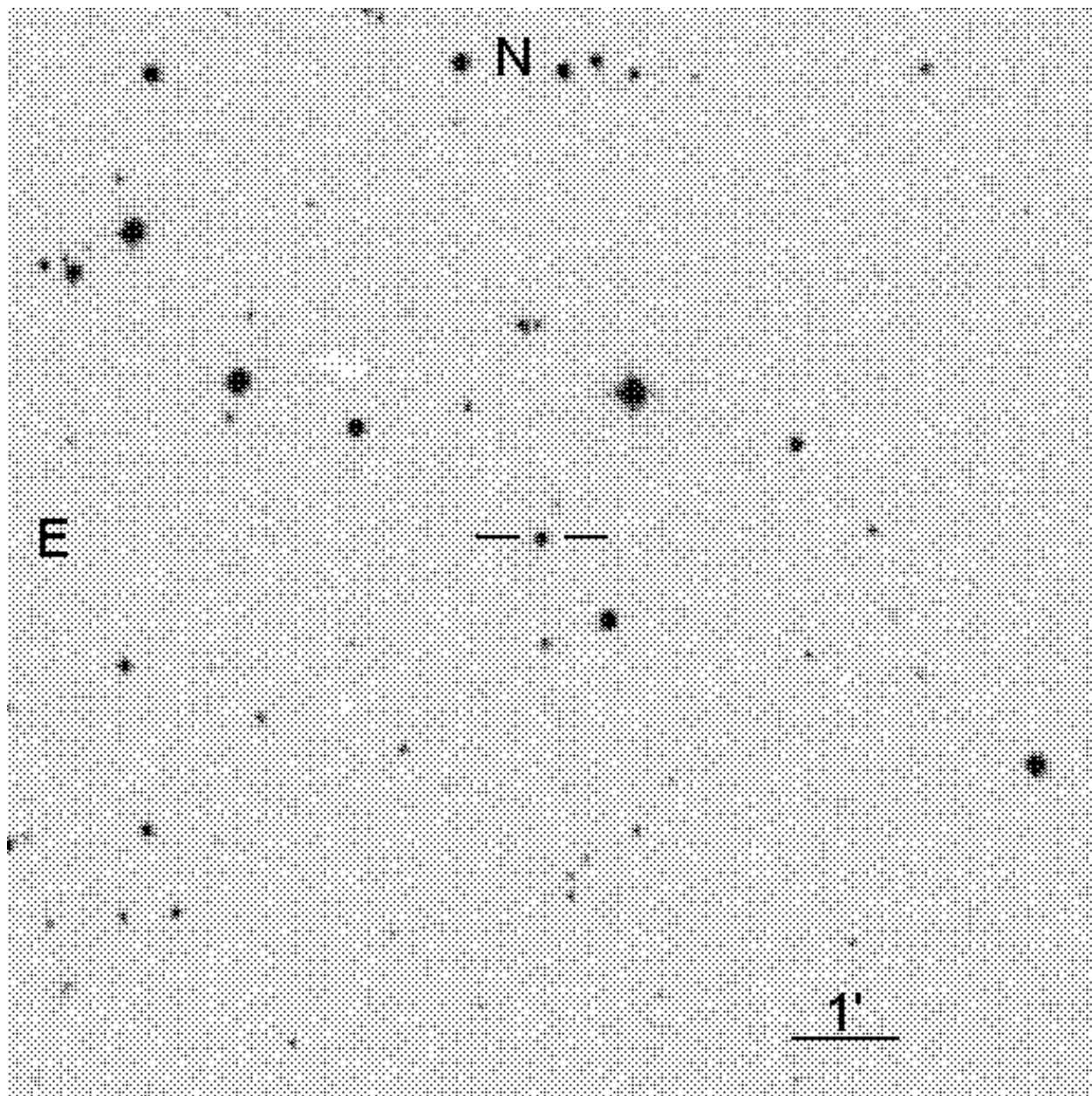


Fig. 19.— The field, 10 arc minutes on a side, of the star G 193-74.

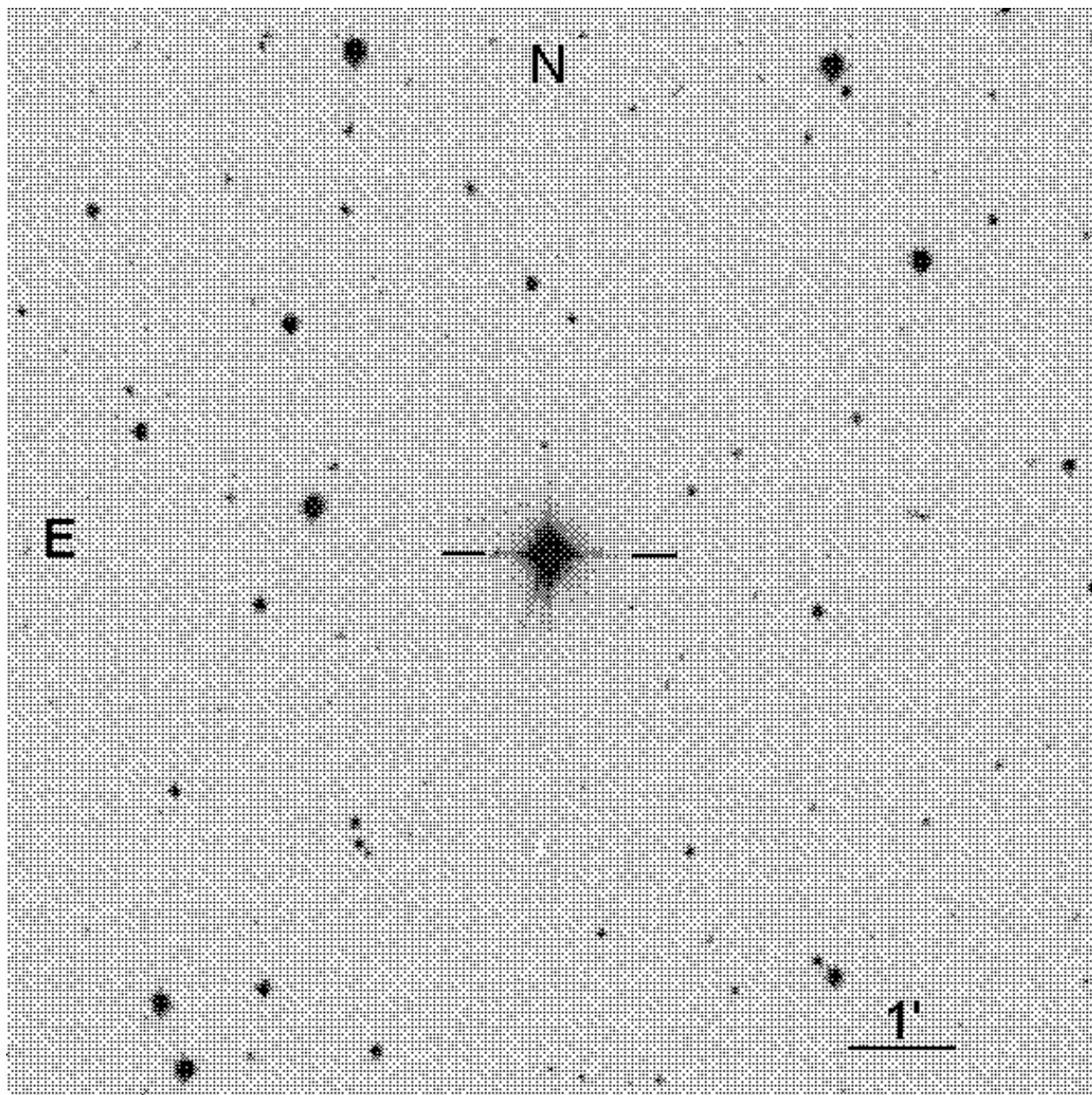


Fig. 20.— The field, 10 arc minutes on a side, of the star BD+75°325.



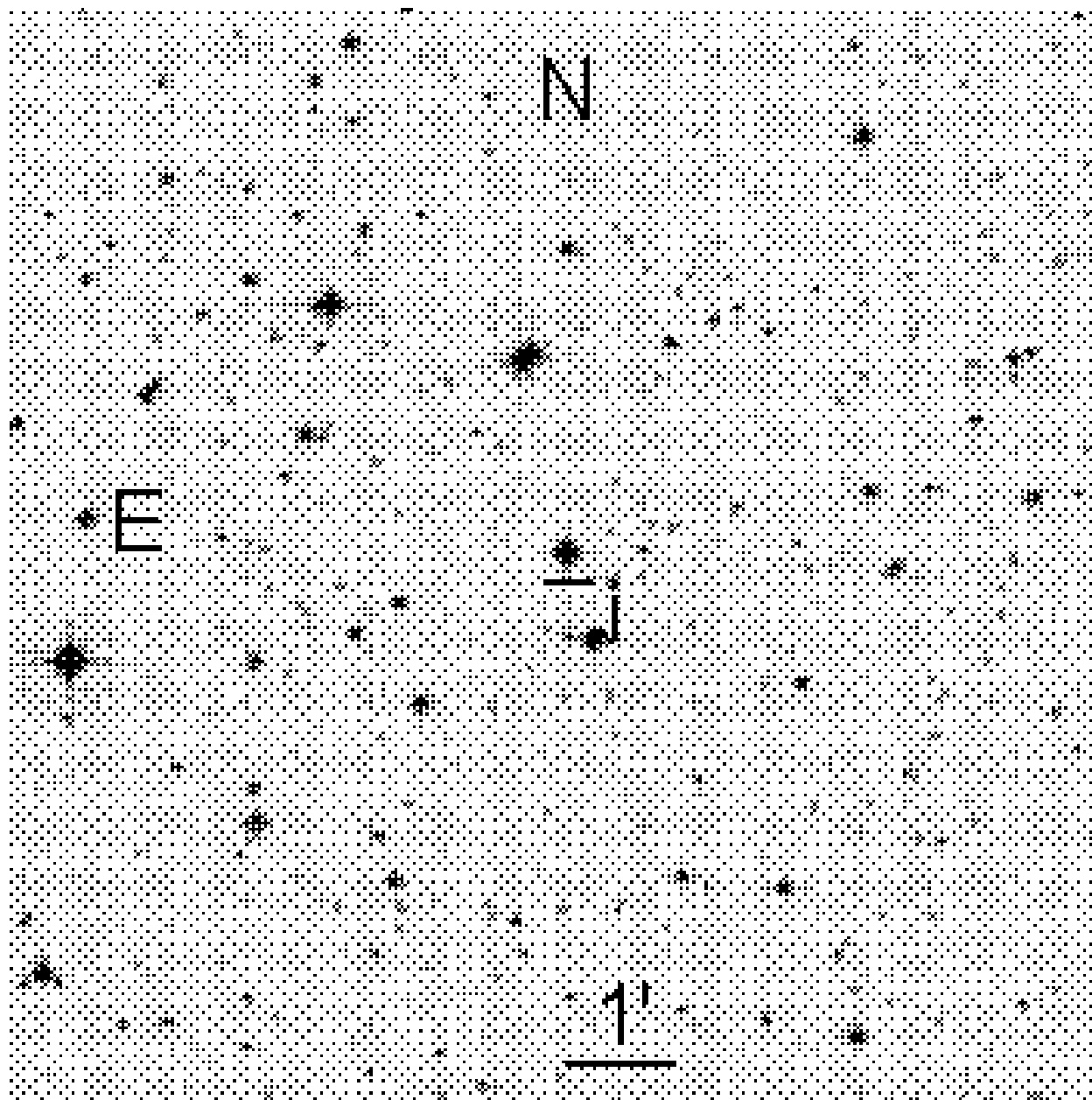


Fig. 21.— The field, 10 arc minutes on a side, of the star LDS 235B.

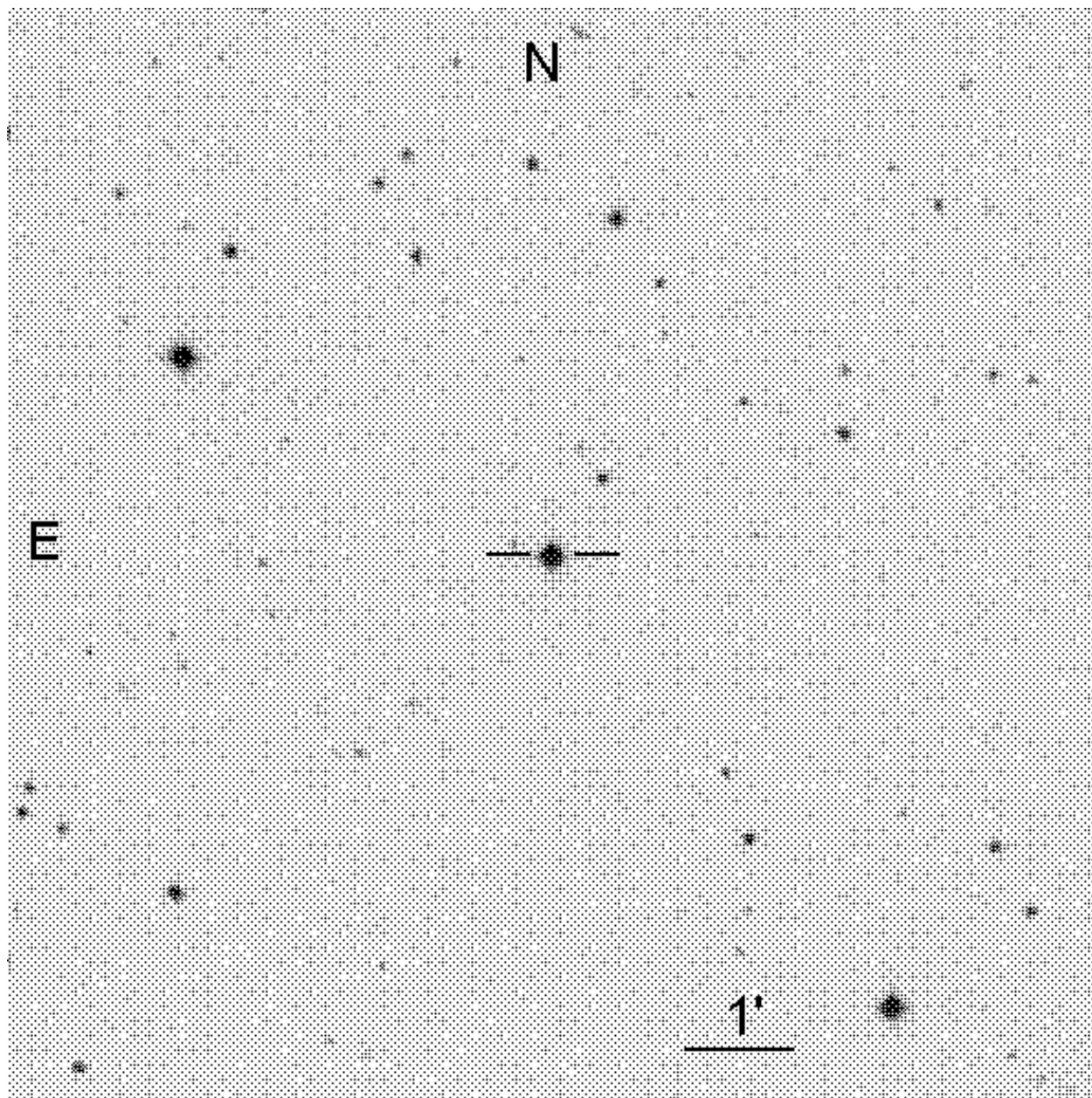


Fig. 22.— The field, 10 arc minutes on a side, of the star AGK+81°266.

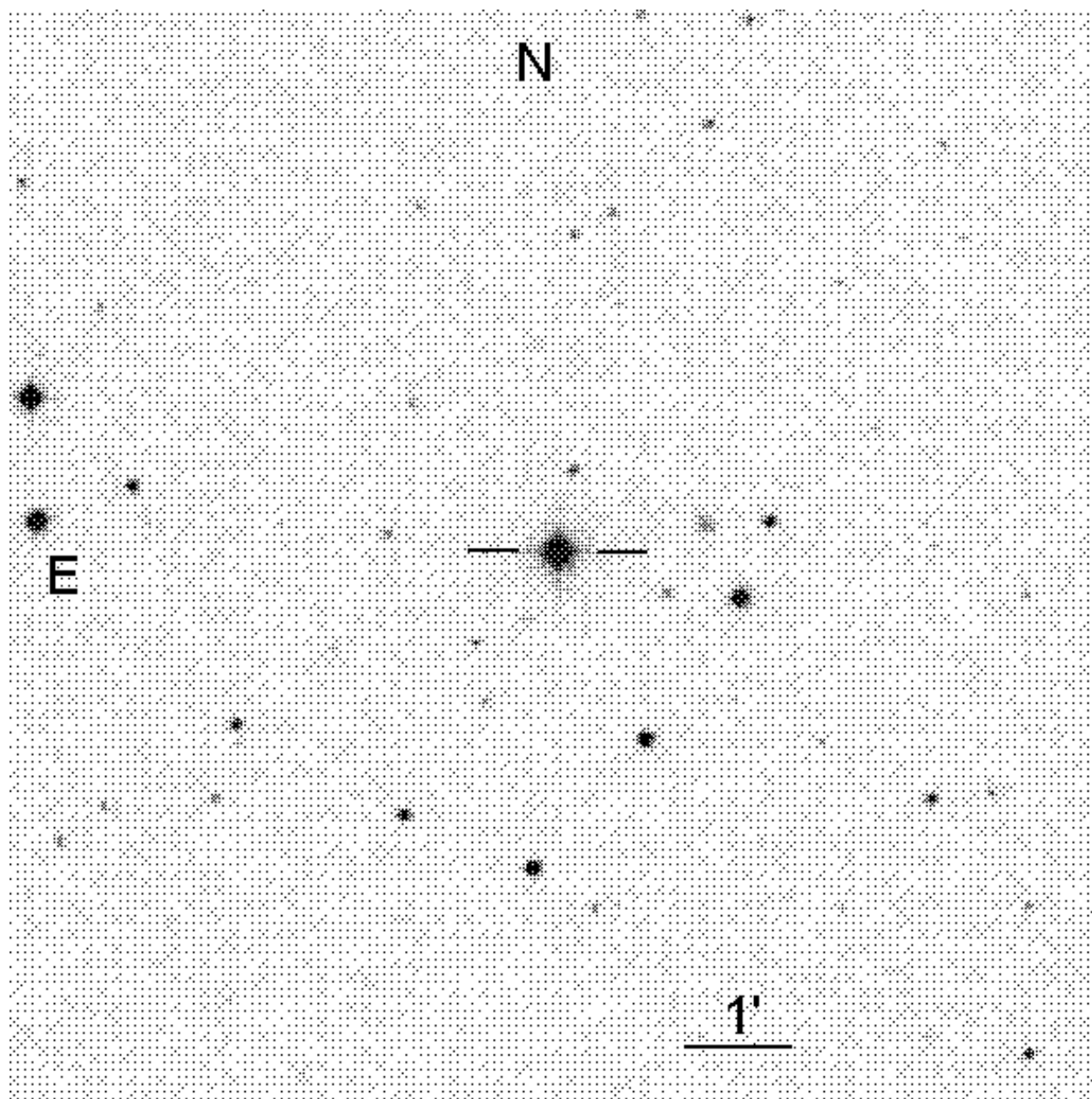


Fig. 23.— The field, 10 arc minutes on a side, of the star Feige 34.

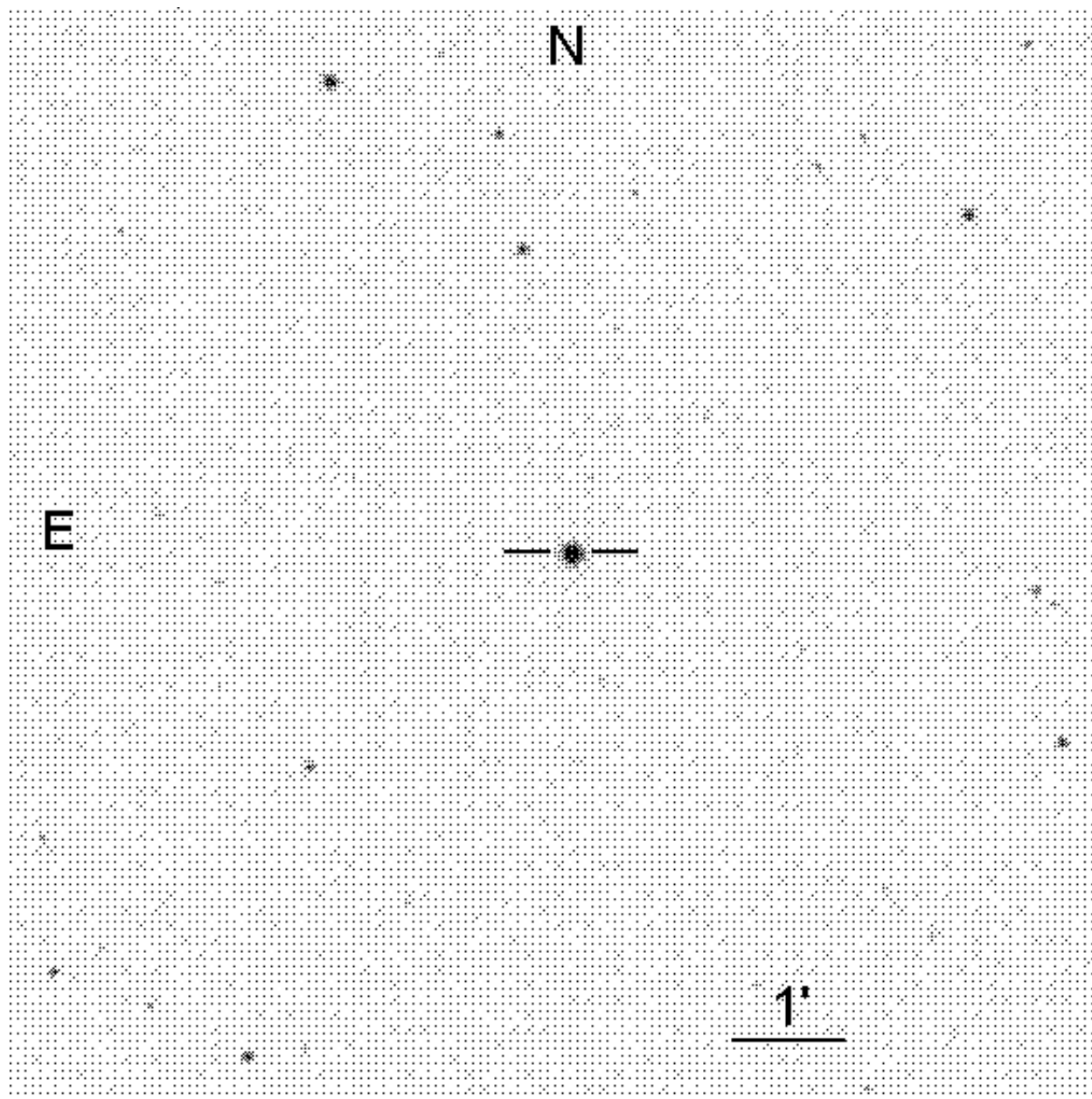


Fig. 24.— The field, 10 arc minutes on a side, of the star GD 140.

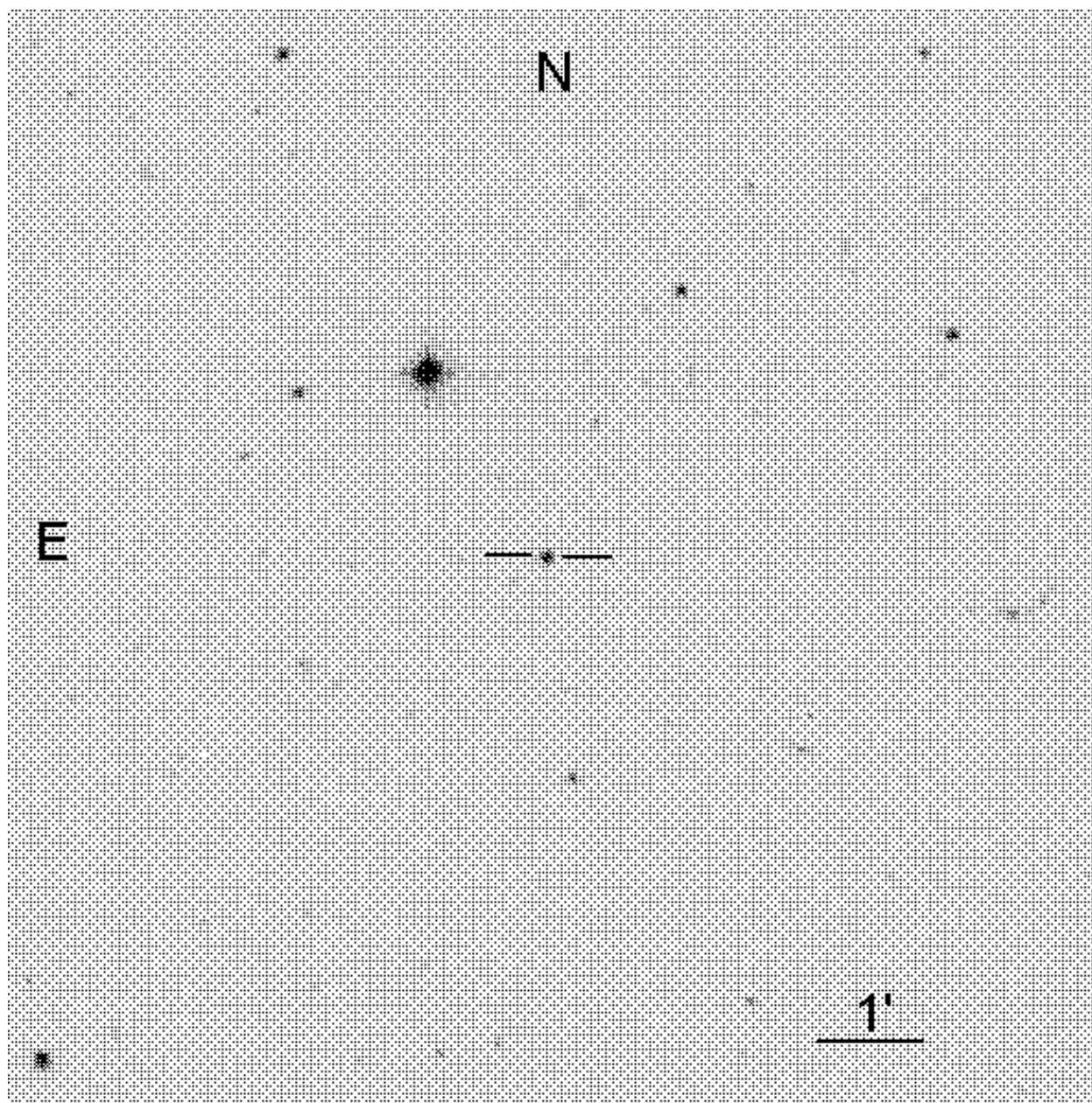


Fig. 25.— The field, 10 arc minutes on a side, of the star HZ 21.

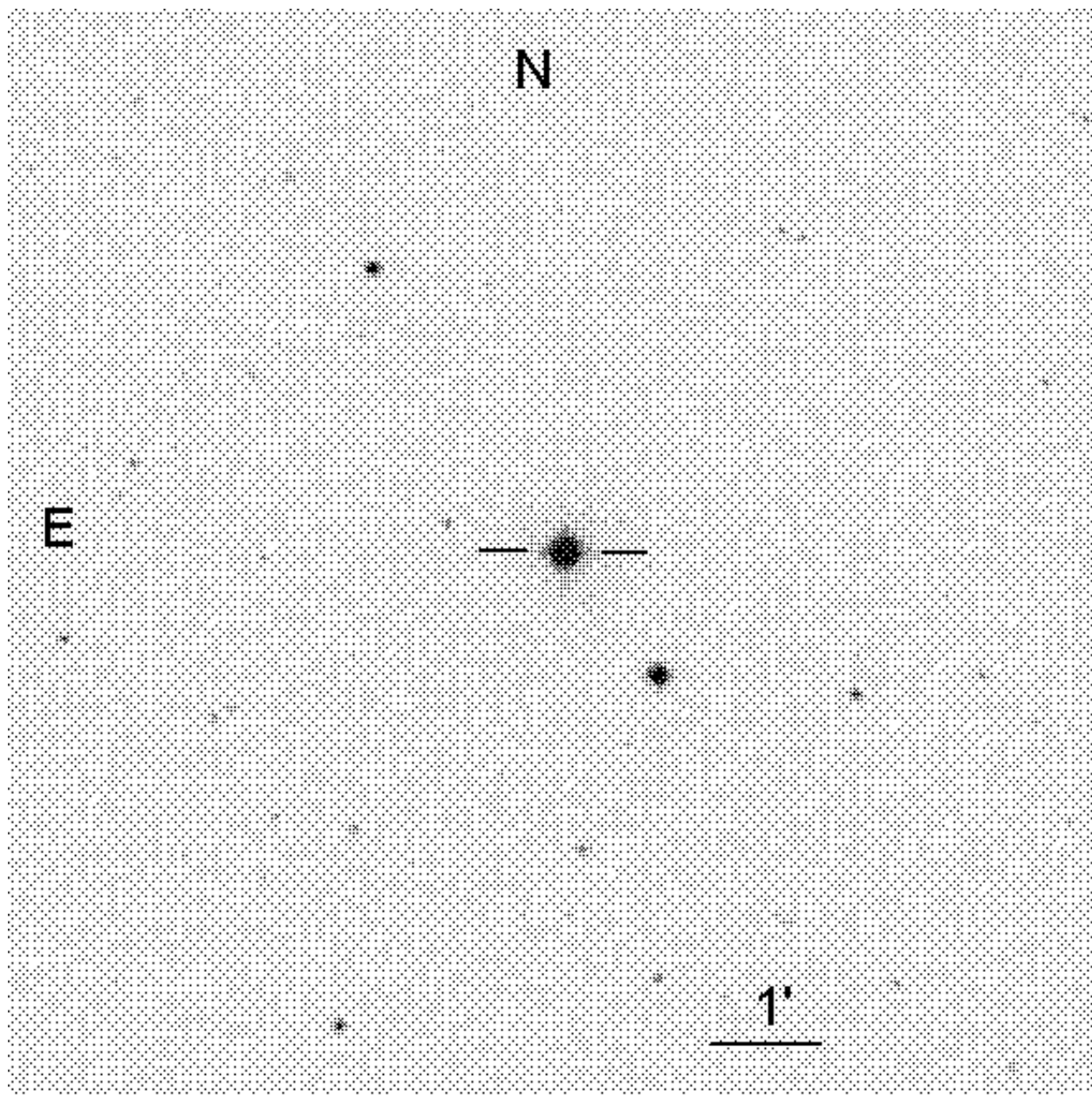


Fig. 26.— The field, 10 arc minutes on a side, of the star Feige 66.

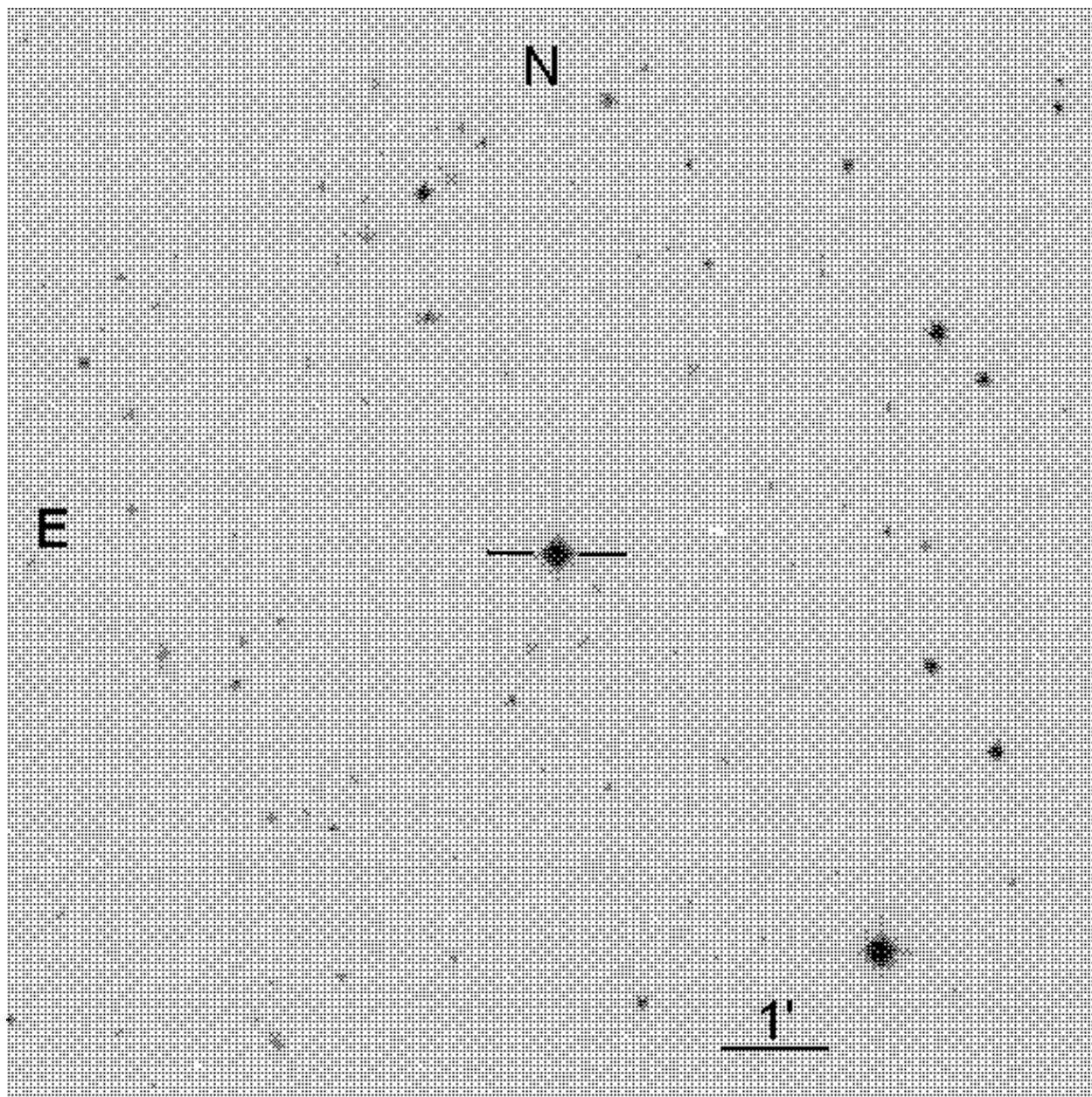


Fig. 27.— The field, 10 arc minutes on a side, of the star Feige 67.

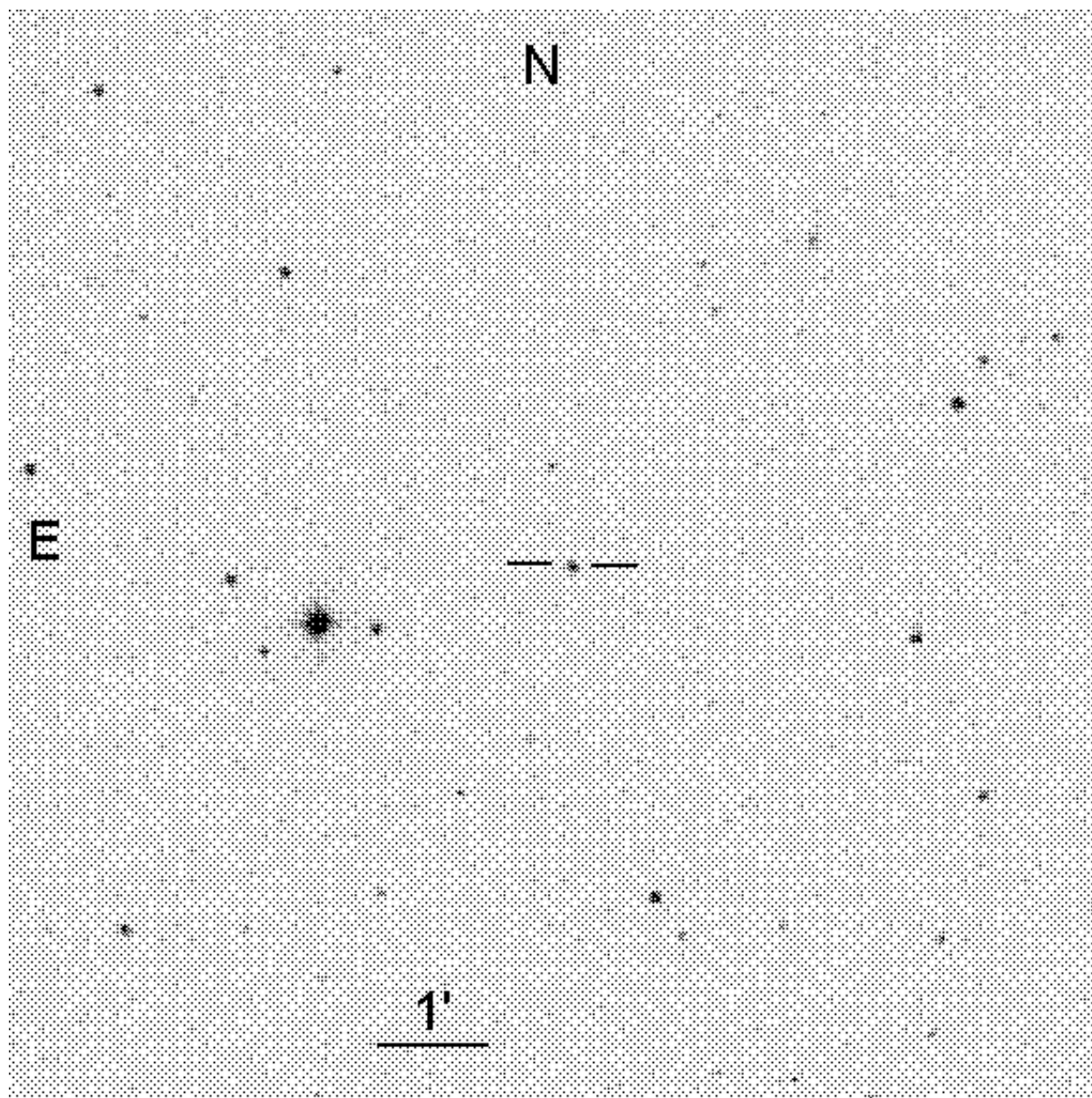


Fig. 28.— The field, 10 arc minutes on a side, of the star G 60-54.



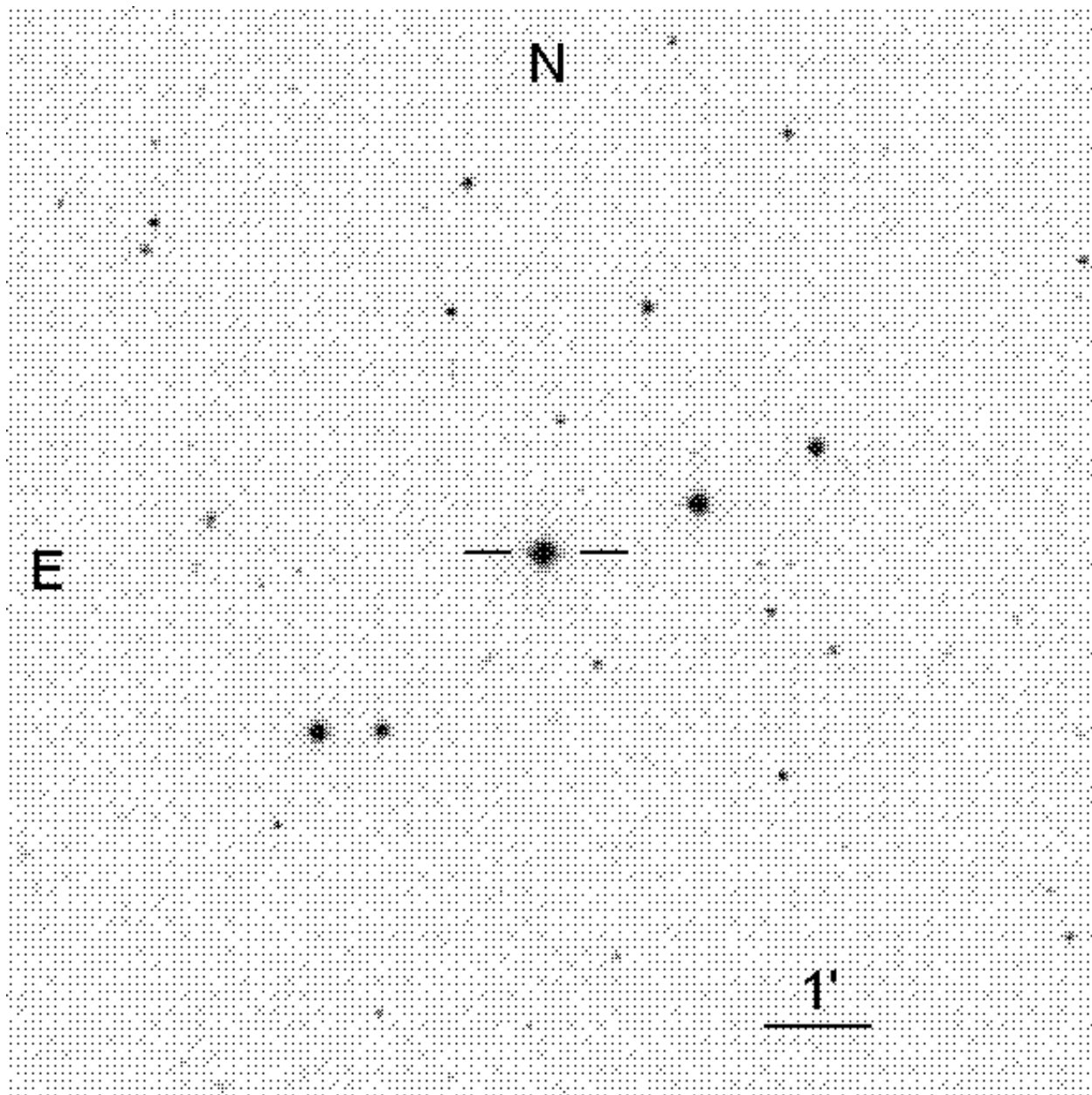


Fig. 29.— The field, 10 arc minutes on a side, of the star HZ 44.

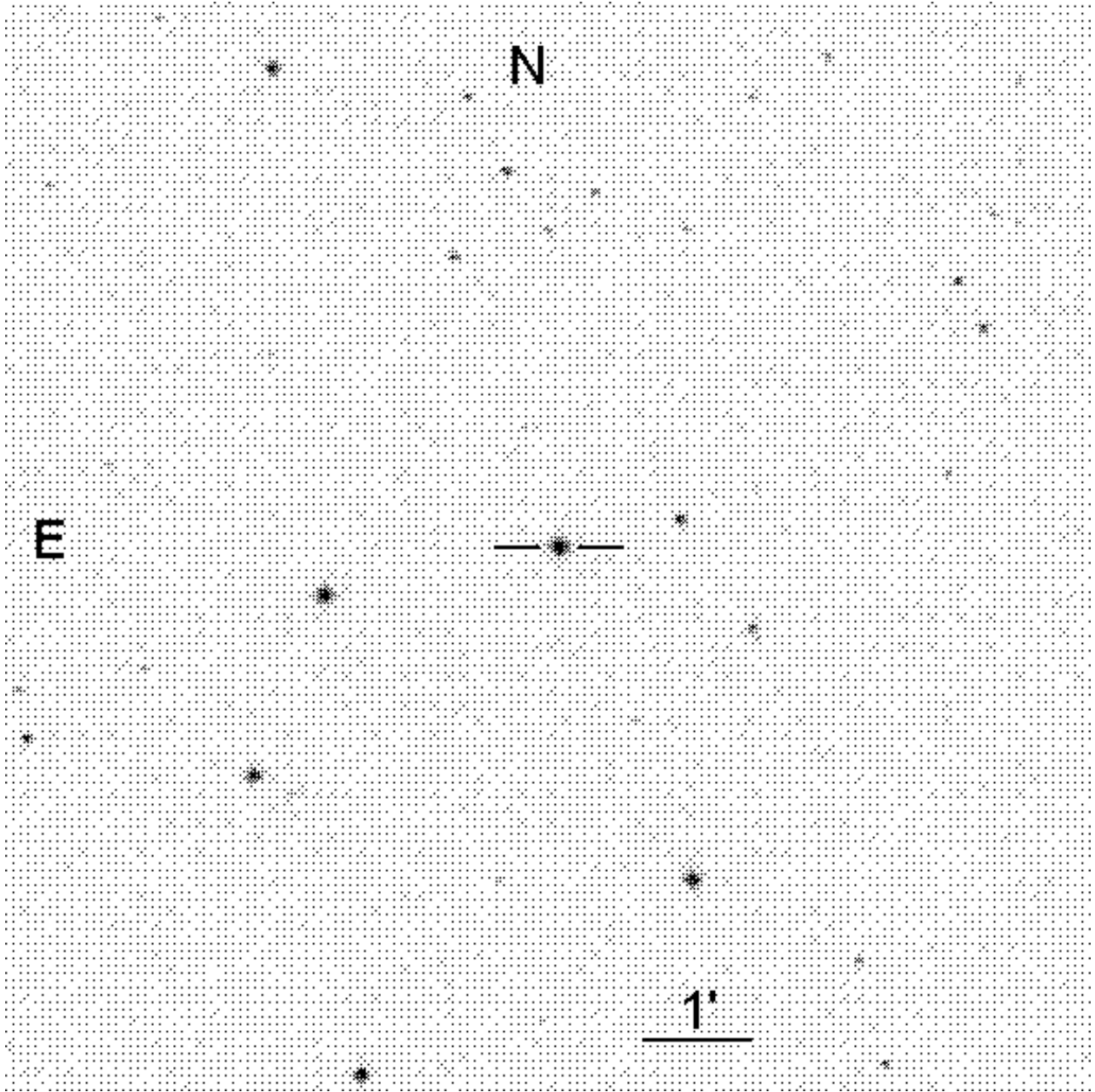


Fig. 30.— The field, 10 arc minutes on a side, of the star GRW+70°5824.

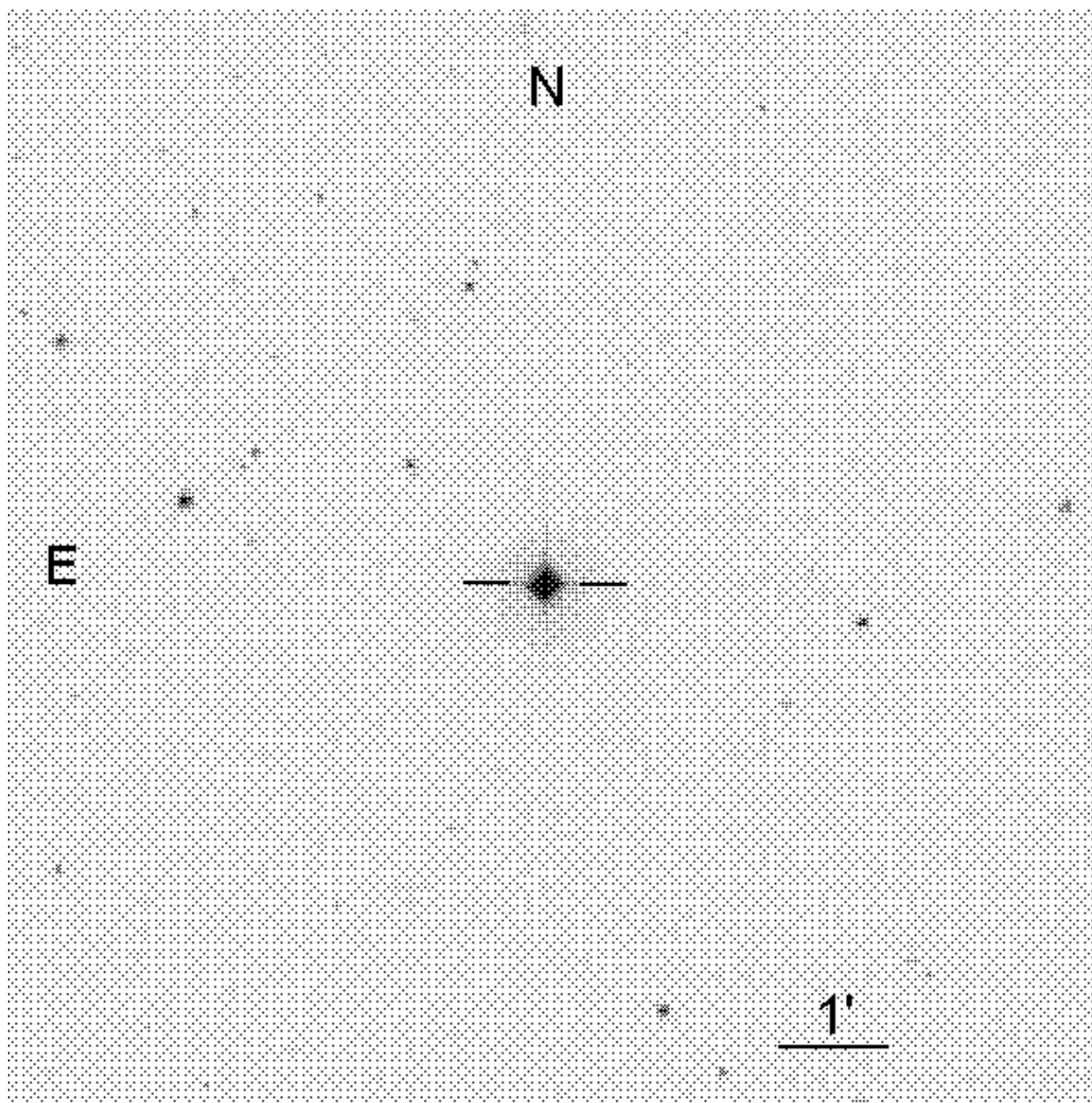


Fig. 31.— The field, 10 arc minutes on a side, of the star BD+26°2606.

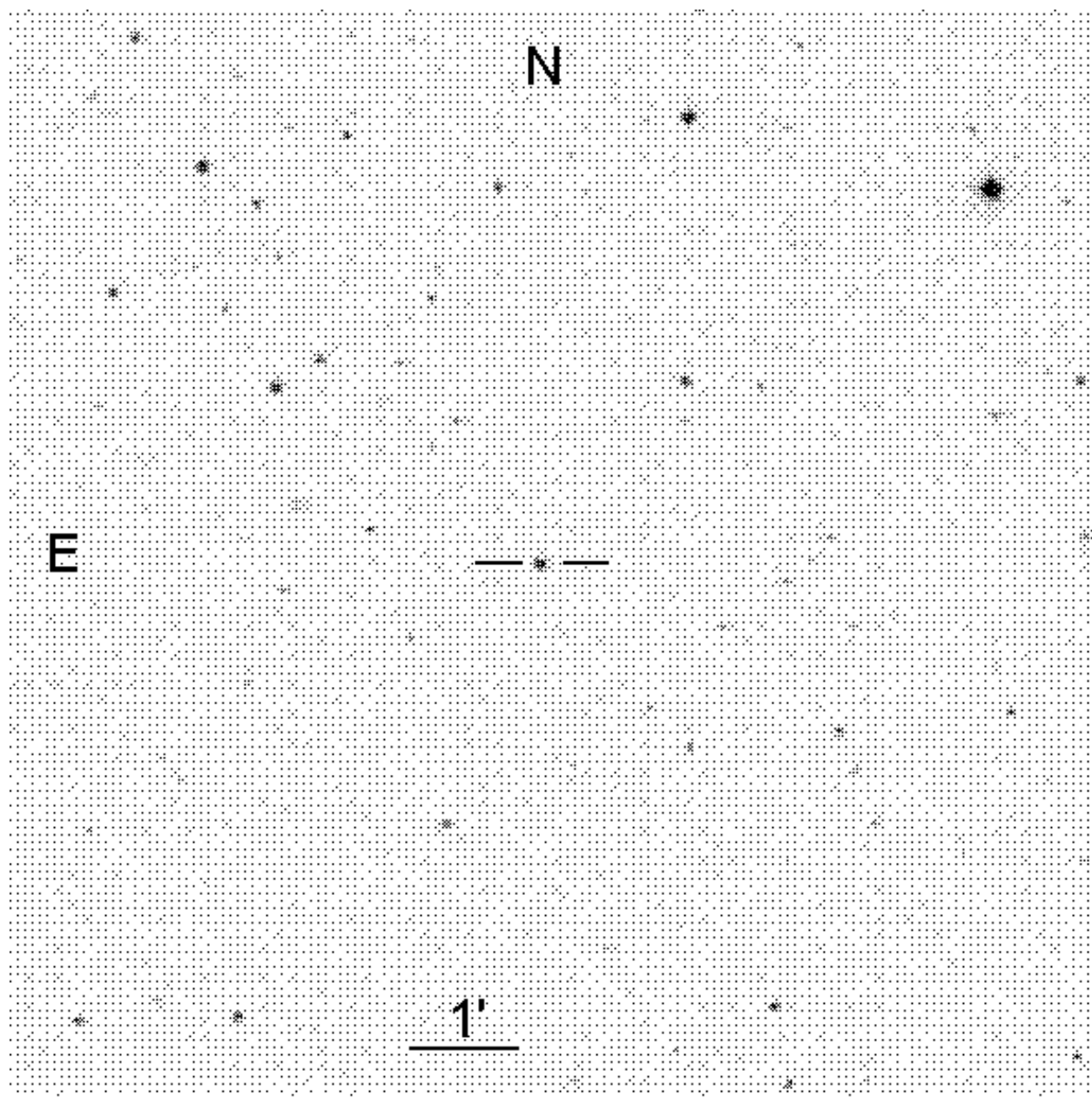


Fig. 32.— The field, 10 arc minutes on a side, of the star GD 190.

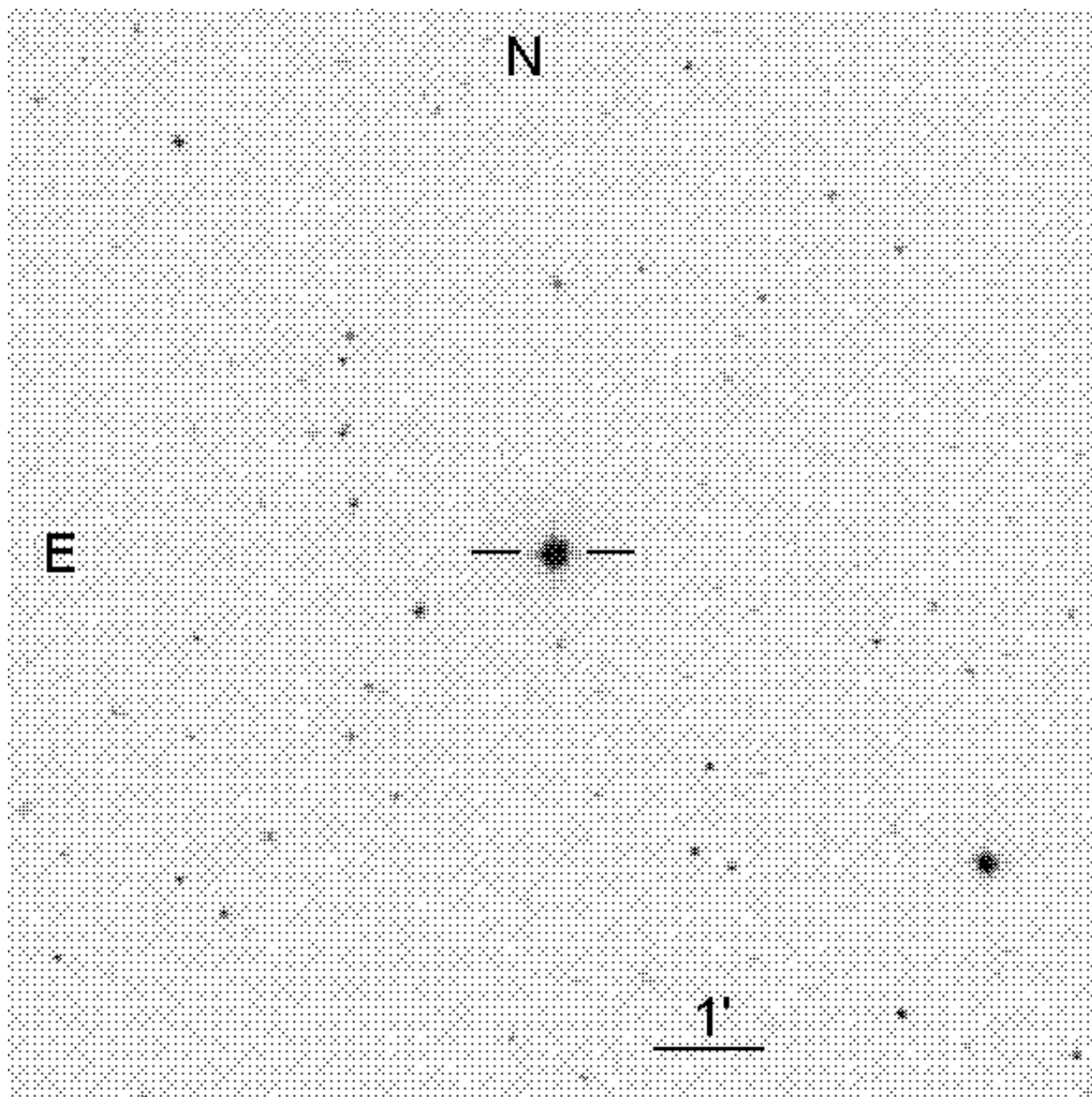


Fig. 33.— The field, 10 arc minutes on a side, of the star BD+33°2642.

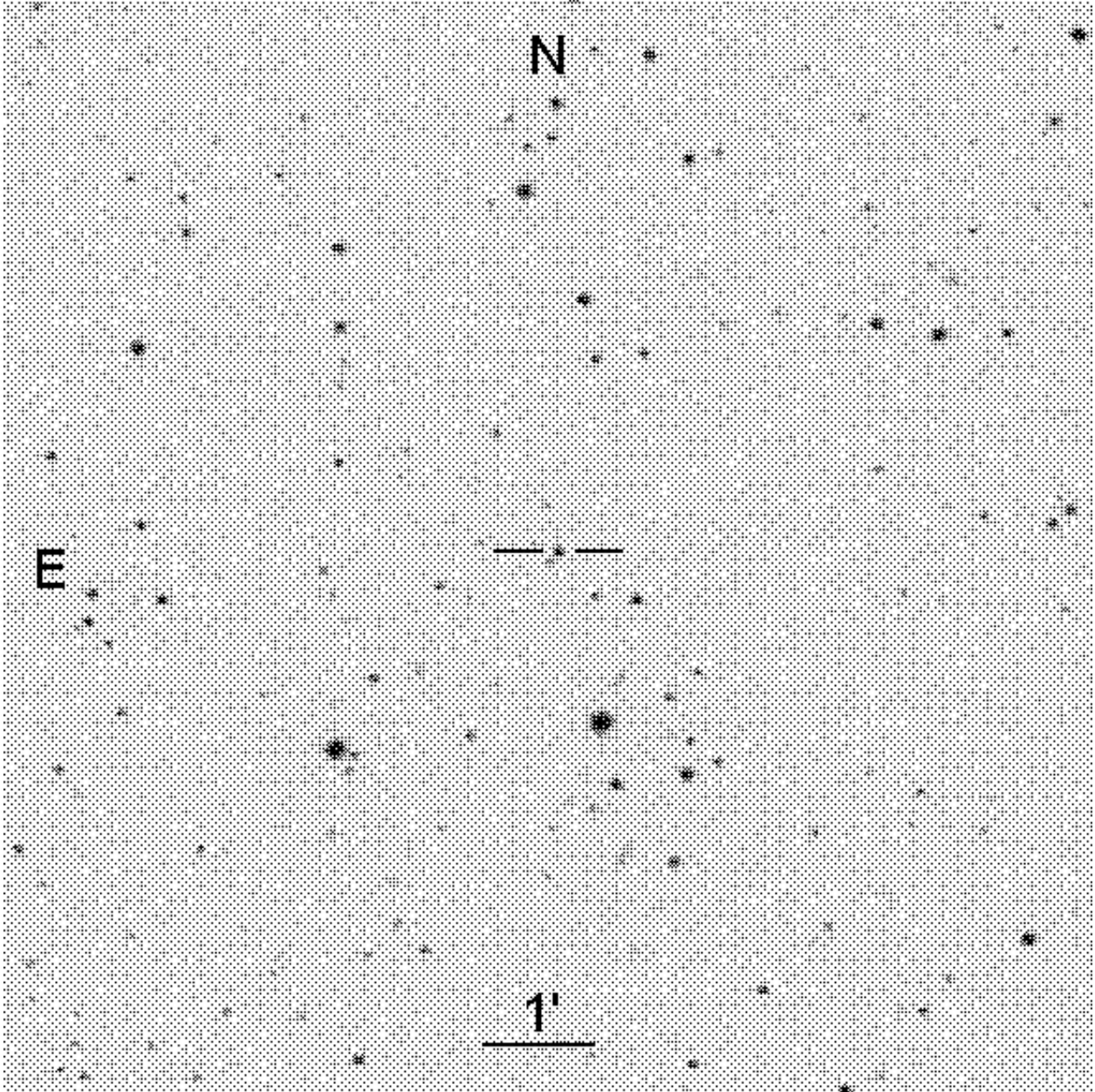


Fig. 34.— The field, 10 arc minutes on a side, of the star G 138-31.

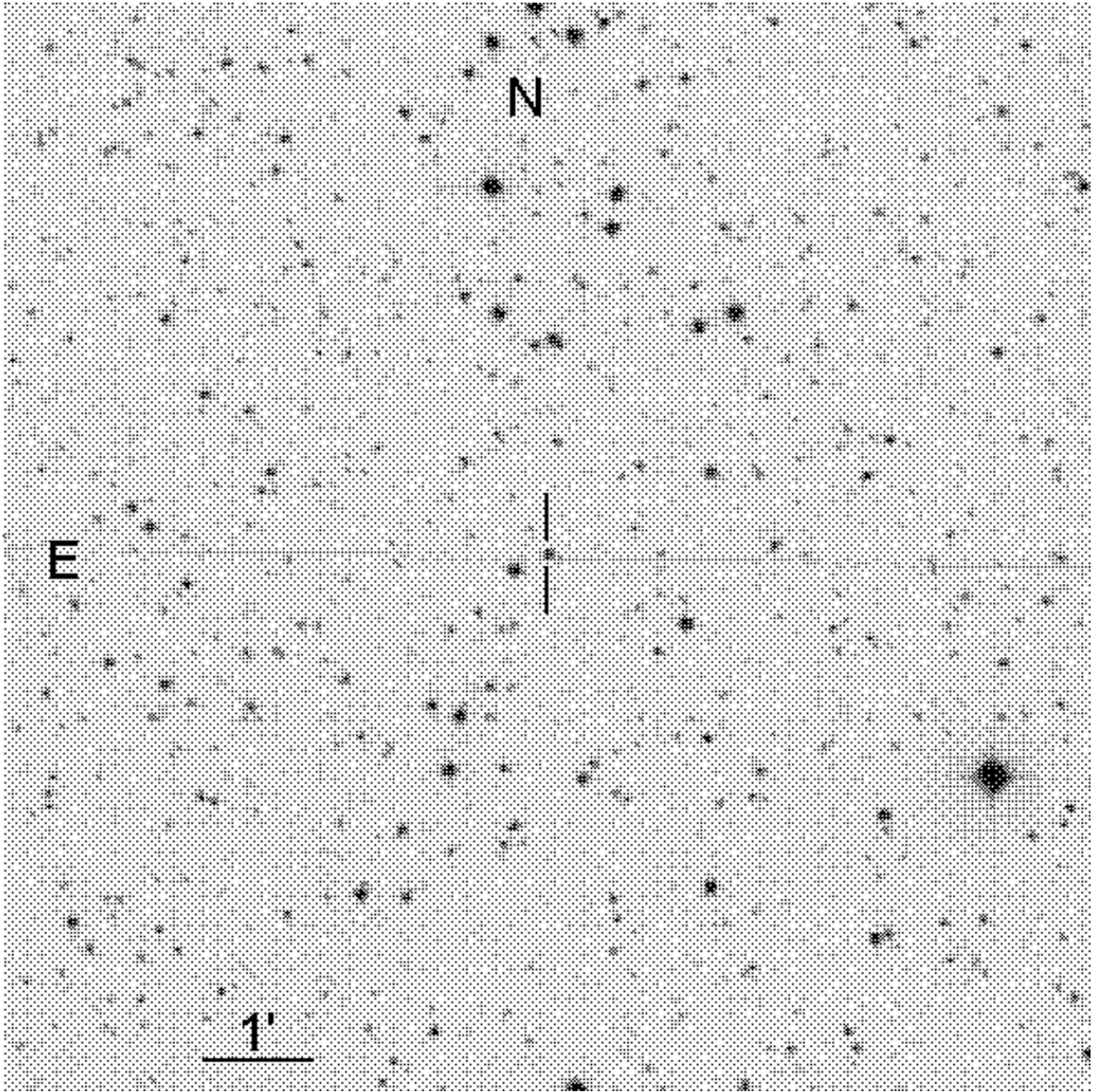


Fig. 35.— The field, 10 arc minutes on a side, of the star G 24-9.

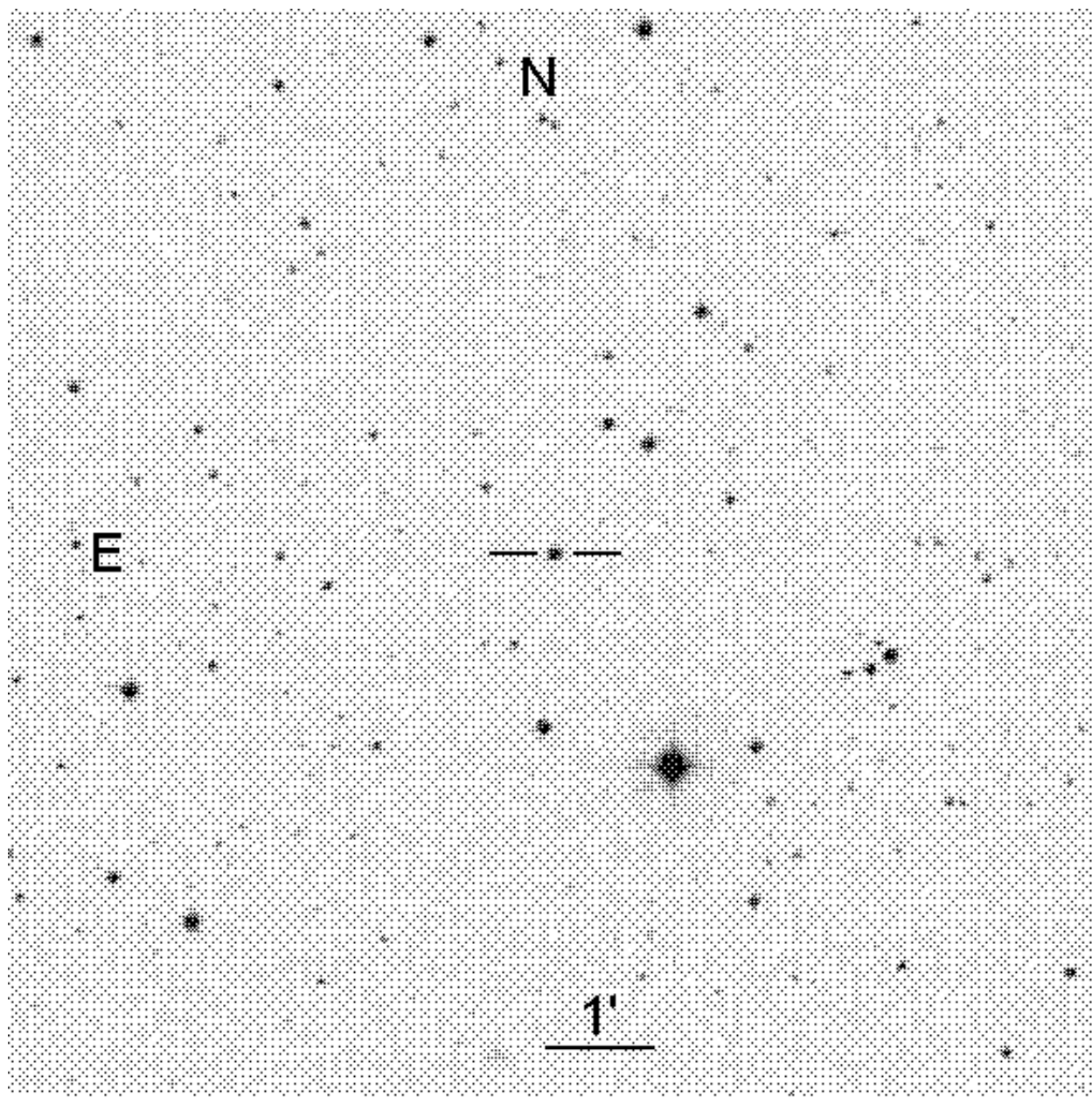


Fig. 36.— The field, 10 arc minutes on a side, of the star LDS 749B.



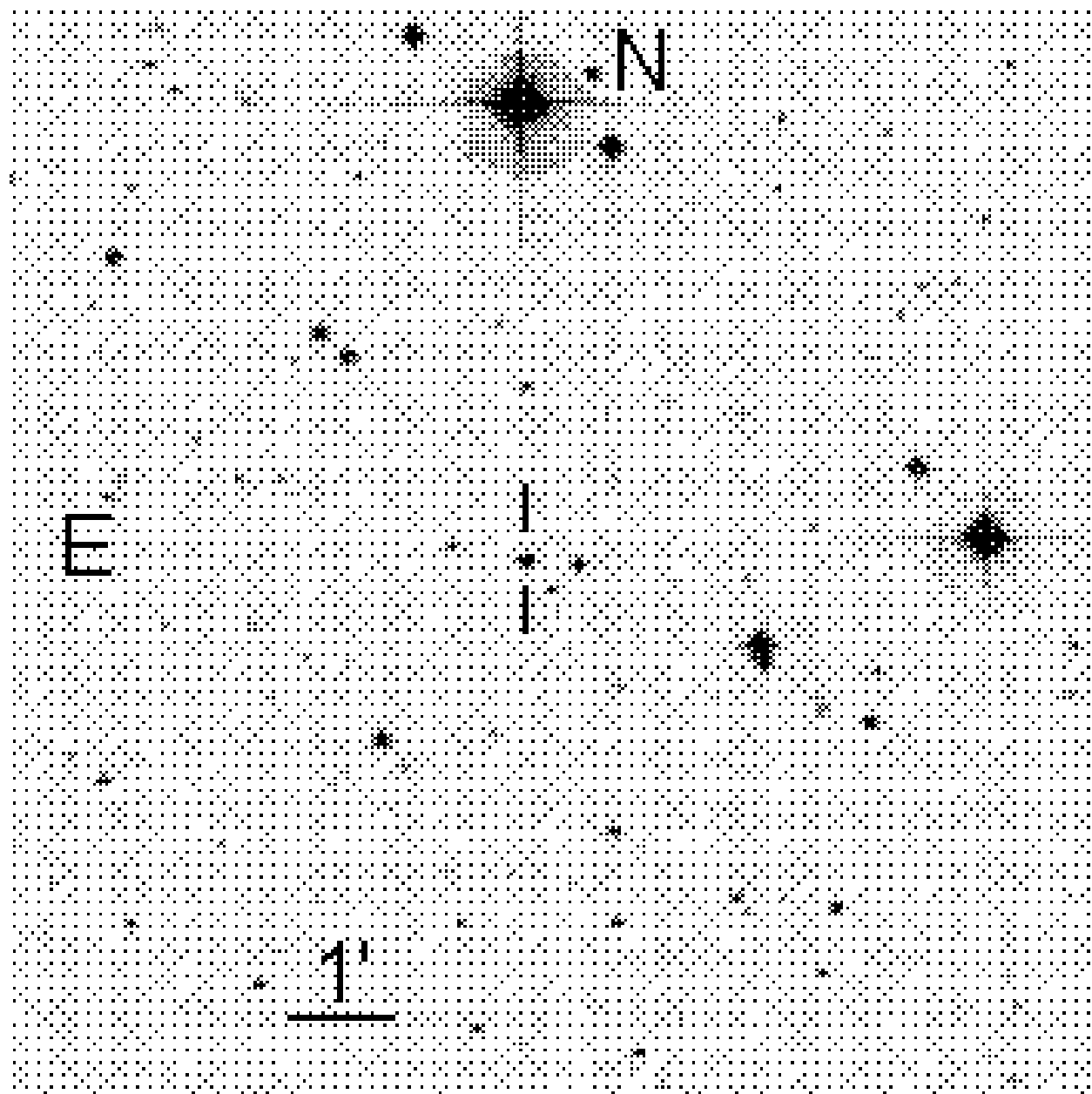


Fig. 37.— The field, 10 arc minutes on a side, of the star L 930-80

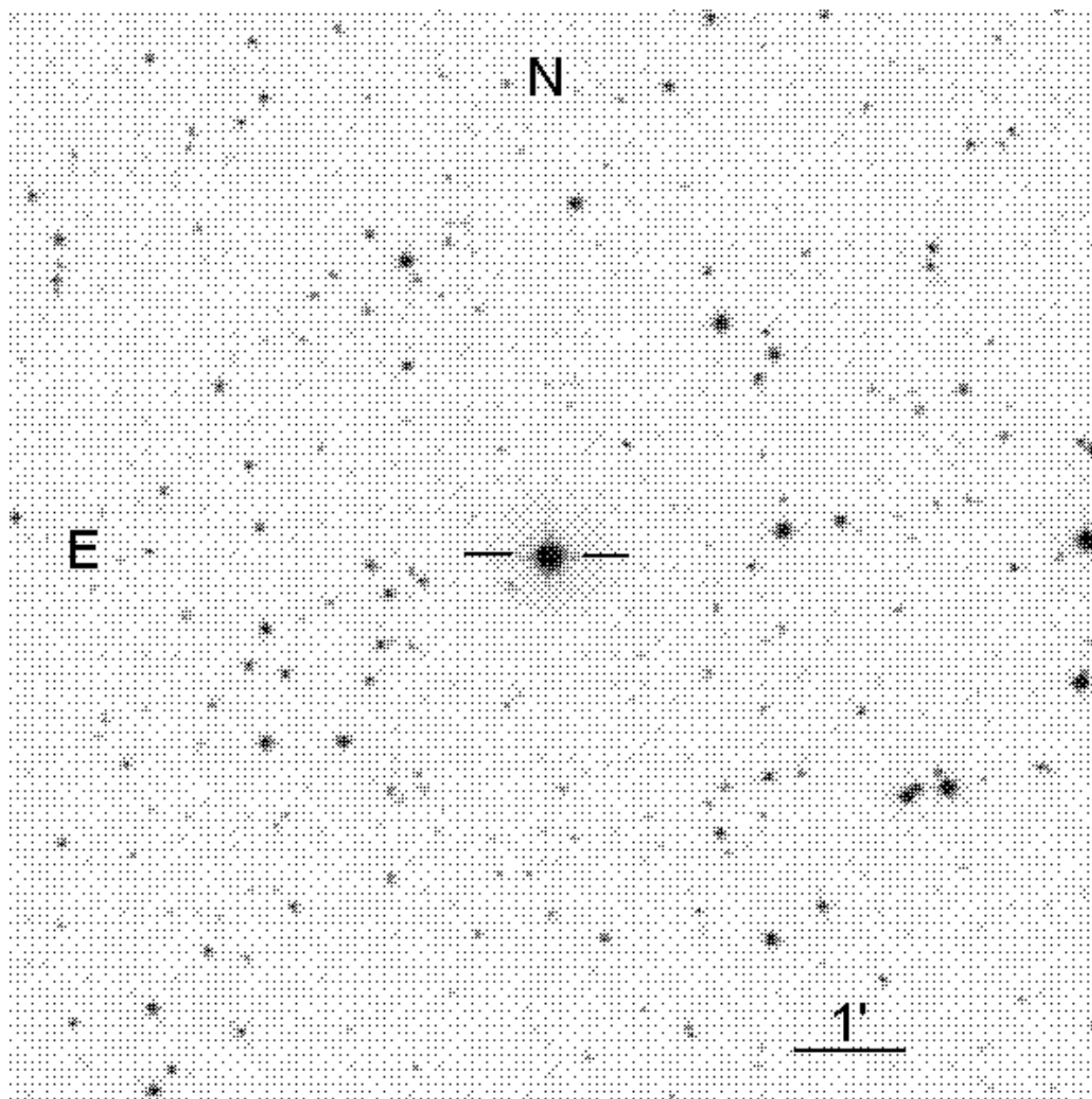


Fig. 38.— The field, 10 arc minutes on a side, of the star BD+28°4211.

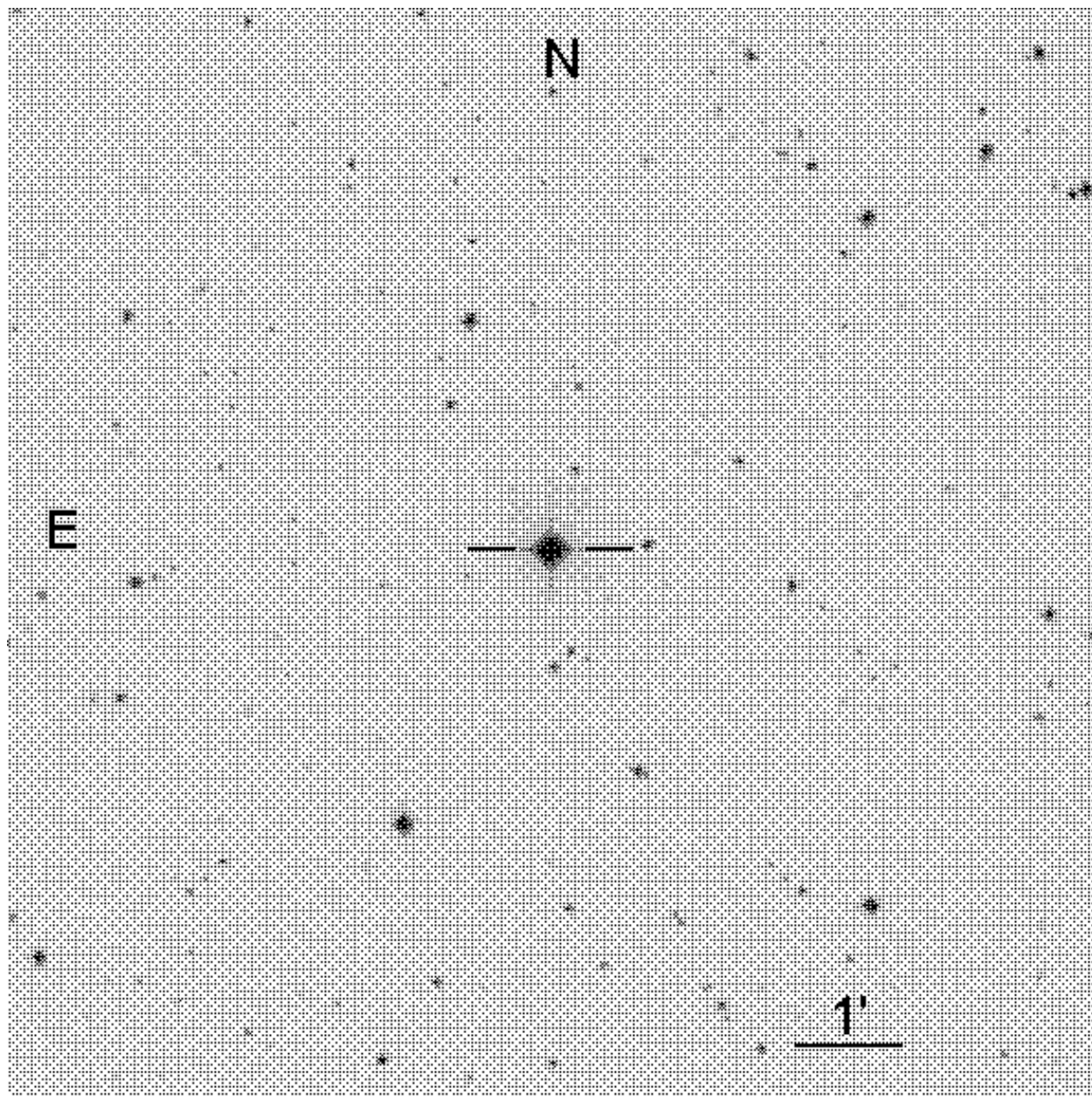


Fig. 39.— The field, 10 arc minutes on a side, of the star BD+17°4708.

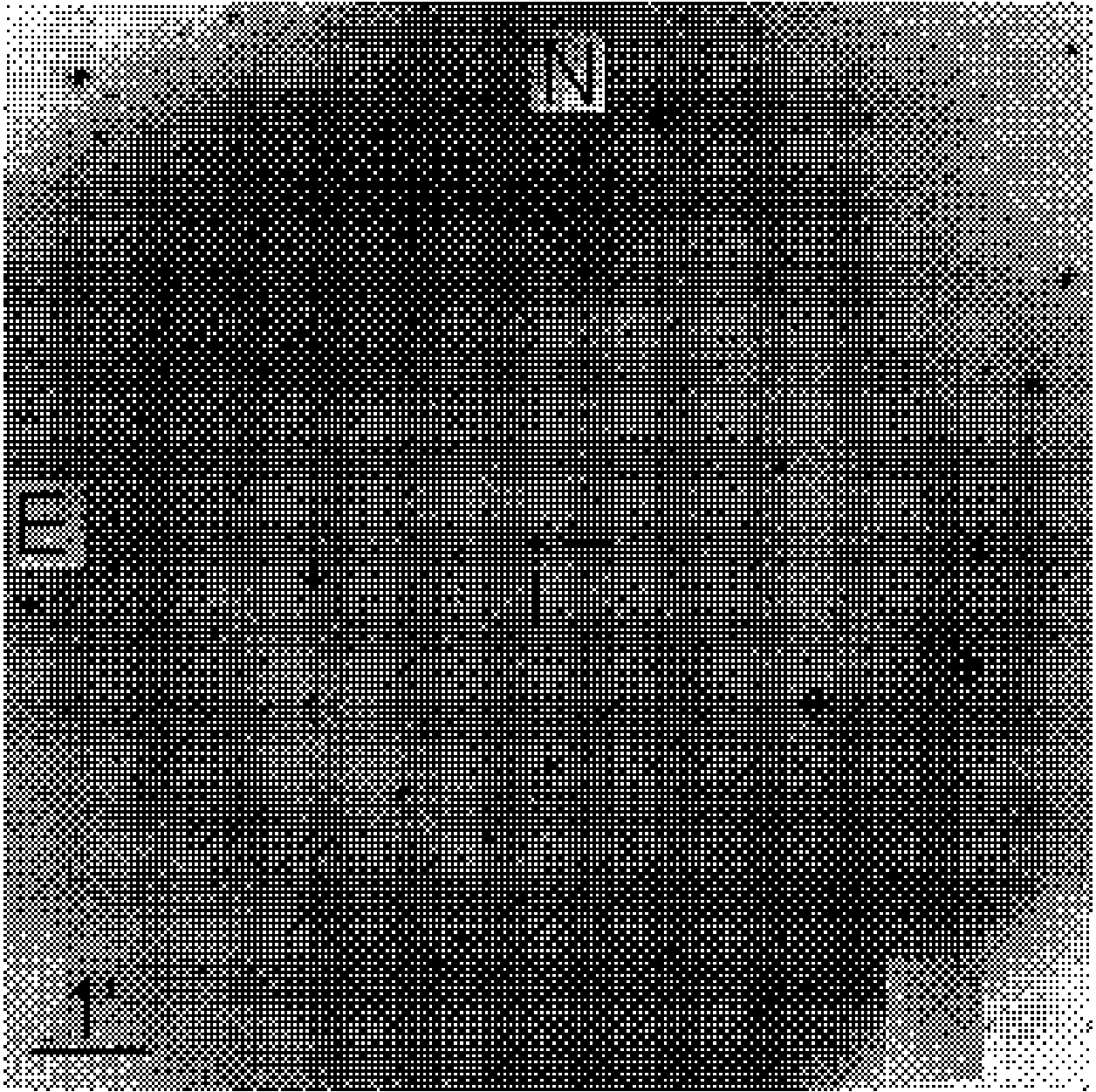


Fig. 40.— The field, 10 arc minutes on a side, of the planetary nebula NGC 7293.

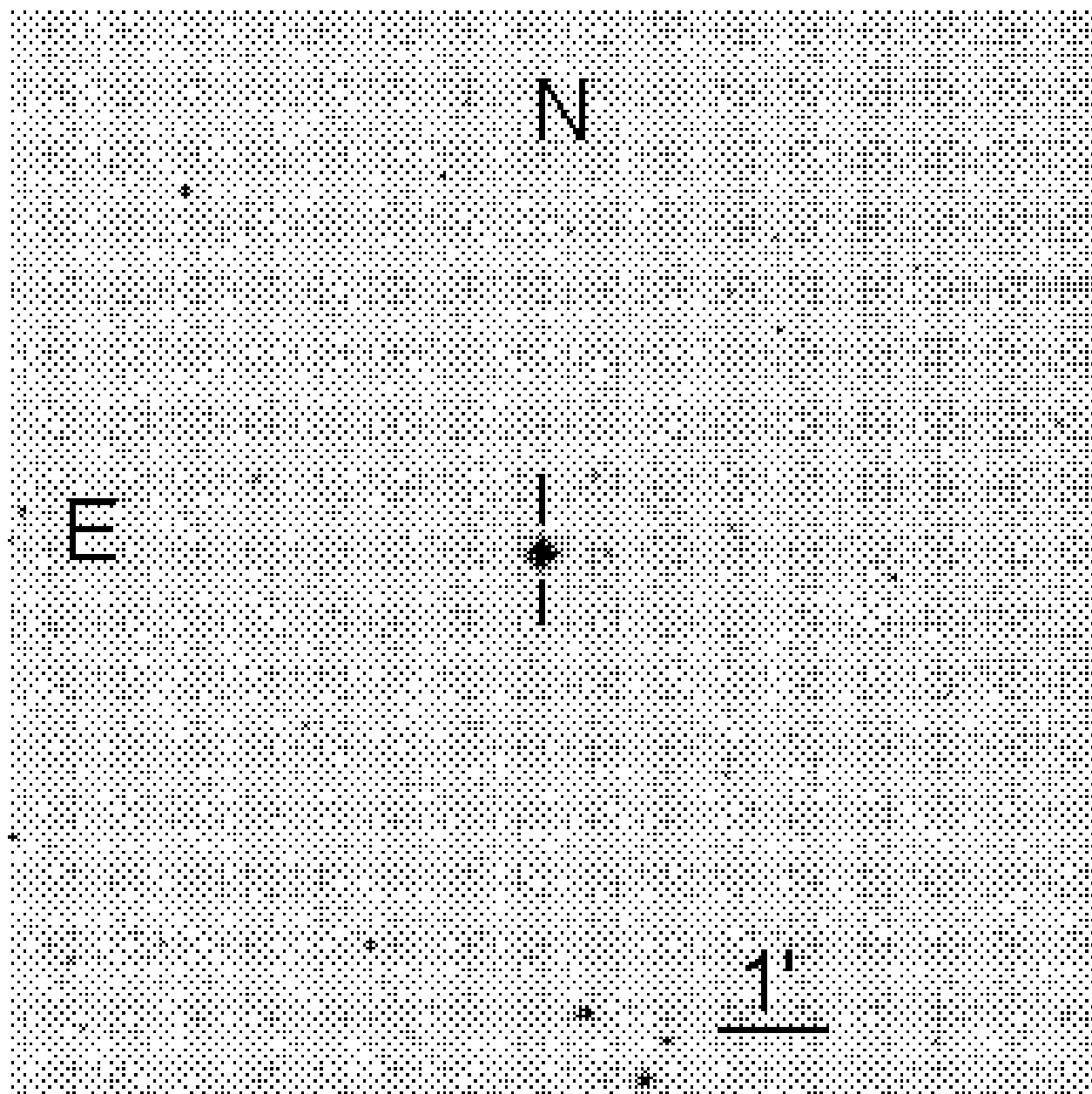


Fig. 41.— The field, 10 arc minutes on a side, of the star Feige 110.

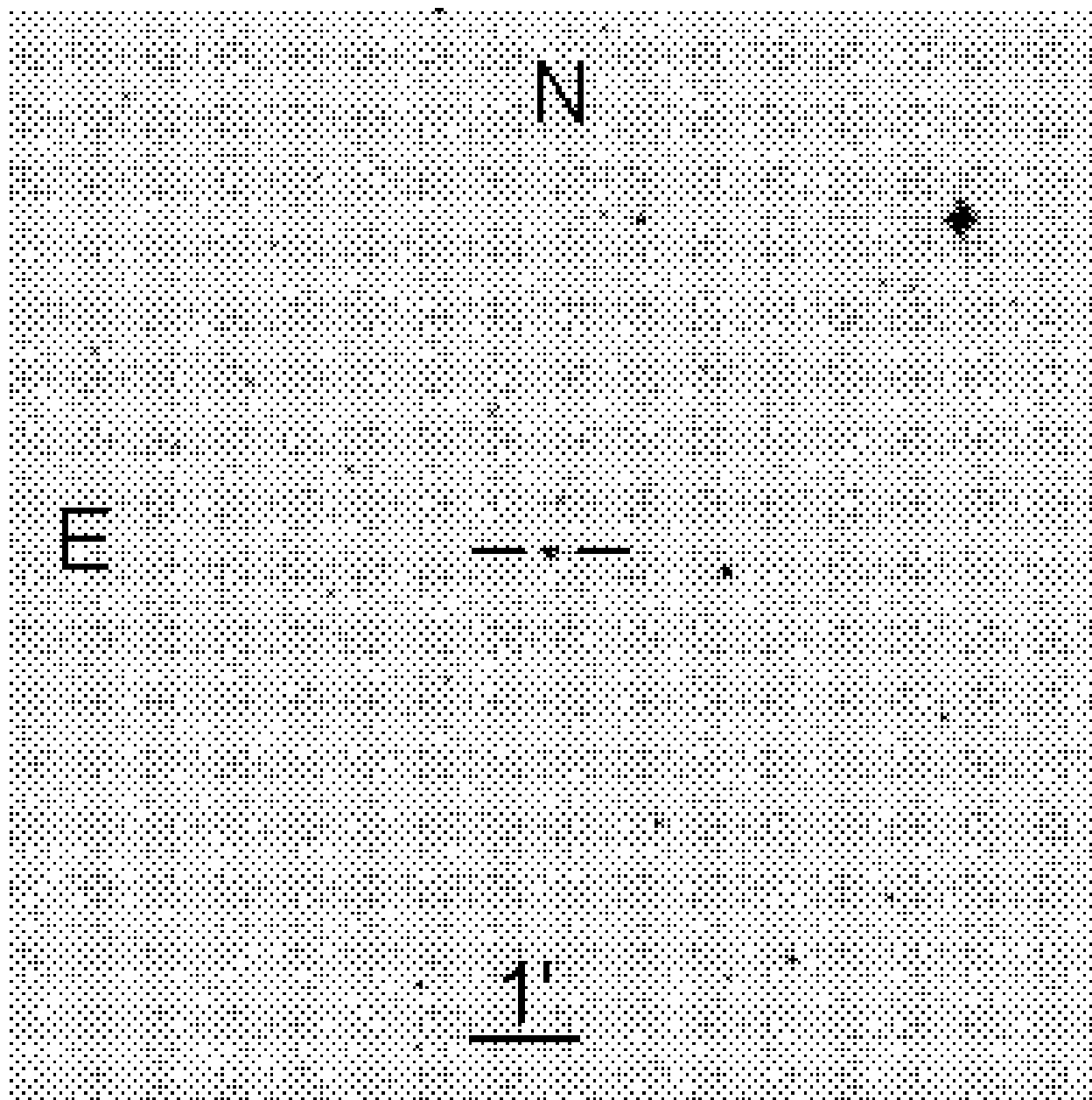


Fig. 42.— The field, 10 arc minutes on a side, of the star LTT 9491.

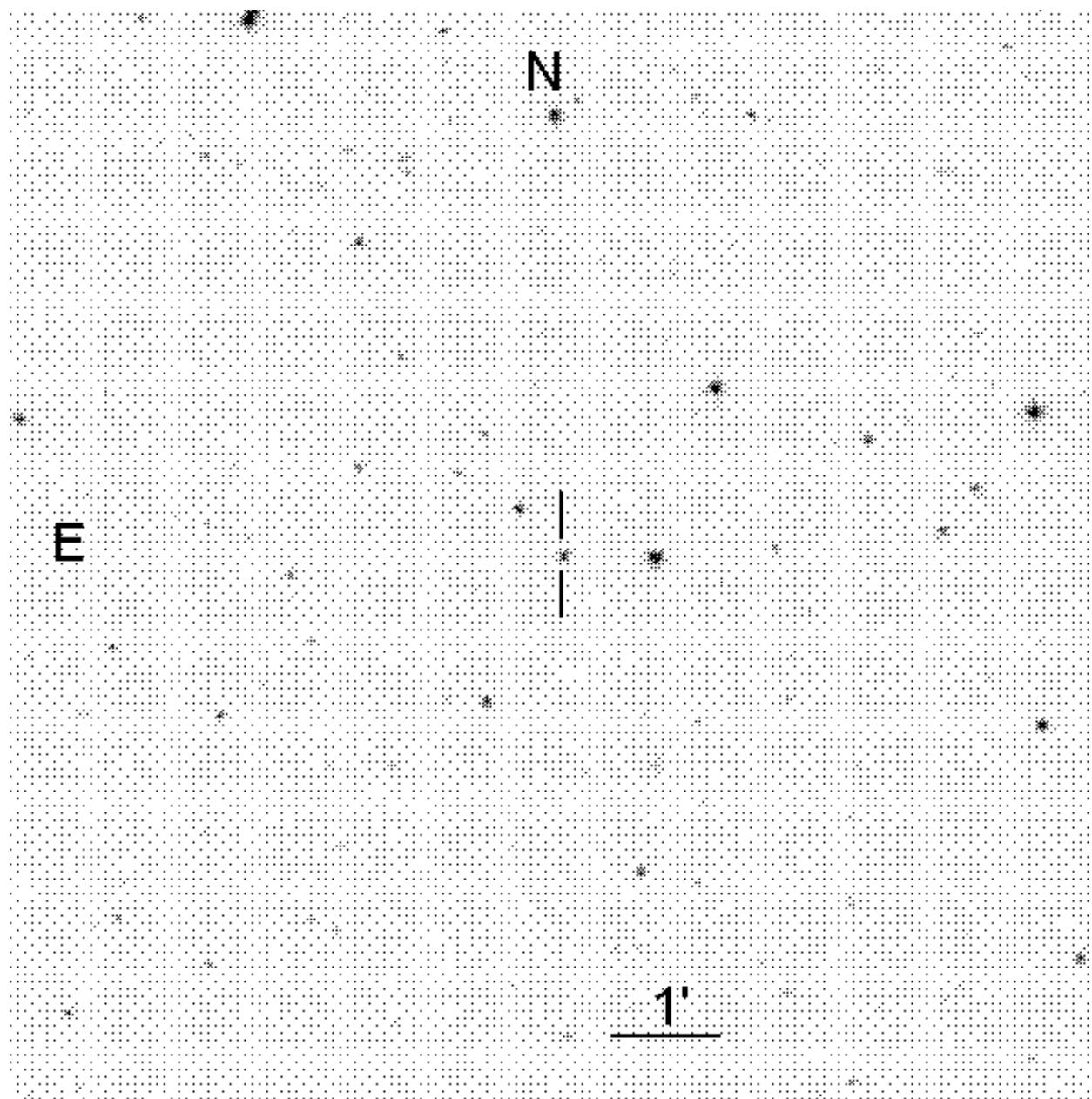


Fig. 43.— The field, 10 arc minutes on a side, of the star GD 248.

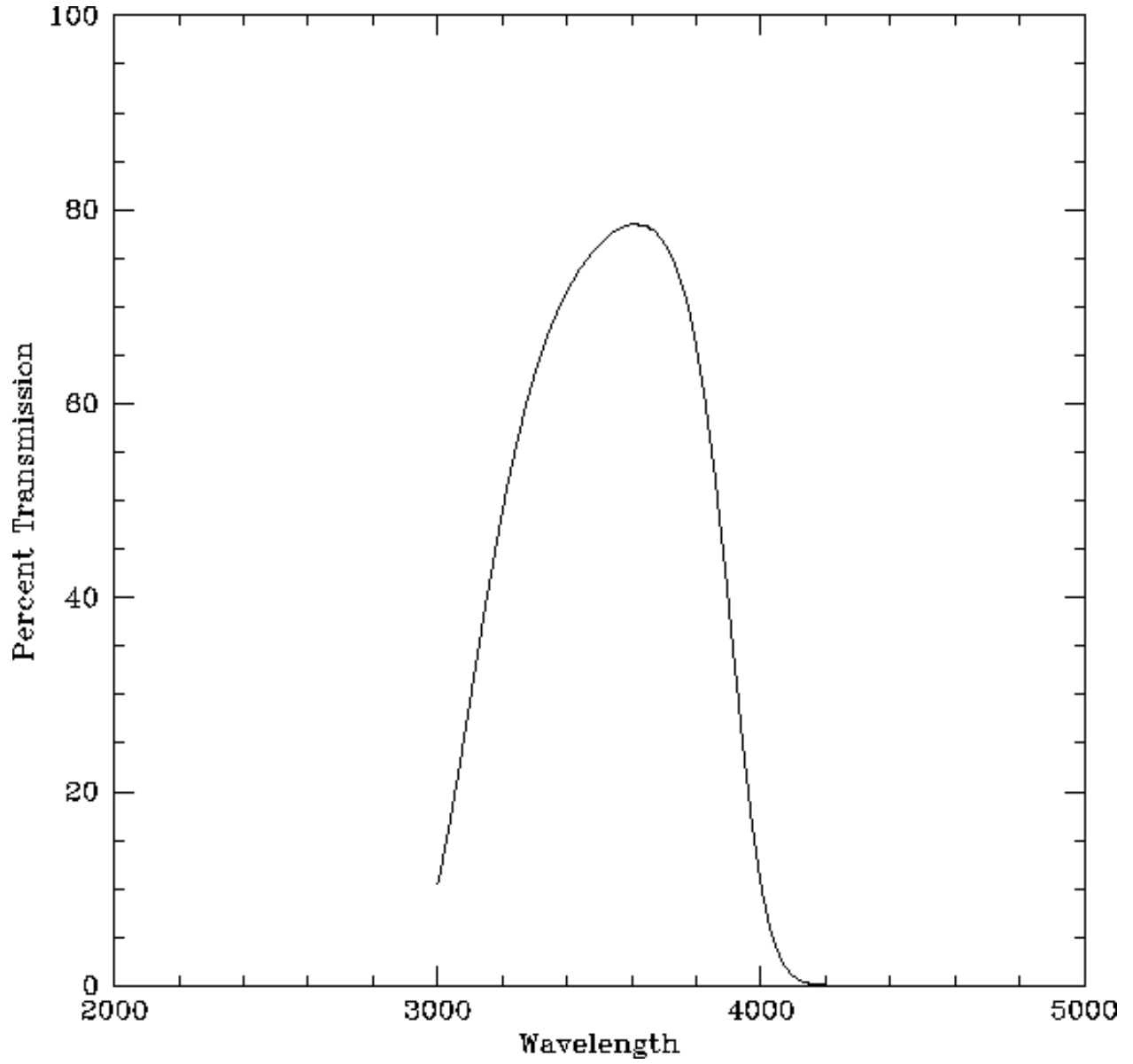


Fig. 44.— The transmission characteristics of the *U* filter: 1mm UG 2 + CuSO<sub>4</sub>.



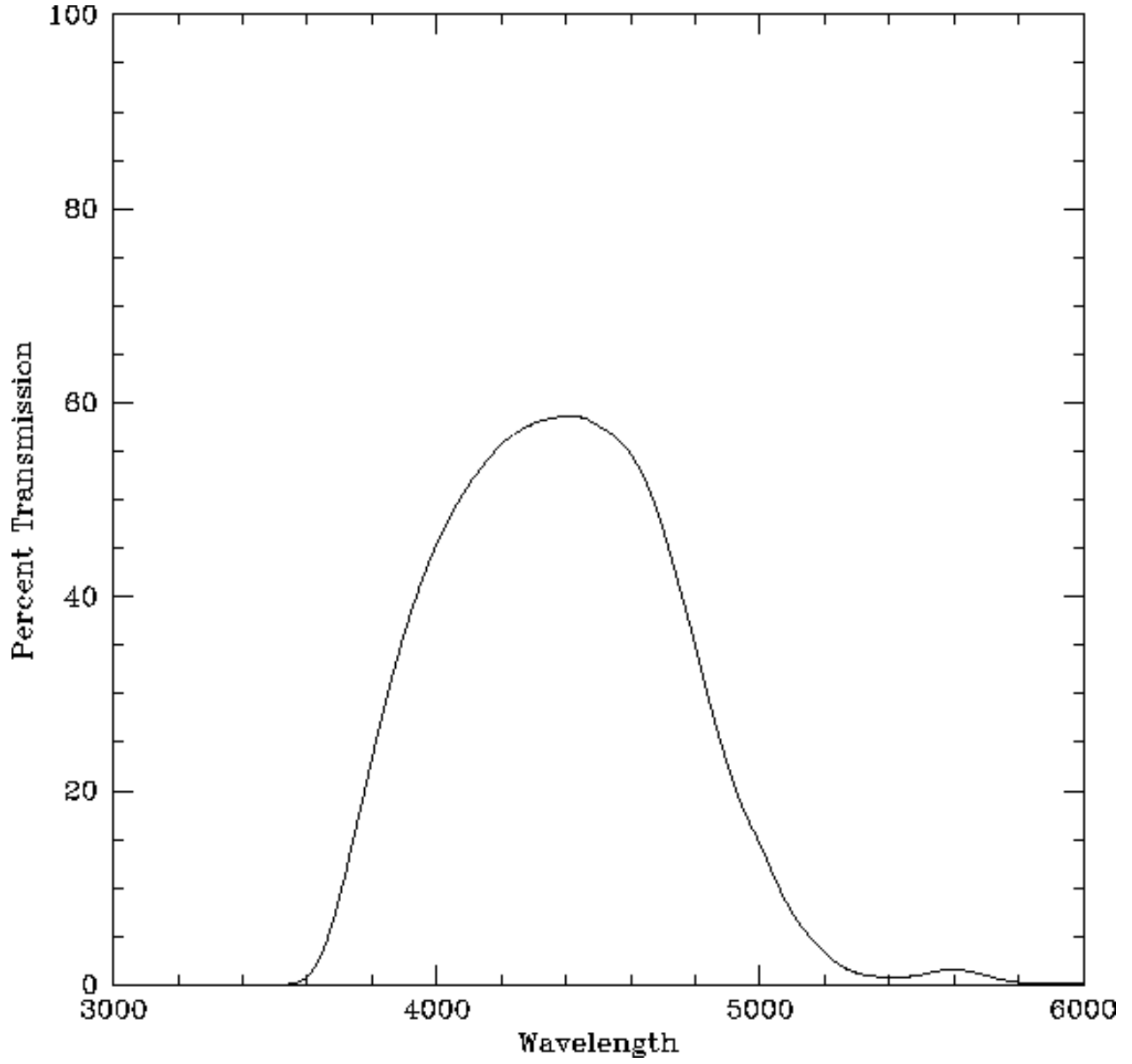


Fig. 45.— The transmission characteristics of the *B* filter: 2mm GG 385 + 1mm BG 12 + 1mm BG 18.

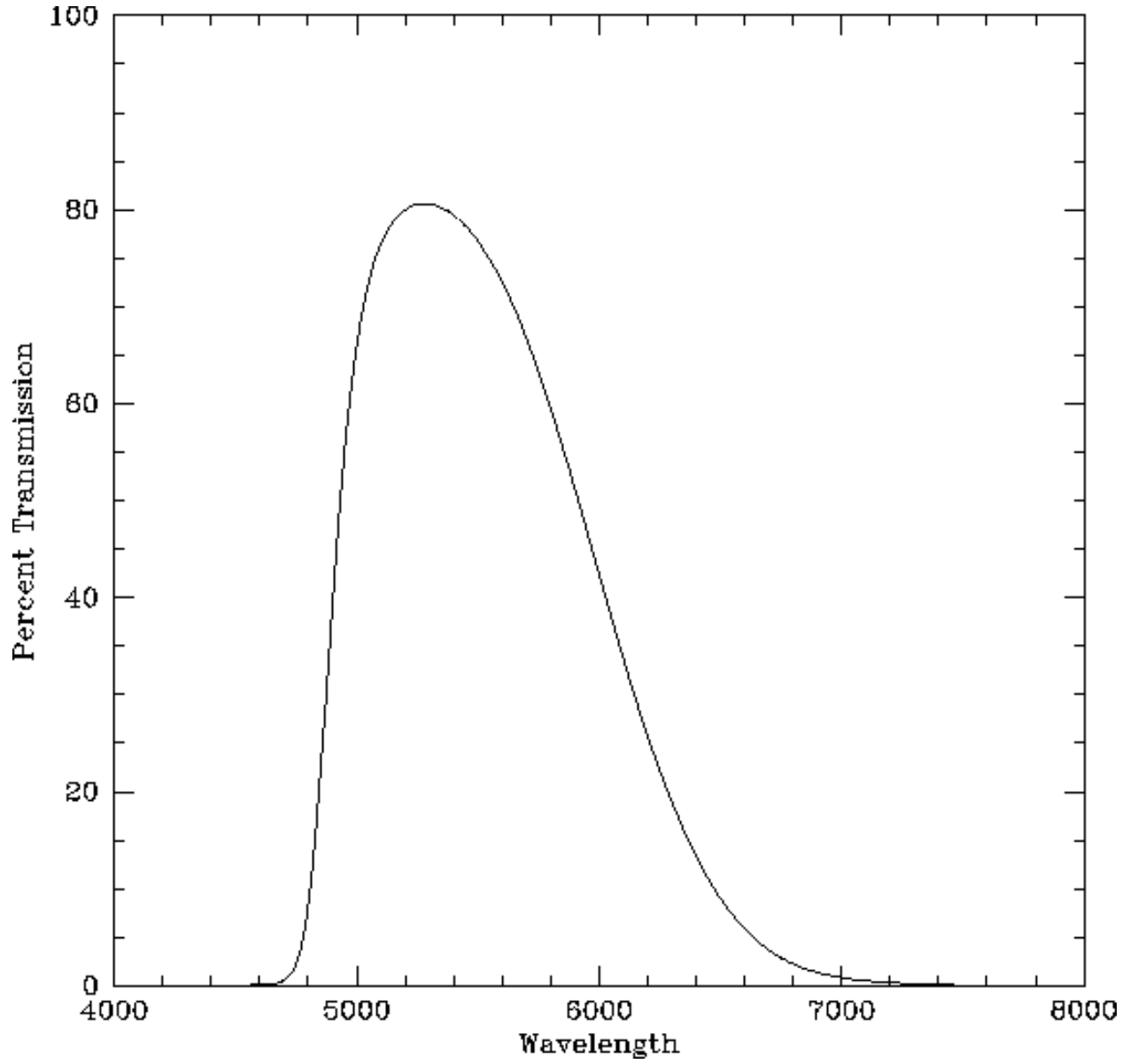


Fig. 46.— The transmission characteristics of the V filter: 2mm GG 495 + 1mm BG 18.

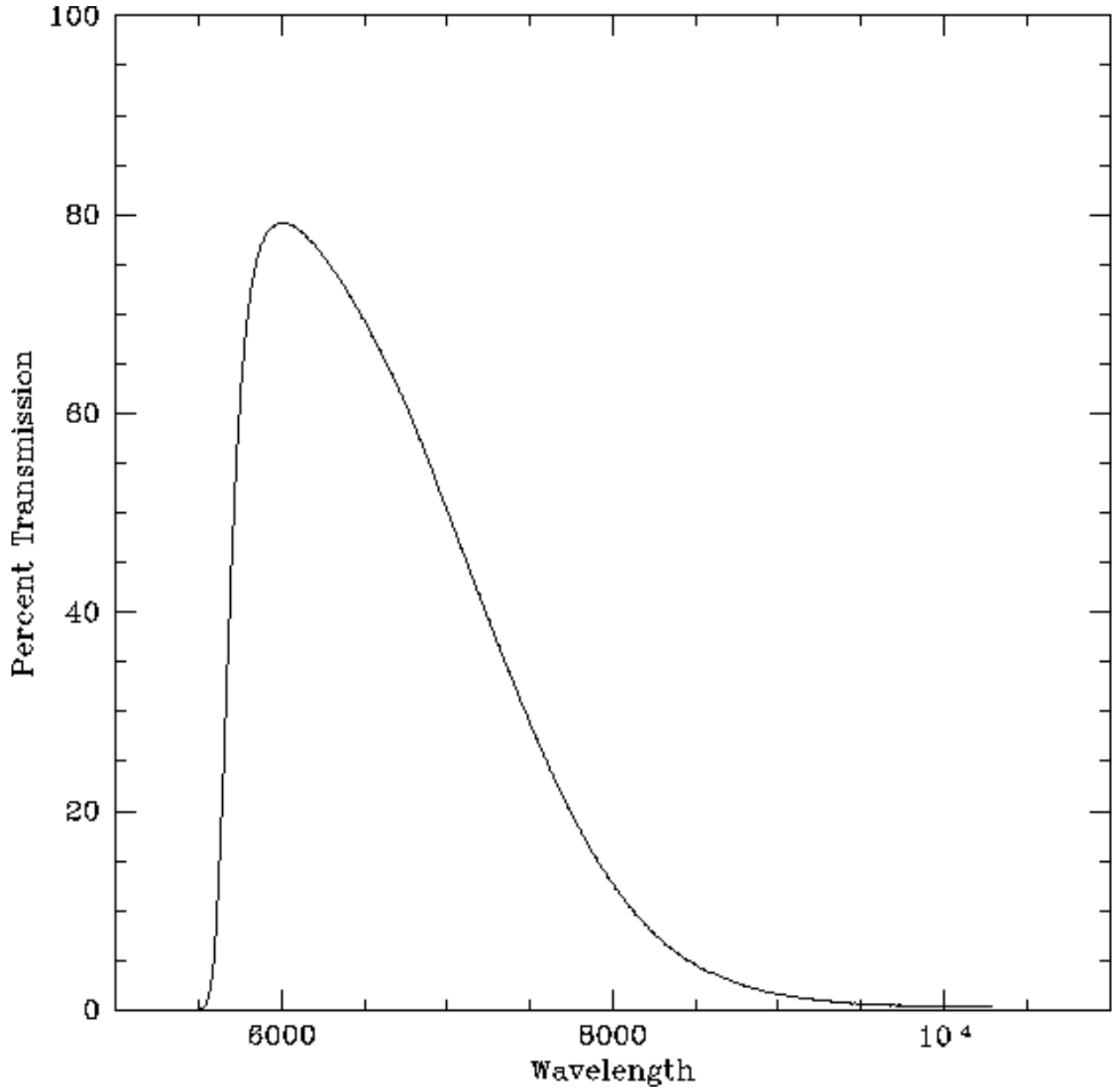


Fig. 47.— The transmission characteristics of the *R* filter: 2mm OG 570 + 2mm KG 3.

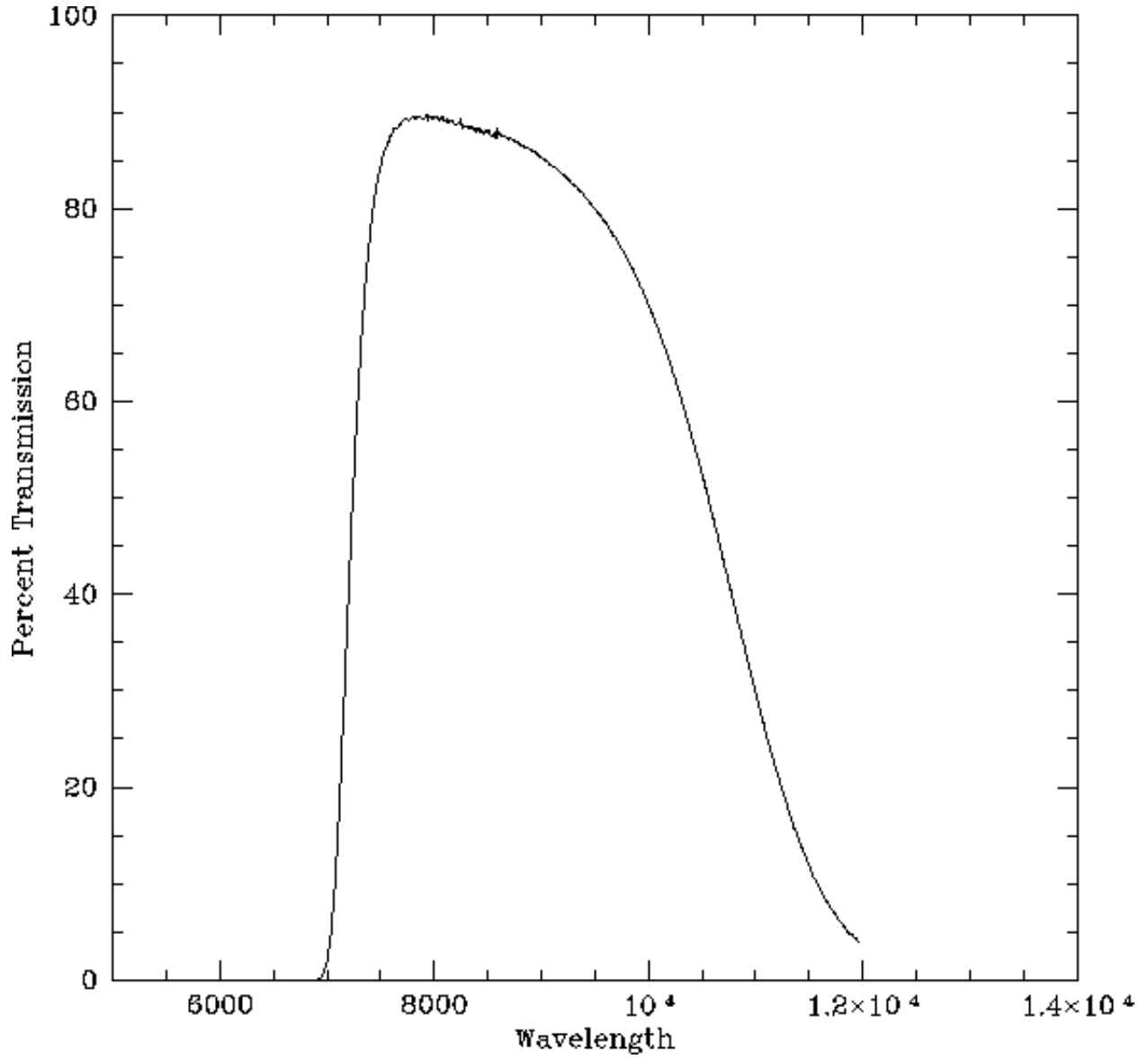


Fig. 48.— The transmission characteristics of the *I* filter: 3mm RGN 9.